

OPTIMUM THRESHOLD DETECTION FOR AN
INFRARED NUTATING DETECTION SYSTEM

William Earl Major

Library
Naval Postgraduate School
Monterey, California 93940

NAVAL POSTGRADUATE SCHOOL

Monterey, California



THESIS

OPTIMUM THRESHOLD DETECTION
FOR AN
INFRARED ROTATING DETECTION SYSTEM

by

William Earl Major, II

Thesis Advisor:

Harold Titus

March 1973

T15 7 43

Approved for public release; distribution unlimited.

Optimum Threshold Detection
for an
Infrared Nutating Detection System

by

William Earl Major, II
Lieutenant, United States Navy
B.S., Auburn University, 1965

Submitted in partial fulfillment of the
requirements for the degree of

ELECTRICAL ENGINEER

from the

NAVAL POSTGRADUATE SCHOOL
March 1973

M 2775
C.1

ABSTRACT

A threshold detection system based on the Neyman-Pearson criterion is derived for an infrared nutating optical system. Detection is optimum for small signal-to-noise ratios and a Gaussian uncertainty in the pointing error of the optical system. The signal spectrum and background power spectral density for a rectangular space filter are computed numerically and used to specify the matched filter for the threshold detection system and evaluate its performance.

TABLE OF CONTENTS

INTRODUCTION -----	7	
SIGNAL PROCESSING -----	10	
TARGET SPECTRUM -----	10	i,
CORRELATION OF BACKGROUND NOISE -----	15	
WHITE NOISE COMPONENT -----	18	
SIGNAL PROCESSING -----	20	or
DETECTION OF A KNOWN SIGNAL -----	21	ice
DETECTION OF SIGNAL WITH UNKNOWN PARAMETERS ---	28	
EVALUATION OF PERFORMANCE -----	32	
THRESHOLD DETECTOR FOR ROTATING SYSTEM -----	37	
ADJUSTMENT FOR RECTANGULAR DETECTOR -----	42	
NUMERICAL RESULTS -----	56	
CONCLUSIONS -----	85	
: DERIVATION OF SIGNAL SPECTRAL COEFFICIENTS -----	88	
: DERIVATION OF BACKGROUND CORRELATION COEFFICIENTS -----	91	
: EXPECTATION OF Λ_{12} -----	96	
: KARHUNEN-LOEVE REPRESENTATION OF EQUIVALENT SIGNAL-TO-NOISE RATIO -----	102	
: NON-ZERO TERMS FOR NUMERICAL INTEGRATION ---	105	
: SUMMATION CHECK -----	108	
: CALCULATED COEFFICIENTS -----	113	
: COMPUTER PROGRAM -----	116	

BIBLIOGRAPHY	-----	131
INITIAL DISTRIBUTION LIST	-----	133
FORM DD 1473	-----	134

LIST OF FIGURES

Figure		
1.1	Optical Imaging -----	11
1.2	Circular Nutation in the Image Plane -----	14
1.3	Power Spectrum of White Noise -----	19
5.1	Nutation with Rectangular Detector -----	43
6.1	Scanned Area of Nutating Detector -----	57
6.2-6.5	Background Power Spectral Density vs. Frequency (Hz) -----	62
6.6-6.8	Point Target Spectrum Envelope vs. Frequency ----	66
6.9-6.10	Averaged Signal Spectrum Envelope vs. Frequency -----	69
6.11-6.13	Filter Spectrum for Threshold Detector vs. Frequency (Hz) -----	71
6.14-6.16	Filter Envelope (Matched to point target) vs. Frequency (Hz) -----	74
6.17-6.19	Probability of Detection vs. Background-to- Noise Ratio -----	77
6.20-6.22	Probability of Detection vs. Signal-to- Noise Ratio -----	80
6.23	Probability of Detection vs. Background-to- Noise Ratio -----	83
6.24	Probability of Detection vs. Number of Nutations -----	84

ACKNOWLEDGEMENTS

The author wishes to express his appreciation to Dr. Harold A. Titus for his full support throughout the period of time this work was done and to DR. Reo Yoshitani, Senior Engineer, Hughes Aircraft Company, who posed the problem and offered many helpful suggestions. Also the author wishes to thank Dr. Richard Franke, Asst. Professor of Mathematics, Naval Postgraduate School, for his guidance in using Gaussian quadrature methods for numerical integration.

I. INTRODUCTION

An infrared (IR) detection system determines the presence or absence of a target in a particular area of space by processing the received IR energy from that area. The target must be found amid ever-present background radiance and any internal noise generated by the detection system. In this thesis, one type of system, called a nutating optical system, is considered.

Infrared detection is a combination of spatial frequency processing and temporal processing. Spatial frequency processing is a means of achieving a modulated output from the IR radiance passing into the optical system so that information may be easily extracted [Ref. 14]. To extract this information, some form of temporal processing is used. In a nutating optical system, the optical axis rotates about an axis perpendicular to the image plane in such a way that a point image traces out a circle in the image plane. The spatial frequency filter is a piece of IR sensitive material in the image plane which produces a voltage output that is amplified and fed into a temporal filter for processing. A nutating optical system is frequently used in a missile seeker because it produces a signal when there is no tracking error and the rotating optics can be made into a gyro that provides the inertial reference.

This work is a synthesis and extension of two recently published articles in the literature. The first, by

Harger [Ref. 3], formulates the detection theory of a known signal in background and white noise. Since in IR target detection the signal is never known completely, Harger's work is extended to the case where the target amplitude and position are unknown. However, a known target shape is assumed as well as a priori statistics of amplitude and position. Since detection is most difficult when the amplitude is small, a test (called the threshold detector) is derived that is optimum for weak signals.

To specify the form of the threshold detector and to calculate its performance, an eigenvalue integral equation must be solved. Ordinarily, this is a difficult undertaking but the solution becomes trivial if the covariance function of the background process is periodic. This is exactly the condition realized for the background process out of a nutating detector provided that the phase, which is physically unimportant, is averaged out.

Samuelsson's results [Ref. 11] specify the form of the signal and background coefficients in terms of the system parameters and signal and background radiance. These derivations were first published in a Swedish internal report [Ref. 10], then re-derived in English by Yoshitani [Ref. 6]. The latter's derivations are included in the appendices.

Samuelsson's equations have been applied to a rectangular IR detector assuming a Wiener spectrum for the random background and the coefficients have been calculated.

Using these coefficients, the optimum filter has been determined and the probability of detection computed as a function of signal-to-noise ratios and background-to-noise ratios.

II. SPATIAL PROCESSING

The spatial frequency filtering portion of the detection system is comprised of a lens system and an IR sensitive detector located in the image plane, the focal plane of the optics. To adequately derive information from the IR radiation, the lens system and detector must be of a nature that causes the voltage output to be modulated in a way that information about a target within the field of view can be processed. In a practical nutating optical system, the lens system moves and the detector is stationary. However, for conceptual purposes, this is equivalent to a stationary lens system and nutating detector.

A. TARGET SPECTRUM

The object to be detected, the target, is located in the object plane a distance R from the lens and parallel to the image plane as shown in Figure 1.1. The angle from the perpendicular axis connecting the planes to the target coordinates measured in the x -direction is called x and is measured in milliradians; the angle in the y -direction is y . The target is considered to be close to the optical axis and at a sufficient distance, R , such that small angle approximations may be made,

$$\begin{aligned}x &\approx \tan x \\y &\approx \tan y\end{aligned}\tag{2.1}$$

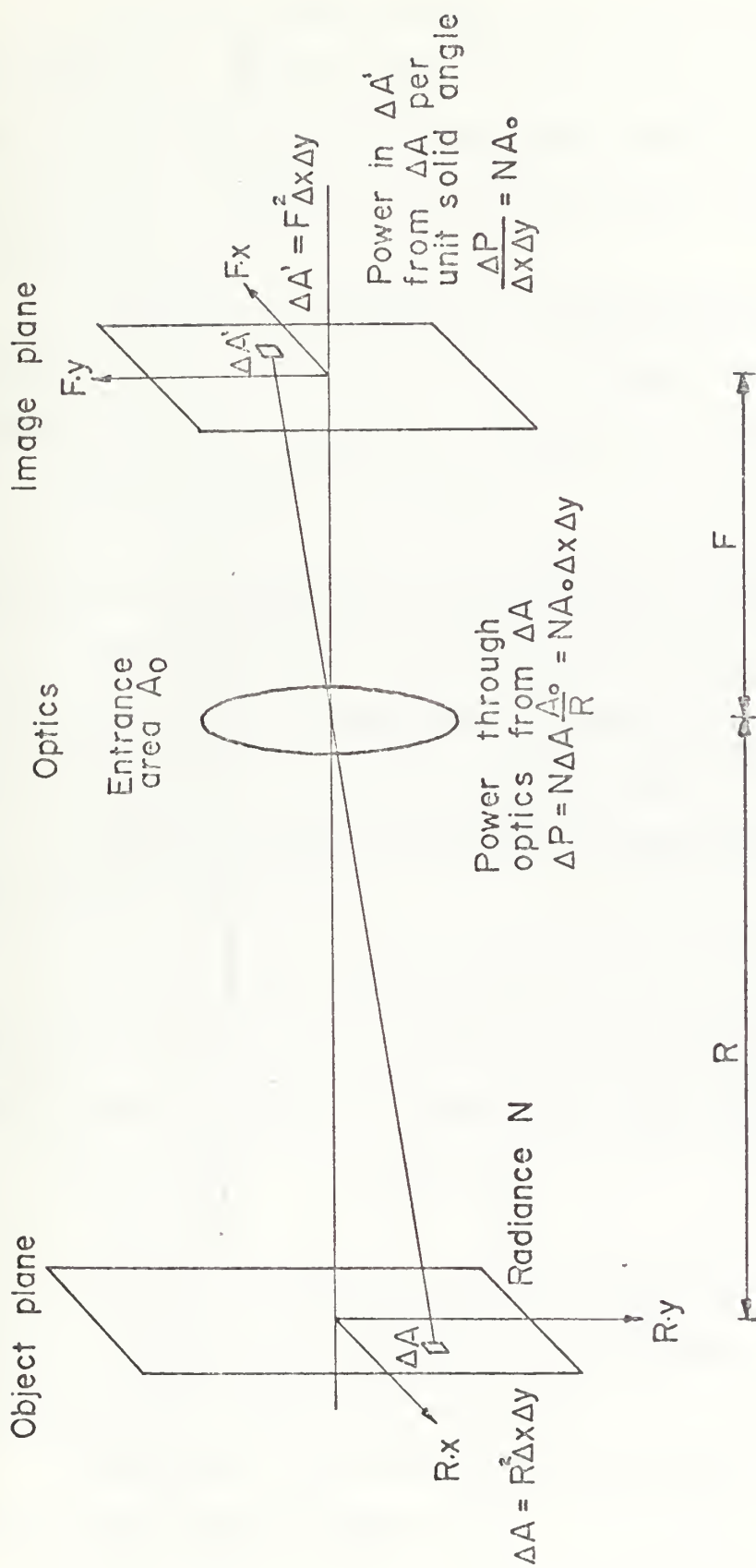


Figure 1.1. Optical Imaging.

Consider a target with a radiance distribution $N(\underline{r})$ ($\text{W}/\text{cm}^2\text{-sr}$) which is the radiant power into a unit solid angle per unit projected area of the sources. $\underline{r} = \underline{r}(x,y)$ is a vector whose origin is the perpendicular axis connecting the coordinates.

Assuming no atmospheric attenuation (this can be included in $N(\underline{r})$ if it exists) and perfect optics, the power distribution in the image plane is

$$P_i(\underline{r}) = N(\underline{r}) \cdot A_0 \text{ (w/sr)} \quad (2.2)$$

where A_0 is the effective entrance area of the optics.

Dividing by A_0 , one can see that the radiance distribution in the image plane is numerically equal to the radiance distribution in the object plane.

However, because the optics is not perfect, a point object given by

$$H_p \delta(\underline{r}) = H_p \delta(x) \delta(y) \text{ (w)} , \quad (2.)$$

(where H_p (W/cm^2) is the irradiance at the optics received from the point source) is imaged as a power distribution

$$H_p \cdot f_0(\underline{r}) \text{ (W/cm}^2 \text{ Sr)} \quad (2.4)$$

where $f_0(\underline{r})$ (sr^{-1}) is the point spread function of the optics. Irradiance is defined as the radiant flux incident on a surface of unit area [Ref. 5].

Therefore, the radiance distribution, $N(\underline{r})$, in the object plane will be imaged as

$$N'(\underline{r}) = \int N(\underline{r}-\underline{s}) f_0(\underline{s}) d^2 \underline{s} \text{ (W/cm}^2 \text{ Sr)} \quad (2.5)$$

where $d^2s = dx dy$ and the integration is over the entire image plane.

The detector is a space filter in the image plane which may be a moving retical or simply an aperture across which the power is integrated.

The power in the image plane incident on the detector is

$$H = \int N'(\underline{r}) \tau(\underline{r}) d^2\underline{r} \quad (W/cm^2) \quad (2.6)$$

where $\tau(\underline{r}) = \tau(x,y)$ is the transmittance of the detector.

When the detector moves as a function of time, the power incident on the detector becomes a function of time,

$$H(t) = \int N'(\underline{r}) \tau(\underline{r}-\underline{\rho}(t)) d^2\underline{r} \quad (W/cm^2) \quad (2.7)$$

where $\rho(t)$ describes the movement of the detector in the image plane.

A nutating detector moves circularly in the image plane but its orientation remains fixed, i.e., the coordinate system (x',y') shown in Fig. 1.2 does not rotate. The nutation radius measured with respect to the optical axis is given by ρ .

Assuming a nutating optics and no relative motion between the target and the optics, the radiance on the detector will be periodic and thus can be expanded in a Fourier series

$$H(t) = \sum_n H_n e^{jn\omega_0 t} \quad 0 \leq t \leq T \quad (2.8)$$

where

$$H_n = \frac{1}{T} \int_0^T H(t) e^{-jn\omega_0 t} dt .$$

Replacing $H(t)$ by equation (2.7),

$$H_n = \frac{1}{T} \int_0^T dt e^{-jn\omega_0 t} \int d^2 \tilde{r} N'(\tilde{r}) (r - \rho(t)) \quad (2.9)$$

The motion describing function, $\rho(t)$, for circular nutation is

$$\rho(t) = \rho(\cos \omega_0 t, \sin \omega_0 t) , \quad (2.10)$$

where $\omega_0 = 2\pi/T$ (rad/sec) is the radian frequency of nutation and T is the period for one nutation.

Substituting (2.10) in (2.9), H_n can be shown (see Appendix A) to be

$$H_n = j^n \int N'(\tilde{k}) \tau^*(\tilde{k}) e^{-jn\phi} J_n(2\pi\rho \sqrt{k_x^2 + k_y^2}) d^2 \tilde{k} \quad (2.11)$$

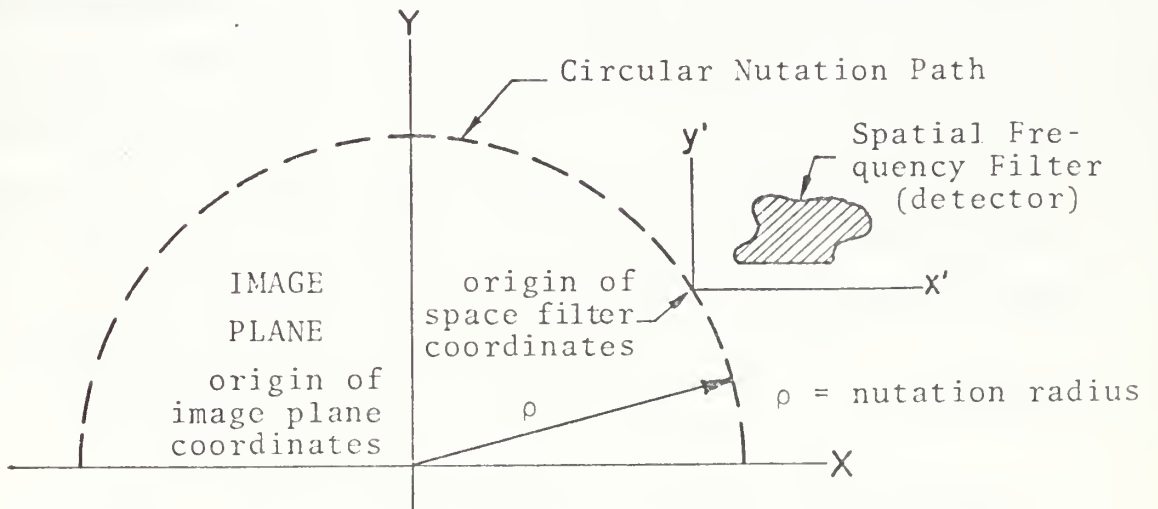


Figure 1.2. Circular Nutation in the Image Plane.

where $\tilde{k} = (k_x, k_y)$, two-dimensional spacial Fourier transform coordinates [Ref. 8],

$N'(\tilde{k})$ = transform of radiance distribution in the image plane,

$\tau^*(\tilde{k})$ = complex conjugate of the transform of the optical transmittance function in the detector coordinate system,

$$\phi = \tan^{-1} k_y/k_x,$$

ρ = nutation radius,

and $J_n(z)$ is the n th order Bessel function of the first kind. It has been assumed that the image plane is very large compared to the radiance distribution from a target so that the image plane may be considered infinite for mathematical purposes.

B. CORRELATION OF BACKGROUND NOISE

The background power incident on the detector is from a sample background scene where a scene is a two-dimensional random process characterized by the radius vector $\tilde{r} = (x, y)$ from the optical axis.

Let $N(\tilde{r})$ be a sample scene radiance distribution on the object plane from an ensemble of scenes which has been given a suitable probability structure. The background power incident on the detector is

$$B(t) = \int N'(\tilde{r}) \tau(\tilde{r}-\tilde{\rho}(t)) d^2\tilde{r}. \quad (2.12)$$

The covariance function is defined by taking the expected value

$$E\{[B(t)] - E\{B(t)\}}[B(u) - E\{B(u)\}] = R_B(t,u) \quad (2.13)$$

where E denotes the expectation over the ensemble of scenes. Because the detector is nutating, the random process, $B(t)$, will not be stationary. However, if the detector and background do not move with respect to each other, then $R_B(t_1, t_2)$ is doubly periodic:

$$R_B(t_1 + MT, t_2 + NT) = R_B(t_1, t_2) \quad (2.14)$$

where M and N are integers.

It can be shown [Ref. 7] that the form of the covariance of a doubly period process is

$$R_B(t_1, t_2) = \sum_{m,n}^{\infty} \beta_{mn} e^{jm\omega_0 t_1} e^{-jn\omega_0 t_2} . \quad (2.15)$$

Because the nutation is periodic, over the ensemble of scenes, there is little significance in the starting time t . Therefore, considering t as a random variable that is uniform over the nutation period, one can "average it out" of the covariance function as

$$R_B(\tau) = \frac{1}{T} \int_0^T R_B(t+\tau, t) dt . \quad (2.16)$$

Substituting (2.16) in (2.15),

$$R_B(\tau) = \sum_{m,n}^{\infty} \beta_{mn} e^{jm\omega_0 \tau} \frac{1}{T} \int_0^T e^{j(m-n)\omega_0 t} dt . \quad (2.17)$$

Using the relation

$$\delta_{uv} = \frac{1}{T} \int_0^T e^{j(u-v)\omega_0 t} dt, \quad (2.18)$$

the correlation function becomes

$$R_B(\tau) = \sum_n \beta_n e^{jn\omega_0 \tau}. \quad (2.19)$$

Equation (2.19) shows that $B(t)$ can be considered a wide sense stationary process and that it is periodic in the mean square sense; i.e.,

$$R_B(\tau) = R_B(T+\tau) \quad \text{for any } \tau \quad (2.20)$$

The power spectral density is the temporal Fourier transform of $R_B(\tau)$. Taking the transform one has

$$S_B(\omega) = 2\pi \sum_n \beta_n \delta(\omega - n\omega_0). \quad (2.21)$$

The coefficients, β_n , can be related to the optical system parameters by

$$\beta_n = \int |\tau(\tilde{k})|^2 |F_0(\tilde{k})|^2 W_B(\tilde{k}) J_n^2(2\pi\rho\sqrt{k_x^2 + k_y^2}) d^2\tilde{k} \quad (2.22)$$

where $F_0(\tilde{k})$ is the transform of the point spread function, and $W_B(\tilde{k})$ is the Wiener spectrum, the transform of the background correlation function. This derivation was first made by Samuelsson [Ref. 10] in an internal Swedish report then again by Yoshitani [Ref. 6]. Yoshitani's derivation has been included as Appendix B.

Equation (2.19) implies that the background, $B(t)$, can be represented by a Fourier series with uncorrelated coefficients [Ref. 7]. Thus,

$$B(t) = \sum_n b_n e^{jn\omega_0 t} \quad (2.23)$$

where the convergence is in the mean square sense.

The coefficients, b_n , satisfy

$$E(b_n) = \begin{cases} E(B(t)) & n = 0 \\ 0 & n \neq 0 \end{cases} \quad (2.24)$$

Moreover, they are uncorrelated

$$E(b_m b_n) = \begin{cases} \beta_n & m = n \\ 0 & m \neq n \end{cases} \quad (2.25)$$

C. WHITE NOISE COMPONENT

In an actual system there will be a certain amount of internal noise generated in the detector and preamplifier which is additive to any background noise or signal. In the frequencies of interest the primary source of this noise is thermal agitation. This type of noise, called Johnson noise, is assumed to be white and Gaussian.

Let $W(t)$ be Gaussian white noise with power spectral density $\frac{N}{2} (V^2/H_z)$. The power spectrum at the output of the preamp with bandwidth B is shown in Figure 1.3.

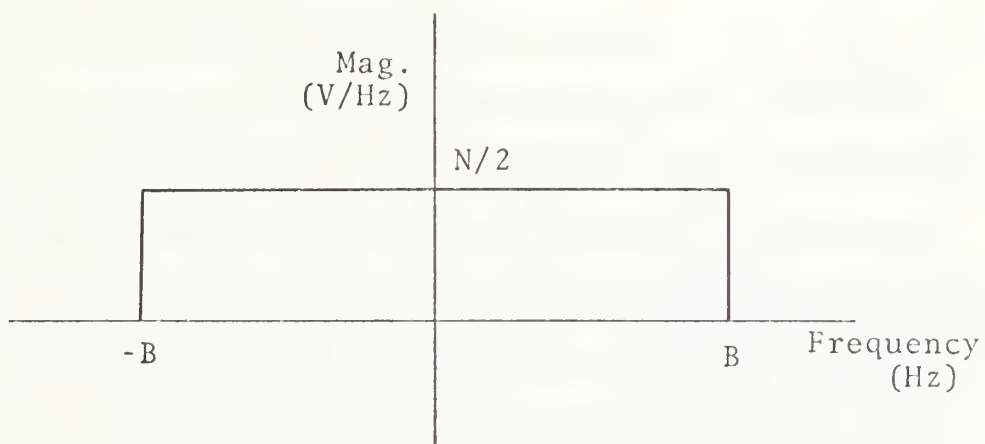


Figure 1.3. Power Spectrum of White Noise.

The RMS voltage measured at the output of the preamp is

$$V_{\text{rms}}^2 = \frac{N}{2} \cdot 2B = NB \text{ (V}^2\text{)} . \quad (2.26)$$

III. TEMPORAL PROCESSING

The output voltage from the detector is temporally processed to determine the presence of a target. The type of processor is determined by applying statistical detection theory to the known behavior of the nutating system and various realistic assumptions about the system and the target. An optimum processor in the sense of small signal amplitudes, called a threshold detector, is developed in this section.

Harger [Ref. 3] derived the detection theory for the known signal case in the presence of additive background and white noise components. In IR detection, the target amplitude and position are usually not known completely. The threshold detector is an extension of Harger's work which accounts for the unknown amplitude and position.

The form of the optimal detector under the Neyman-Pearson criterion will be derived for multiple observations. It is assumed that the image plane and object plane remain parallel and stationary with respect to each other during the observations.

The detection of the target under the Neyman-Pearson criterion becomes a problem of hypothesis testing. The task of the detector is one of choosing between two hypotheses, H_0 that only noise is present and H_1 that in addition to the noise there is a target present. The design of the detector is one that permits the correct choice of hypothesis H_1 (a detection) with maximum probability of detection, Q_d , in a fixed probability, Q_{FA} , of choosing

H_1 when H_0 is true (a false alarm). The structure of the Neyman-Pearson criterion requires forming a likelihood ratio, Λ_{10} , which is compared to a known threshold, V_t , specified for a given false alarm probability. If the likelihood ratio exceeds the threshold, hypothesis H_1 is assumed true and if not, hypothesis H_0 is assumed true. The logic process may be written

$$\Lambda_{10} \underset{H_0}{\overset{H_1}{>}} V_t \quad (3.1)$$

where the threshold, V_t , is derived from the expression

$$Q_{FA} = \int_{V_t}^{\infty} p(Z|H_1) dZ \quad (3.2)$$

and Z is a sufficient statistic of the received data.

A. DETECTION OF A KNOWN SIGNAL

The data for processing is a set of M functions of time $\{Z_n(t), n=1, \dots, M\}$ where each function is the output of the preamp during one nutation $(0, T)$. T is the nutation period. The output may be represented as

$$Z_n(t) = S_n(t) + B(t) + N_n(t); 0 \leq t \leq T, n=1, \dots, M \quad (3.3)$$

$S_n(t)$ represents the output due to a target. The component, $B(t)$, represents an additive background and is a sample function of a random field (B) . The relative size of the target in the field of view is assumed sufficiently small that the background is additive while $B(t)$ is assumed to be

the sample function during each of the M nutations observed. $N_n(t)$ represents the additive noise component due to the internal noise of the detector-preamplifier combination. It is a sample function of a white Gaussian random process (N_n) of zero mean and power spectral density $N/2(V^2/H_Z)$.

The two hypotheses for the likelihood ratio may be written as

$$H_1: \{Z_n(t) = S_n(t) + B(t) + N_n(t) ; n=1, \dots, M\} \quad (3.4)$$

$$H_0: \{Z_n(t) = B(t) + N_n(t) ; n=1, \dots, M\}$$

Denote the likelihood ratio as $\Lambda_{10}(\{Z_n\})$ where the likelihood ratio is defined as

$$\Lambda_{10}(\{Z_n\}) = \frac{p(\{Z_n\} | H_1)}{p(\{Z_n\} | H_0)} \quad (3.5)$$

The likelihood ratio is complicated by the fact Z_n and Z_m are not independent because of a common noise component, $B(t)$. To simplify the derivation Harger introduced an auxiliary hypothesis

$$H_2: \{Z_n = N_n ; n=1, \dots, M\}. \quad (3.6)$$

Then the likelihood ratio, Λ_{10} , can be computed using the chain rule for likelihood ratios:

$$\begin{aligned} \Lambda_{10} &= \frac{p(\{Z_n\} | H_1)}{p(\{Z_n\} | H_0)} = \frac{p(\{Z_n\} | H_1)/p(\{Z_n\} | H_2)}{p(\{Z_n\} | H_0)/p(\{Z_n\} | H_2)} \\ &= \Lambda_{12}/\Lambda_{02}. \end{aligned}$$

If the sample functions for the background, B , were non-random, $Z_i(t)$ and $Z_j(t)$, $i \neq j$, would be mutually independent because of white noise. Accordingly, if B were fixed, one can write the conditional likelihood for the n^{th} observation $\Lambda_{12}^n(\{Z_n\}|\tilde{B})$. Moreover, the likelihood ratio for M observations would be the product of the likelihood ratios for each single observation,

$$\Lambda_{12}(\{Z_n\}|\tilde{B}) = \prod_{n=1}^M \Lambda_{12}^n(Z_n|\tilde{B}).$$

The conditioning is then removed by averaging over the ensemble of backgrounds

$$\Lambda_{12}(\{Z_n\}) = E_B[\Lambda_{12}(\{Z_n\}|\tilde{B})].$$

Since the noise is white Gaussian, the conditional likelihood ratio is that for detecting a known signal $S_n + B_n$ in white Gaussian noise and has the well known form ([Ref. 15], page 253)

$$\begin{aligned} \Lambda_{12}^n(\{Z_n\}|\tilde{B}) = \exp \left\{ \frac{2}{N} \sum_{n=1}^M \int_0^T Z_n(t) (S_n(t) + B(t)) dt \right. \\ \left. - \frac{1}{N} \sum_{n=1}^M \int_0^T (S_n(t) + B(t))^2 dt \right\} \end{aligned}$$

which may be rewritten as

$$\begin{aligned} \Lambda_{12}^n(\{Z_n\}|\tilde{B}) = \exp \left\{ \frac{2}{N} \sum_{n=1}^M \int_0^T Z_n(t) S_n(t) dt \right. \\ \left. - \frac{1}{N} \sum_{n=1}^M \int_0^T S_n^2(t) dt \right\} \exp \alpha(b) \quad (3.14) \end{aligned}$$

where

$$\alpha(b) = \frac{2}{N} \sum_{n=1}^M \int_0^T (Z_n(t) + S_n(t)) B(t) dt - \frac{M}{N} \int_0^T B^2(t) dt. \quad (3.15)$$

To find $\Lambda_{10}(\{Z_n\})$, one must evaluate $E_B[\Lambda_{12}^n(\{Z_n\}|B)]$

where

$$\begin{aligned} E_B[\Lambda_{12}^n(\{Z_n\}|B)] &= \exp \left\{ \frac{2}{N} \sum_{n=1}^M \int_0^T Z_n(t) S_n(t) dt \right. \\ &\quad \left. - \frac{1}{N} \sum_{n=1}^M \int_0^T S_n^2(t) dt \right\} \cdot E_B \{ \exp \alpha(b) \}. \end{aligned} \quad (3.16)$$

Assuming the background is Gaussian the expectation can be evaluated by representing the background in a Karhunen-Loeve (K-L) expansion

$$B(t) = \sum_k b_k \phi_k(t), \quad 0 \leq t \leq T \quad (3.17)$$

where $\phi_k(t)$ is the eigenfunction corresponding to eigenvalue λ_k of the homogeneous integral equation

$$\lambda_k \phi_k(t) = \int_0^T R_B(t,u) \phi_k(u) du, \quad 0 \leq t \leq T. \quad (3.18)$$

$R_B(t,u)$ is the covariance function of background

$$R_B(t,u) = E\{[B(t) - m_B(t)][B(u) - m_B(u)]\} \quad (3.19)$$

where $m_B(t)$ is the mean of the background.

Then $E_B(\exp \alpha(b))$ can be calculated in a straightforward manner. After the lengthy calculation shown in Appendix C

$$\begin{aligned} \ln E_B \{ \exp \alpha(b) \} = & - \frac{1}{2} \sum_k \ln \left(1 + \frac{M}{N_0} \lambda_k \right) \\ & + \frac{2}{N} \int_0^T dt \sum_{n=1}^M (Z_n(t) - S_n(t)) \int_0^T du \sum_{m=1}^M (Z_m(u) - S_m(u)) q(t, u) \\ & - \frac{1}{2} \int_0^T dt \{ m_B(t) - \frac{2}{M} \sum_{n=1}^M (Z_n(t) - S_n(t)) \} h(t) \end{aligned} \quad (3.20)$$

where $q(t, u)$ satisfies the integral equation

$$\frac{N}{2M} q(t, u) + \int_0^T R_B(t, \tau) q(\tau, u) d\tau = R_B(t, u) \quad 0 \leq u, t \leq T \quad (3.21)$$

and $h(t)$ satisfies

$$\frac{N}{2M} h(t) + \int_0^T R_B(t, \tau) h(\tau) d\tau = m_B(t) \quad 0 \leq t \leq T. \quad (3.22)$$

$q(t, u)$ is the impulse response of the filter that gives the minimum mean square error estimate \hat{B} of the background when the mean is zero [Ref. 15]. The additive white noise is reduced in amplitude by $1/M$. Using the K-L representation, one can also write

$$q(t, u) = \sum_k \frac{\frac{N}{2M} \lambda_k}{\frac{N}{2M} + \lambda_k} \phi_k(t) \phi_k^*(u) \quad 0 \leq u, t \leq T \quad (3.23)$$

Using equations (2.9), (3.10), (3.14) and (3.20) and

observing that

$$\Lambda_{02}(\{Z_n\}) = \Lambda_{12}(\{Z_n\}) | S_n = 0 \quad (3.24)$$

it can be shown (see Appendix C) that the likelihood function for hypotheses H_1 and H_0 is

$$\Lambda_{10}(\{Z_n\}) = \exp \left\{ \sum_{n=1}^M \int_0^T Z_n(t) q_n(t) dt + K' \right\} \quad (3.25)$$

where

$$q_n(t) = \frac{2}{N} \left[S_n(t) - \frac{1}{M} \int_0^T \sum_{\ell=1}^M S_\ell(u) q(t,u) du \right] \quad (3.25a)$$

and

$$\begin{aligned} K' = & - \frac{1}{N} \sum_{n=1}^M \int_0^T S_n^2(t) dt + \frac{1}{NM} \int_0^T \int_0^T \sum_{n=1}^M \sum_{\ell=1}^M S_n(t) S_\ell(u) q(t,u) dt du \\ & - \frac{2}{m} \sum_{n=1}^M \int_0^T S_n(t) h(t) dt \end{aligned} \quad (3.25b)$$

The logarithm is a monotonic function. Thus it offer no loss of information but greatly simplifies the calculations. In the remaining work

$$\Lambda'_{10}(\{Z_n\}) = \ln \Lambda_{10}(\{Z_n\}) . \quad (3.26)$$

Rewriting equation (3.25),

$$\Lambda'_{10}(\{Z_n\}) = L(\{Z_n\}) + K' \quad (3.27)$$

where

$$L(Z_n) = \sum_{n=1}^M \int_0^T Z_n(t) q_n(t) dt .$$

K' does not depend on the input data so it may be included in the threshold. The hypotheses test now becomes

$$L(Z_n) \underset{H_0}{\overset{H_1}{>}} \text{Threshold} . \quad (3.28)$$

It is also possible, as Harger has shown, to derive tests similar to (3.28) without making the Gaussian background assumption. In particular, if the background fluctuates many times over $(0, T)$ such that $\alpha(b)$ of (3.15) is approximately Gaussian, then the test is

$$\sum_{n=1}^M \int_0^T Z_n(t) g_n(t) dt \underset{H_0}{\overset{H_1}{>}} \text{Threshold} \quad (3.29)$$

where

$$g_n(t) = \frac{1}{N} [S_n(t) - \frac{2M}{N} \int_0^T R_B(t,u) [\frac{1}{M} \sum_{\ell=1}^M S_{\ell}(u)] du] .$$

Since by Mercer's theorem

$$R_B(t,u) = \sum_k^{\infty} \lambda_k \phi_k(t) \phi_k^*(u), \quad 0 \leq t, u \leq T \quad (3.30)$$

on comparing q_n , g_n and (3.21), it is seen that the above model approaches the Gaussian model if

$$\frac{N}{2M} \gg \max_k \lambda_k .$$

The above condition, which implies a weak background, is sufficient but by no means necessary. The two models approximate each other whenever the second term of q_n and g_n are nearly identical. The point is that while the Gaussian background assumption may not fit the reality, a processor based on the assumption is probably not far from being the optimum. Also, the Gaussian assumption allows one to compute the processor performance.

B. DETECTION OF SIGNAL WITH UNKNOWN PARAMETERS

The likelihood ratio derived in section A is applicable only if the signal is known completely. Such is seldom the case in IR target detection and in general the signal is a function of some unknown parameters. Typically, the amplitude, a , of the target and its position \vec{r}_0 in the image plan are the unknown parameters, and the form of the signal can be rewritten to include these parameters:

$$S_n = S_n(t; a, \vec{r}_0)$$

Furthermore, by assuming that only point targets are of interest and including the assumption of fixed image and object planes over the number of nutations of interest, the shape of the waveform will be the same during each nutation. However, the amplitude is allowed to vary between successive nutations.

The signal waveform may now be written as

$$S_n(t; a, \vec{r}_0) = a_n f(t, \vec{r}_0) \quad (3.31)$$

where a_n is the signal amplitude and $f(t, \vec{r}_0)$ is the signal shape for a target at \vec{r}_0 .

Rewriting hypothesis H_1 under these assumptions gives

$$H_1': \{Z_n(t) = a_n f(t, \vec{r}_0) + B(t) + N_n(t); n=1, \dots, M \\ 0 \leq t \leq T\} \quad (3.32)$$

The likelihood ratio Λ_{10} becomes the conditional likelihood ratio $\Lambda_{10}(\{Z_n\} | a, \vec{r}_0)$ obtained by replacing $S_n(t)$ by $a_n f(t, \vec{r}_0)$ everywhere in (3.25).

Assuming a priori statistical knowledge of \underline{a} and \vec{r}_0 , and their independence, the likelihood ratio may be averaged over the respective density functions to produce an unconditional likelihood ratio

$$\Lambda_{10}(\{Z_n\}) = \iint \Lambda_{10}(\{Z_n\} | \underline{a}, \vec{r}_0) p(\underline{a}) p(\vec{r}_0) d\underline{a} d\vec{r}_0. \quad (3.33)$$

Instead of averaging as above, one could estimate \underline{a} and \vec{r}_0 by the maximum likelihood procedure and substitute the

estimated values \hat{a} and $\hat{\vec{r}}_0$ in the conditional likelihood ratio and try to maximize the generalized likelihood ratio $\Lambda_{10}(\{Z_n\}|\hat{a},\hat{\vec{r}}_0)$. However, this procedure is not followed here because the maximum likelihood estimates are difficult to obtain.

Since the main interest is in detection of the weak target, the small signal case is of primary interest. Expanding $\Lambda_{10}(\{Z_n\}|\hat{a},\hat{\vec{r}}_0)$ in powers of signal amplitudes

$$\begin{aligned} \Lambda_{10}(\{Z_n\}|\hat{a},\hat{\vec{r}}_0) &= 1 + \sum_{n=1}^M a_n \frac{\partial}{\partial a_n} \Lambda_{10}(\{Z_n\}|\hat{a},\hat{\vec{r}}_0) \Big|_{\hat{a}=0} \\ &+ \frac{1}{2} \sum_{n=1}^M \sum_{k=1}^M a_n a_k \frac{\partial^2}{\partial a_n \partial a_k} \Lambda_{10}(\{Z_n\}|\hat{a},\hat{\vec{r}}_0) \Big|_{\hat{a}=0} \\ &+ \dots \end{aligned} \quad (3.34)$$

Integrating (3.34) as in (3.33) term by term and retaining only the first non-zero term that depends on the data provides a statistic which is optimum for weak signals and is called a threshold detector [Ref. 4].

The evaluation is made easier by the fact

$$\frac{\partial}{\partial a_k} \Lambda_{10}(\{Z_n\}|\hat{a},\hat{\vec{r}}_0) \Big|_{\hat{a}=0} = \frac{\partial}{\partial a_k} \ln \Lambda_{10}(\{Z_n\}|\hat{a},\hat{\vec{r}}_0) \Big|_{\hat{a}=0} \quad (3.35)$$

which results from

$$\Lambda(\{Z_n\}|0,\vec{r}_0) = 1 .$$

The first non-zero term becomes

$$\begin{aligned}
 \frac{\partial}{\partial a_k} \ln \Lambda_{10}(\{Z_n\} | \tilde{a}, \vec{r}_0) \Big|_{\tilde{a}=0} &= \frac{2}{N} \int_0^T Z_n(t) f(t, \vec{r}_0) dt \\
 &- \frac{2}{N} \int_0^T Z_n(t) dt \int_0^T q(t, u) f(u, \vec{r}_0) du \\
 &- \int_0^T f(t, \vec{r}_0) h(t) dt
 \end{aligned} \tag{3.36}$$

Performing the integration over \vec{r}_0 ,

$$\begin{aligned}
 \Lambda_{10}(\{Z_n\}) &\cong 1 + \frac{2}{N} \sum_{n=1}^M \bar{a}_n \int_0^T Z_n(t) [\bar{f}(t) - \int_0^T q(t, u) \bar{f}(u) du] \\
 &- \int_0^T \bar{f}(t) h(t) dt
 \end{aligned} \tag{3.37}$$

where the bar denotes the averaged quantities. The first and last terms are independent of the data and may be included in the threshold value. Moreover, if the amplitudes are identically distributed, as is generally the case, the threshold detector performs the test

$$W = \sum_{n=1}^M \int_0^T Z_n(t) \bar{q}(t) dt \begin{matrix} > \\ < \end{matrix} \begin{matrix} H_1 \\ H_0 \end{matrix} W_t \tag{3.38}$$

where W_t is the threshold and

$$\bar{q}(t) = \frac{2}{N} [\bar{f}(t) - \int_0^T q(t, u) \bar{f}(u) du] . \tag{3.39}$$

Thus the threshold detector can be mechanized either as a correlator or matched filter followed by an accumulator.

The filter function $\bar{q}(t)$ may be represented in a series expansion in terms of the eigenfunctions of $R_B(t,u)$ and the coefficients of the signal expansion. Expanding $\bar{f}(t)$ in terms of the eigenfunctions:

$$\bar{f}(t) = \sum_k^{\infty} \bar{f}_k \phi_k(t) . \quad (3.40)$$

Substituting (3.40) in (3.39) and using (3.23)

$$\bar{q}(t) = \frac{N}{2M} \sum_k^{\infty} \frac{\bar{f}_k}{\frac{N}{2M} + \lambda_k} \phi_k(t) . \quad (3.41)$$

C. EVALUATION OF PERFORMANCE

The Gaussian assumption was made in deriving the threshold statistic; therefore, the threshold statistic itself is Gaussian. This means that the probability of detection, Q_d , and probability of false alarm, Q_{FA} , are uniquely determined by second-order statistics, e.g., the means and variances of W under hypotheses H_0 and H_1 .

Recall that the threshold statistic is

$$W = \sum_{n=1}^M \int_0^T Z_n(t) \bar{q}(t) dt. \quad (3.42)$$

The means and variances of W are:

$$E(W|H_0) = \sum_{n=1}^M \int_0^T \bar{q}(t) E(B(t) + N_n(t)) dt$$

$$= \sum_{n=1}^M \int_0^T \bar{q}(t) m_B(t) dt$$

$$E(W|H_1) = \sum_{n=1}^M \int_0^T \bar{q}(t) E[a_n f(t, \vec{r}_0) + B(t) + N_m(t)] dt$$

$$= E(W|H_0) + \sum_{n=1}^M \int_0^T \bar{f}(t) \bar{q}(t) dt$$

$$\text{VAR}(W|H_0) = \text{VAR}(W|H_1) = \text{VAR}$$

$$= \frac{NM}{2} \int_0^T \bar{q}^2(t) dt + M^2 \int_0^T \bar{q}(t) \int_0^T \bar{q}(u) R_B(t, u) du dt \quad (3.43)$$

Letting $p_w(\cdot|H_i)$ be the Gaussian density function of W under H_i which is specified by the equations above, then

$$Q_{FA} = \int_{W_t}^{\infty} p_w(x|H_0) dx \quad (3.44)$$

and

$$Q_d = \int_{W_t}^{\infty} p_w(x|H_1) dx \quad (3.45)$$

where W_t is the threshold voltage.

Equations (3.43) and (3.44) can be solved to yield

$$Q_{FA} = \phi_c(x) \quad (3.46)$$

and

$$Q_d = \phi_c(x-d) \quad (3.47)$$

where

$$x = \frac{W_t - E[W|H_0]}{\sqrt{VAR}},$$

d is the equivalent signal-to-noise ratio

$$d = \frac{E(W|H_1)}{\sqrt{VAR}}$$

$$= \frac{\sum_{n=1}^M a_n \int_0^{T-} \bar{f}(t) \bar{q}(t) dt}{\sqrt{\frac{NM}{2} \int_0^T \bar{q}^2(t) dt + M^2 \int_0^T \bar{q}(t) \int_0^T \bar{q}(u) R_B(t,u) du dt}} \quad (3.48)$$

and $\phi_c(g)$ is the complementary error function of the kind

$$\phi_d(g) = \frac{1}{\sqrt{2\pi}} \int_g^\infty e^{-v^2/2} dv \quad (3.49)$$

By setting a desired probability of false alarm, x may be determined from equation (3.46). The probability of detection is then determined by solving for d and using equation (3.47).

By substituting (3.41) and (3.42), and using (3.23), the numerator of d is

$$\sum_{n=1}^M a_n \int_0^T f(t) q(t) dt = \sum_{n=1}^M \frac{N}{2M} \sum_k \frac{|\bar{f}_k^*|^2}{\frac{N}{2M} + \lambda_k} \quad (3.50a)$$

while the denominator of d (see Appendix D) is

$$\sqrt{\text{VAR}} = \frac{N}{2M} \left[\sum_k \frac{|\bar{f}_k|^2}{\frac{N}{2M} + \lambda_k} \right]^{\frac{1}{2}} \quad (3.50b)$$

Therefore the effective signal-to-noise ratio is

$$d = \frac{1}{M} \sum_{n=1}^M \bar{a}_n \sqrt{\frac{2M}{N}} \left[\sum_k \frac{|\bar{f}_k|^2}{1 + \frac{2M}{N} \lambda_k} \right]^{\frac{1}{2}}. \quad (3.51)$$

Knowledge of d along with (3.46) and (3.47) completely specifies the performance of the threshold detector.

The equivalent signal-to-noise ratio for a target whose amplitude and position are known is easily shown to be

$$d' = \frac{1}{M} \sum_{n=1}^M a_n \sqrt{\frac{2M}{N}} \left[\sum_k |f_k(\vec{r}_0)|^2 \frac{1}{1 + \frac{2M}{N} \lambda_k} \right]^{\frac{1}{2}} \quad (3.52)$$

By letting the background be zero it will now be shown that d' reduces to the equivalent signal-to-noise ratio for a known signal in white Gaussian noise which is well known [Ref. 4].

The energy dissipated during one observation in a resistor of 1 ohm if the signal $a_n f(t, \vec{r}_0)$ is the voltage across that resistor is

$$\begin{aligned}
\underline{E}_n &= a_n^2 \int_0^T \sum_k^\infty f_k(\vec{r}_0) \phi_k(t) \sum_\ell^\infty f_\ell^*(\vec{r}_0) \phi_\ell^*(t) dt \\
&= a_n^2 \sum_k^\infty |f_k(\vec{r}_0)|^2 .
\end{aligned} \tag{3.53}$$

The voltage resulting from M observations then is

$$\sqrt{E} = \frac{1}{M} \sum_{n=1}^M \sqrt{E_n} = \frac{1}{M} \sum_{n=1}^M a_n \left[\sum_k^\infty |f_k(\vec{r}_0)|^2 \right]^{\frac{1}{2}} . \tag{3.54}$$

Substituting (3.54) in (3.52) with $\lambda_k = 0$,

$$d' = \sqrt{E} \sqrt{\frac{2M}{N}} = \sqrt{\frac{2E}{N}} \sqrt{M} ,$$

which shows the familiar result that detectability depends only upon the signal energy and the signal-to-noise ratio increases as the square root of the number of observations.

IV. THRESHOLD DETECTOR FOR ROTATING SYSTEM

In an infrared detection system the output voltage to be processed is obtained from a detector-preamplifier combination. The irradiance on the detector in W/cm^2 is converted to volts with a linear scale factor. The voltage output can be written as

$$v(t, \vec{r}_0) = KH(t, \vec{r}_0) \quad (4.1)$$

where $H(t, \vec{r}_0)$ is the irradiance on the detector from a target at position \vec{r}_0 , and K is a scale factor in (V/W/cm^2) . Also the covariance function may be written as

$$R_{vB}(\tau) = E[KB(t+\tau) KB(t)] = K^2 R_B(\tau), \quad (4.2)$$

where $B(t)$ is the irradiance on the detector due to a particular background scene. The output voltage due to this scene is

$$v_B = KB(t) \quad (4.3)$$

The problem now is to relate the detector-preamplifier output to the equations derived for the threshold detector.

It was shown in Part III that an optimum processor for weak signals was a threshold detector that performed a certain linear operation on the data. The linear filter was specified in terms of the eigenvalues and eigenfunctions of the integral equation (3.18), where the kernel $R_B(t, u)$ is the covariance function for the background.

In Part II, the covariance function was noted to be periodic. Rewriting (4.2) in terms of the output voltage

$$R_{vB}(t,u) = K^2 \sum_k^{\infty} \beta_k e^{jk\omega_0(t-u)} \quad (4.4)$$

Substituting (4.4) into integral equation (3.18), the solution for the eigenvalues and eigenfunctions is trivial with

$$\phi_k(t) = \frac{e^{jk\omega_0 t}}{\sqrt{T}}$$

and

$$\lambda_k = K^2 \beta_k T \quad (4.5)$$

where T is the nutation period.

The signal coefficients were also noted to be periodic and could be expanded in a Fourier series

$$v(t) = K \sum_k^{\infty} H_k(\vec{r}_0) e^{jk\omega_0 t} \quad (4.6)$$

Recognizing the similarity between equations (4.6) and (3.41), the signal coefficients for a known signal which is expanded using the basis set above become

$$f_k(\vec{r}_0) = KH_k(\vec{r}_0)\sqrt{T} \quad (4.7)$$

For the threshold detector, the signal is averaged with respect to an a priori density function for \vec{r}_0 . Averaging can be done with the coefficients to give

$$\begin{aligned}
\tilde{f}_k &= \int p(\vec{r}_o) f_k(\vec{r}_o) d\vec{r}_o \\
&= K\sqrt{T} \int H_k(\vec{r}_o) p(\vec{r}_o) d\vec{r}_o \\
&= K\sqrt{T} \bar{H}_k.
\end{aligned} \tag{4.8}$$

Using equation (2.10), the coefficients \bar{H}_k can be written as

$$\bar{H}_k = j^n \int d\vec{r}_o p(\vec{r}_o) \int N'(k, \vec{r}_o) \tau^*(\underline{k}) e^{-jn\phi} J_n \left(2\pi\rho \sqrt{k_x^2 + k_y^2} \right) d^2 \underline{k} \tag{4.9}$$

The transform of the radiance distribution from a target, $N'(k, \vec{r}_o)$ is a function of the target radiance, $R(\underline{k})$, the position of the target, \vec{r}_o , and the point spread function of the optics, $F_o(k)$. Rewriting (4.9),

$$\begin{aligned}
\bar{H}_k &= j^n \int d^2 \underline{k} R(\underline{k}) \tau^*(\underline{k}) J_n \left(2\pi\rho \sqrt{k_x^2 + k_y^2} \right) e^{-jn\phi} \\
&\quad \int d\vec{r}_o p(\vec{r}_o) e^{-j2\pi \underline{k} \cdot \vec{r}_o}
\end{aligned} \tag{4.10}$$

If the density function, $p(\vec{r}_o)$, is assumed Gaussian with a standard deviation p_o , then the averaged coefficients become

$$\bar{H}_k = j^n \int R(\underline{k}) e^{-2\pi p_o^2 (k_x^2 + k_y^2)} \tau^*(\underline{k}) e^{-jn\phi} J_n \left(2\pi\rho \sqrt{k_x^2 + k_y^2} \right) d^2 \underline{k}. \tag{4.11}$$

The Gaussian assumption on \vec{r}_o is reasonable because \vec{r}_o often represents a pointing error from some designated target position. Then p_o describes the accuracy of the pointing mechanism. Substituting (4.8) into (3.42), the filter function for the threshold detector becomes

$$\bar{q}(t) = K \sum_k \bar{H}_k \sqrt{T} \left(\frac{1}{1 + \frac{2M}{N} K^2 \beta_k T} \right) \frac{e^{jk\omega_o t}}{\sqrt{T}} \tag{4.12}$$

Rewriting the equivalent signal-to-noise ratio in terms of equations (4.8) and (4.12) one has

$$d = \frac{M \sum_{n=1}^M \bar{a}_n \sqrt{T} \sqrt{M}}{\sqrt{N/2}} \left[\sum_k |\bar{H}_k|^2 \frac{1}{1 + \frac{MTK^2 \beta_k}{N/2}} \right]^{\frac{1}{2}} \quad (4.13)$$

It will be shown in Part V that β_k may be represented as

$$\beta_k = \sigma_B^2 \Omega^2 Q_k$$

where σ_B^2 is the amplitude of the background noise correlation function, Ω^2 is the instantaneous field-of-view of the detector and Q_k is an integral function of the optical and detector parameters and correlation length of the background radiance.

Define the following terms:

$$\text{Signal-to-noise ratio (SNR)} = \frac{K \frac{1}{M} \sum_{n=1}^M \bar{a}_n \sqrt{T}}{\sqrt{N/2}} \quad (4.14a)$$

$$\text{Background-to-noise ratio (BNR)} = \frac{\sigma_B^2 \Omega K \sqrt{T}}{\sqrt{N/2}} \quad (4.14b)$$

Using (4.14a) and (4.14b), d may be rewritten as

$$d = \text{SNR} \sqrt{M} \left[\sum_k |\bar{H}_k|^2 \frac{1}{1 + MQ_k \text{BNR}^2} \right]^{\frac{1}{2}} \quad (4.15)$$

Noise equivalent irradiance (NEI) may be defined at the detector-preamplifier output to be

$$K \cdot NEI = \sqrt{\frac{N}{2} \cdot 2B_w} = \sqrt{NB_w} \quad (4.16)$$

where B_w is the detector-preamplifier bandwidth.

The SNR and BNR may now be written in terms of the NEI as

$$\sqrt{M} \text{ SNR} = \frac{\langle a \rangle \sqrt{NTB}}{NEI} = \text{SNR}' \sqrt{NTB}$$

where NTB is number-time-bandwidth product and

$$\sqrt{M} \text{ BNR} = \frac{\sigma_B}{NEI} \sqrt{NTB} = \text{BNR}' \sqrt{NTB}.$$

Expressing d in terms of NEI one has

$$d = \text{SNR}' \sqrt{NTB} \sum_k^\infty |H_k|^2 \left[\frac{1}{1 + Q_k \text{ NTB BNR}'^2} \right]^{\frac{1}{2}}. \quad (4.17)$$

V. SOLUTION FOR RECTANGULAR DETECTOR

The equations in Part II for the detector-preamplifier output voltage and the correlation function of the background must be solved to obtain the filter function and specify the detection system performance.

The two general equations obtained in Part II are

$$H_n(\vec{r}_0) = j^n \int R(k) e^{-j\pi \vec{k} \cdot \vec{r}_0} \vec{F}_0(\vec{k}) \tau^*(\vec{k}) e^{-jn\phi} J_n \left(2\pi \rho \sqrt{k_x^2 + k_y^2} \right) d^2 \vec{k} .$$

where $H_n(\vec{r}_0)$ is the n^{th} Fourier series coefficient for the radiation on the spatial filter and

$$\beta_n = \int |\tau(\vec{k})|^2 |F_0(\vec{k})|^2 W_B(\vec{k}) J_n^2 \left(2\pi \rho \sqrt{k_x^2 + k_y^2} \right) d^2 \vec{k}$$

where B_n is the n^{th} coefficient of the background correlation function at the spatial filter.

A rectangular shaped detector was chosen for the calculations because it exhibited the simplest form of the equations. For circular nutation the filter is represented graphically in Figure 5.1.

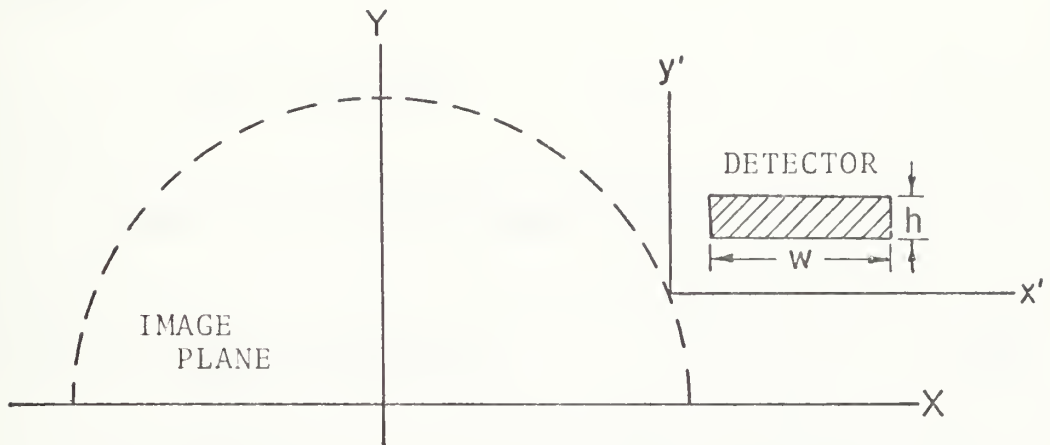


Figure 5.1. Nutation with Rectangular Detector.

If the detector function is given by

$$\tau(x', y') = \begin{cases} 1 & x_o - w/2 \leq x' \leq x_o + w/2 \\ & y_o - h/2 \leq y' \leq y_o + h/2 \\ 0 & \text{otherwise} \end{cases}$$

then its transform is

$$\tau(k_x, k_y) = \frac{e^{-j2\pi(k_x x_o + k_y y_o)}}{\pi^2 k_x k_y} \sin(\pi k_x w) \sin(\pi k_y h)$$

so that

$$|\tau(k)|^2 = \frac{\sin^2(\pi k_x w)}{\pi^2 k_x^2} \frac{\sin^2(\pi k_y h)}{\pi^2 k_y^2} . \quad (5.1)$$

The point spread function of the optics is assumed to be Gaussian:

$$f_o(\tilde{r}) = \frac{1}{2\pi\sigma^2} e^{-\frac{|\tilde{r}|^2}{2\sigma^2}}$$

Its transform is

$$F_o(\tilde{k}) = e^{-2\pi^2\sigma^2(k_x^2+k_y^2)} \quad (5.2)$$

The correlation of the background radiance is assumed to be of the form

$$\phi_B(x,y) = \sigma_B^2 e^{-\alpha|x|} e^{-\beta|y|} \quad (5.3a)$$

where α^{-1} and β^{-1} are the correlation lengths in the x- and y- directions, respectively. The Wiener spectrum is the Fourier transform of ϕ_B :

$$W_B(\tilde{k}) = \sigma_B^2 \frac{2\alpha}{\alpha^2 + (2\pi k_x)^2} \frac{2\beta}{\beta^2 + (2\pi k_y)^2} \quad (5.3b)$$

Substituting (5.1), (5.2) and (5.3b) into (2.10), the radiance from a point target becomes

$$\begin{aligned} H_n(\vec{r}_o) &= j^n \int e^{-j2\pi(k_x r_x + k_y r_y)} e^{-2\pi^2\sigma^2(k_x^2+k_y^2)} \\ &\quad \cdot e^{j2\pi(k_x x_o + k_y y_o)} \frac{\sin\pi k_x w}{\pi k_x} \frac{\sin\pi k_y h}{\pi k_y} \\ &\quad e^{-jn \tan^{-1}(k_y/k_x)} J_n \left(2\pi\rho \sqrt{k_x^2+k_y^2} \right) dk_x dk_y. \end{aligned} \quad (5.4)$$

Letting

$$u_x = \sqrt{2}\pi\sigma k_x$$

$$u_y = \sqrt{2}\pi\sigma k_y$$

equation (5.4) becomes

$$\begin{aligned}
 H_n(\vec{r}_0) = & \frac{j^n}{\pi^2} \int e^{-(u_x^2 + u_y^2)} \\
 & \cdot e^{-j \frac{\sqrt{2}}{\sigma} [(r_x - x_0)u_x + (r_y - y_0)u_y]} \\
 & e^{-jn \tan^{-1}(u_y/u_x)} J_n \left(\frac{\sqrt{2}\rho}{\sigma} \sqrt{u_x^2 + u_y^2} \right) du_x du_y \quad (5.5)
 \end{aligned}$$

If \vec{r}_0 is random, the radiance from a target may be averaged with respect to the density function $p(\vec{r}_0)$ as shown in Part IV. In particular, if \vec{r}_0 is Gaussian distributed, with standard deviation p_0 the averaged coefficients become

$$\begin{aligned}
 \bar{H}_n = & j^n \int e^{-2\pi^2 \gamma^2 (k_x^2 + k_y^2)} e^{j2\pi(k_x x_0 + k_y y_0)} \\
 & \frac{\sin \pi k_x w}{\pi k_x} \frac{\sin \pi k_y h}{\pi k_y} e^{-jn \tan^{-1}(k_y/k_x)} \\
 & J_n \left(2\pi\rho \sqrt{k_x^2 + k_y^2} \right) dk_x dk_y \quad (5.6)
 \end{aligned}$$

where

$$\gamma^2 = p_0^2 + \sigma^2.$$

Letting

$$u'_x = \sqrt{2}\pi\gamma k_x$$

$$u'_y = \sqrt{2}\pi\gamma k_y$$

equation (5.6) becomes

$$\bar{H}_n = \frac{j^n}{\pi^2} \int e^{-(u_x'^2 - u_n'^2)} e^{j \frac{\sqrt{2}}{\gamma} (u_x' x_o + u_y' y_o)} e^{-jn \tan^{-1}(u_x'/u_y')} \cdot J_n \left(\frac{\sqrt{2}\rho}{\gamma} \sqrt{u_x'^2 + u_y'^2} \right) du_x' du_y' \quad (5.7)$$

And finally substituting equations (5.1), (5.2) and (5.3b) into equation (2.22), the correlation coefficients become

$$\beta_n = \int e^{-4\pi^2 \sigma^2 (k_x^2 + k_y^2)} \frac{\sin^2(\pi k_x w)}{(\pi k_x)^2} \frac{\sin^2(\pi k_y h)}{(\pi k_y)^2} \sigma_B^2 \frac{2\alpha}{\alpha^2 + (2\pi k_x)^2} \frac{2\beta}{\beta^2 + (2\pi k_y)^2} J_n^2 \left(2\pi\rho \sqrt{k_x^2 + k_y^2} \right) dk_x dk_y \quad (5.8)$$

Letting

$$u_x'' = 2\pi\rho k_x$$

$$u_y'' = 2\pi\rho k_y$$

equation (5.8) becomes

$$\beta_n = \frac{\sigma_B^2 \Omega^2 \alpha \beta \sigma^2}{\pi^2} \int e^{-u_x'^2 - u_y'^2} \left(\frac{\sin \frac{w}{\sqrt{2}\sigma} u_x'}{\frac{w}{\sqrt{2}\sigma} u_x''} \right)^2 \left(\frac{\sin \frac{h}{\sqrt{2}\sigma} u_y'}{\frac{h}{\sqrt{2}\sigma} u_y''} \right)^2 \frac{1}{(\alpha\sigma)^2 + u_x'^2} \frac{1}{(\beta\sigma)^2 + u_y'^2} J_n^2 \left(\frac{\rho}{\sigma} \sqrt{u_x''^2 + u_y''^2} \right) du_x'' du_y'' \quad (5.9)$$

where

$$\Omega^2 = w^2 h^2. \quad (5.9)$$

The integrals in (5.5), (5.7) and (5.9) were difficult to evaluate. Although the components of the integrand are relatively simple functions, the argument of the Bessel function prohibited separating the integral into two one-dimensional integrals. No closed form solutions were found so the integrals were evaluated numerically. The numerical method used is based on work by Pierce [9] who applied Gaussian quadrature formulas to two dimensional integration by integrating over a planar annulus in the (x,y) plane.

Gaussian quadrature formulas are a means of evaluating the integral by summing weighted values of the integrand at specific points. For the one dimensional case,

$$\int_a^b g(x)dx = \int_a^b w(x)f(x)dx \quad (5.10)$$

where $g(x)$ is the integrand to be integrated and $w(x)$ is a weight function for which the specific integration was derived. For well behaved functions the integral may be evaluated as

$$\int_a^b g(x)dx = \sum_{i=1}^m A_i f(x_i) + \text{error} \quad (5.11)$$

where the x_i 's are the m zeros of the m^{th} polynomial

$$P_m(x) = \prod_{i=1}^m (x-x_i)$$

of the set of polynomials mutually orthogonal on the interval $[a,b]$ with respect to the weight function $w(x)$. The weights are given by

$$A_i = \int_a^b w(x) L_i(x) dx \quad (5.13)$$

where $L_i(x) = P_m(x)/[(x-x_i)P'_m(x_i)]$ is the Lagrange interpolation coefficient.

For a weight function $w(x)$ and interval $[a,b]$ the polynomial $P_m(x)$ and its zeros x_i and weight factors A_i need be computed only once. For a number of weight functions and intervals the set of orthogonal polynomials is known. Stroud and Secrest [13] give x_i 's and A_i 's for a variety of weight functions and intervals. The degree of the formula determines the number of x_i 's and A_i 's. A $2M-1$ degree formula will have M points and is exact for polynomial integrands of degree $2M-1$ or less.

Pierce applied Gaussian quadrature integration to two dimensions where the solution is of the form

$$\iint g(x,y) dx dy \approx \sum_i \sum_j D_{ij} g(x_{ij}, y_{ij})$$

The integration is over an annulus in the x,y plane with inner radius R and outer radius 1 . Rewriting the integral in polar coordinates

$$\int_R^1 \int_0^{2\pi} r G(r, \theta) d\theta dr \approx \sum_i \sum_j D_{ij} G(r_j, \theta_i) \quad (5.14)$$

Pierce showed the summation could be rewritten as

$$\sum_{i=1}^{4(m+1)} \sum_{j=1}^{m+1} A_i B_j G(r_i \cos \theta_j, r_i \sin \theta_j) \quad (5.15)$$

where A_i and B_j are the weights for the radial and angular directions respectively and $4M+3$ is the degree of accuracy.

For an arbitrary annulus the formula may be obtained by rewriting equation (5.14)

$$I = \int_0^{2\pi} \int_{r_1}^{r_2} f(r, \theta) r dr d\theta \quad (5.16)$$

and letting

$$\rho = \frac{r}{r_2}$$

$$I = r_2^2 \int_0^{2\pi} \int_{r_1/r_2}^1 \rho f(r_2 \rho, \theta) d\rho d\theta. \quad (5.17)$$

The approximate solution can be derived as

$$I = \sum_{i=1}^{4(m+1)} \sum_{j=1}^{m+1} A_i B_j f \left(\sqrt{r_1^2 + \sigma_j^2 (r_2^2 - r_1^2)}, \theta_i \right) \quad (5.18)$$

where

$$A_i = 2\pi/4(m+1)$$

and

$$B_j = w_j (r_2^2 - r_1^2)/2, \quad w_j = \text{weight}$$

$M+1$ is the order of the orthogonal polynomial, in this case the Legendre polynomial on the interval $(0,1)$ and σ_j 's are the zeros of this polynomial. This type of formula is known as a spherical product Gauss formula [12].

The annuli were picked at radii corresponding to the zeros of $J_0(z)$ because $J_0(z)$ is the fastest damping component

of the integrands. One additional annulus inside the first zero was found necessary to account for the $\frac{1}{\alpha+x^2}$ term when α is small and x (and y) approach zero. The distances between annuli outside the first five to eight zeros were found not to be critical and thus spaced arbitrarily.

The Gaussian Quadrature formula used was a Gauss-Legendre 24-point formula as listed in [13] thus giving a degree of accuracy of 99. The integration is limited to only the first quadrant as mentioned below. Thus for a 24-point formula, $(M+1)^2$ or 576 points per annulus were used to evaluate the integral.

The expression for β_n is easily seen to be an even function both radially and about both planer axes, therefore, only integration over the first quadrant was necessary. With a little more difficulty, $H_n(\vec{r}_0)$ and \bar{H}_n can be shown (see Appendix E) to exhibit the same property provided one expression is used for even n and another for odd n . By calculating only over the first quadrant computer time was considerably shortened.

In order to solve for coefficients of arbitrary order, the Bessel functions of that order must first be obtained. The available library subroutines were found inadequate for this use for two reasons. First, these routines have an upper limit of 100 on the order of the Bessel function that can be computed and second, the routine had to be called for each individual order.

The recursive relation

$$J_n(y) = \frac{2n}{y} J_{n+1}(y) - J_{n+2}(y) \quad (5.19)$$

provides a basis for generating an array of Bessel functions of various orders. However for accuracy $J_{n+1}(y)$ and $J_{n+2}(y)$ must be known.

The most accurate method to numerically calculate Bessel functions of various orders and arguments was found to be a uniform asymptotic expansion involving Airy functions [1]:

$$J_n(nz) \approx \left(\frac{4\Delta}{1-z} \right)^{\frac{1}{4}} \left\{ \frac{A_i(n^{2/3}\Delta)}{n^{1/3}} \sum_{k=0}^{\infty} \frac{a_k(\Delta)}{n^{2k}} + \frac{A'_i(n^{2/3}\Delta)}{n^{5/3}} \sum_{k=0}^{\infty} \frac{b_k(\Delta)}{n^{2k}} \right\} \quad (5.20)$$

where A_i and A'_i are two types of Airy functions and

$$\frac{2}{3} \Delta^{3/2} = \ln \left\{ \left(1 + \left| \sqrt{1-z^2} \right| / z \right) \right\} - \sqrt{1-z^2} \quad z < 1$$

$$a_0(\Delta) = 1$$

$$b_0(\Delta) = -5/48 \Delta^2 + \frac{1}{\sqrt{\Delta}} \left\{ \frac{5}{24(1-z^2)^{3/2}} - \frac{1}{8(1-z^2)^{1/2}} \right\} \quad z < 1$$

$$\left. \begin{aligned} a_k(\Delta) &<< a_0(\Delta) \\ b_k(\Delta) &<< b_0(\Delta) \end{aligned} \right\} \quad k > 1 \quad (5.21)$$

The Airy functions are calculated using the equations

$$A_i(x) = \frac{1}{2} x^{-1/2} e^{-\delta} f(-\delta)$$

and

$$A'_i(x) = -\frac{1}{2} x^{1/4} e^{-\delta} g(-\delta)$$

where

$$\delta = \frac{2}{3} x^{3/2} \quad (5.22)$$

and

$$x = n^{2/3} \Delta$$

The functions $f(-\delta)$ and $g(-\delta)$ are tabulated and linear interpolation is used to determine their values. Δ is guaranteed to always be positive if n is selected to be larger than the argument.

By picking an order much higher than the argument, v , and J_{v-1} , using the asymptotic expansion, the recursive relationship (5.19) may be used to generate an array of successive orders of the Bessel function down to and including J_0 . However, error builds up rapidly using this method. A second relation

$$1 = J_0(y) + 2J_2(y) + 2J_4(y) + \dots \quad (5.23)$$

may be used to generate a normalizing factor

$$C = 1/[J_0(y) + 2J_2(y) + 2J_4(y) + \dots] \quad (5.4)$$

Multiplying each Bessel function value generated in the recursive relation by C resulted in very accurate values being obtained. The computer program used to solve the equations is listed as Appendix H.

To evaluate the numerical results a check was used which summed the coefficients and compared this summation to an analytic expression for a sum that could easily be solved numerically.

For a particular phase angle of the nutation cycle, $\omega_0 t$, the radiance function for a target is

$$H(\omega_0 t) = \sum_k^\infty H_k(\vec{r}_0) e^{jk\omega_0 t} \quad (5.25)$$

For a point target and a rectangular, circularly nutating detector

$$H(\omega_0 t) = \int e^{-2\pi^2 \sigma^2 k_x^2} \frac{\sin \pi w k_x}{\pi k_x} e^{j2\pi k_x (\rho \cos \omega_0 t - (r_x - x_0))} dk_x \\ \cdot \int e^{-2\pi^2 \sigma^2 k_y^2} \frac{\sin \pi h k_y}{\pi k_y} e^{j2\pi k_y (\rho \sin \omega_0 t - (r_y - y_0))} dk_y \quad (5.26)$$

which has the solution (see Appendix F)

$$H(\omega_0 t) = \frac{1}{4} \left[F_1(r_x, x_0, w) - F_1(r_x, x_0, -w) \right] \left[E_2(r_y, y_0, h) - E_2(r_y, y_0, -h) \right]$$

where

$$E_1(r, z, \alpha) = \text{Erf} \left[\frac{r - z - \rho \cos \omega_0 t}{\sqrt{2}\sigma} + \frac{\alpha}{2\sqrt{2}\sigma} \right]$$

$$E_2(r, z, \alpha) = \text{Erf} \left[\frac{r - z - \rho \sin \omega_0 t}{\sqrt{2}\sigma} + \frac{\alpha}{2\sqrt{2}\sigma} \right]$$

and Erf is the error function

$$\text{Erf}(x) = \frac{2}{\sqrt{\pi}} \int_0^x e^{-u^2} du \quad (5.27)$$

By evaluating the analytic expression at the phase instant ($\omega_0 t$) that the detector crosses the target and comparing

it against equation (5.27) for an appreciably high n , a reasonable check was made on the accuracy of the individual signal coefficients.

For the coefficients averaged over \vec{r}_0 , the check was made at $\omega_0 t = 0$ where

$$H(0) = \sum_k^{\infty} \bar{H}_k \quad (5.28)$$

and the analytic expression is

$$H(0) = \frac{1}{4} \left[E_1(r_x, k_0, w) - E_1(r_x, x_0, -w) \right] \left[E_3(r_y, y_0, h) - E_3(r_y, y_0, h) \right]$$

where

$$E_3(r, z, \alpha) = E_2(r, z, \alpha) \Big|_{\omega_0 t=0} \quad (5.29)$$

The rms background voltage was used to check the coefficients in the correlation function. The mean square voltage is

$$\bar{e}_B^2 = E\{B^2(t)\} = R_B(0) = \sum_k^{\infty} \beta_k \quad (5.30)$$

Appendix B shows that the correlation function may be written as

$$R_B(\tau) = \int |\tau(\tilde{k})|^2 W_B'(\tilde{k}) J_0 \left(4\pi \rho \tilde{k} \sin \frac{\omega_0 \tau}{2} \right) d^2 \tilde{k} \quad (16B)$$

Substituting (5.1), (5.2), and (5.36) in (16B) and evaluating at $\tau = 0$

$$\begin{aligned} \bar{e}_B^2 = & \sigma_B^2 \alpha \int \frac{\sin^2(\pi k_x w)}{(\pi k_x)^2} \frac{e^{-4\pi^2 \sigma^2 k_x^2}}{\alpha^2 + (2\pi k_x)^2} dk_x \\ & \cdot \sigma_B^2 \beta \int \frac{\sin^2(\pi k_y h)}{(\pi k_y)^2} \frac{e^{-4\pi^2 \sigma^2 k_y^2}}{\beta^2 + (2\pi k_y)^2} dk_y . \end{aligned} \quad (5.31)$$

It can be shown (see Appendix F) that an analytic expression is

$$\bar{e}_B^2 = 4\alpha\beta\sigma_B^2 R(w;\alpha) R(h;\beta)$$

where

$$\begin{aligned} R(\mu, \alpha) = & \frac{\mu}{\alpha^2} \left\{ 1 - \text{Erfc} \left(\frac{2\mu}{\sigma} \right) - \frac{2\sigma}{\sqrt{\pi}\mu} \left[1 - e^{-\left(\frac{\mu}{2\sigma}\right)^2} \right] \right\} \\ & + \frac{e^{\alpha^2 \sigma^2}}{2\alpha^3} \left[e^{\alpha\mu} \text{Erfc} \left(\alpha\sigma + \frac{\mu}{2\sigma} \right) \right. \\ & \left. + e^{-\alpha\mu} \text{Erfc} \left(\alpha\sigma - \frac{\mu}{2\sigma} \right) - 2\text{Erfc}(\alpha\sigma) \right] \end{aligned} \quad (5.32)$$

and Erfc is the complimentary error function

$$\text{Erfc}(x) = \frac{2}{\sqrt{\pi}} \int_x^\infty e^{-u^2} du . \quad (5.33)$$

The computer program used to solve equations (5.6), (5.7) and (5.9) and calculate the infinite summations is listed as Appendix H.

VI. NUMERICAL RESULTS

Numerical results constitute solving for the signal and background coefficients and using these coefficients to specify the form of the filter to be used in the threshold detector as well as to calculate the probability of detection as a function of signal-to-noise ratio (SNR), background-to-noise ratio (BNR) and number of nutations (M) used to make the decision. The probability of detection is determined for the averaged equivalent signal-to-noise ratio and for specific point targets.

Many different values for system parameters and target locations were used to compute the coefficients. A typical set of parameters is¹:

```

    nutation radius = 15
    width of detector = 30
    height of detector = 1
    blur circle standard deviation = .5
    background correlation length x-direction = 20
    background correlation length y-direction = 20
    position of detector in detector coordinate system
        x direction = 15
        y direction = 0
    target coordinates (if desired)
        x direction = 0
        y direction = 0
    pointing error standard deviation = 7.5
```

A detector utilizing the parameters above would trace out the area in the image plane shown in Figure 6.1.

¹All units are in milliradians.

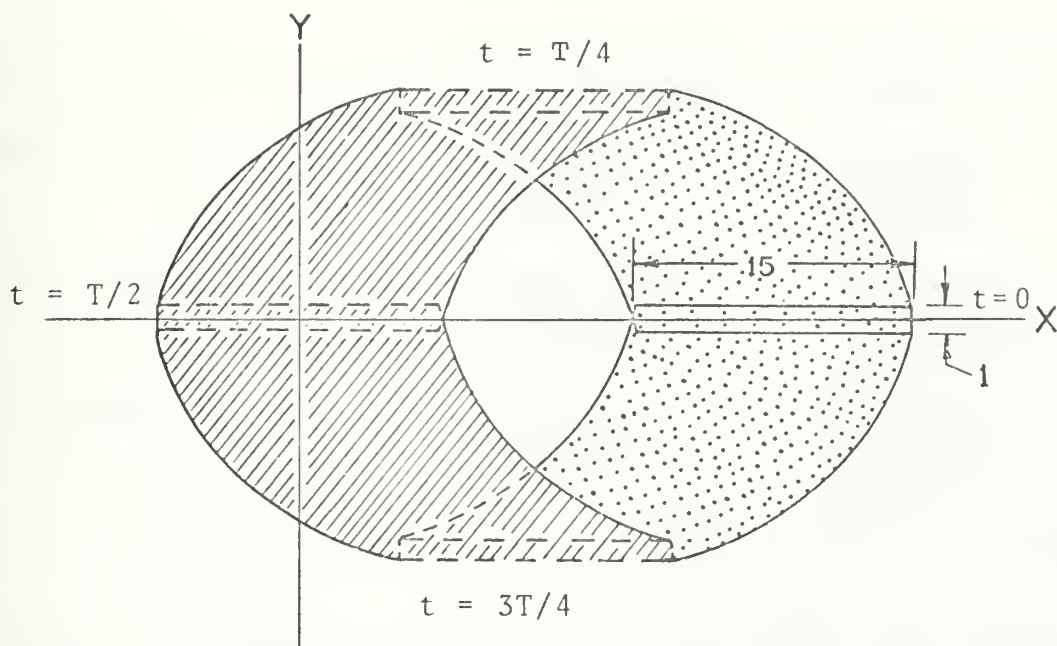


Figure 6.1. Scanned Area of Nutating Detector.

This type scan was chosen because it crossed the center of the coordinate system which would be the center of the target blur circle for zero pointing error. Also, in the case of a random pointing error in the absence of bias zero mean is the center of the coordinates. This is important because the threshold detector design is based on a Gaussian pointing error with zero mean.

A sample calculation of 121 coefficients using the parameters above is listed in Appendix G. The equations shown in Part V were used to check the accuracy of the coefficients. Table 6.1 lists typical values for the summation of 121 coefficients for various sets of parameters and the calculated summation values.

TABLE 6.1

	<u>Calculated Sum</u>	<u>Actual Sum</u>
Signal (point target)	.6826894 .6826895 .5438002	.6826993 .6826994 .5438087
Signal (averaged)	.2990664D-6 .2328138D-4 .2651595D-1	.2991232D-6 .2328142D-4 .2651595D-1
Background	.6013477 .2347420 .8335525	.6012230 .2347420 .8319764

Besides the general shapes of the background and signal spectra, variations in the spectra due to detector size, background correlation lengths and coordinates of the detector are of interest. Curves in the following figures show the effects of these variations.

Figures 6.2 through 6.5 show the envelope of the one side of the two-sided background power spectral density

$$S_B(\omega) = \sum_k^{\infty} \beta_k \delta(\omega - k\omega_0)$$

where ω_0 is normalized to 2π . The curves of Figures 6.2 and 6.3 illustrate the effect of varying the background correlation lengths. In Figure 6.2 the correlation lengths are the same in both x- and y-directions. Practical measurements, however, indicate that correlation lengths in the horizontal (x-) direction may be longer than in the vertical (y-) direction. The curves in Figure 6.3 are for this case.

The curves of Figure 6.4 and 6.5 relate the spectrum to changes in size of the detector. In Figure 6.4, only the detector with BNR equal to 9 and number of nutations equal to 100 are shown in Figures 6.11 through 6.13. Each figure shows the envelope of one side of a double sided spectrum. Two cases are considered. First, threshold detection systems designed for different Gaussian pointing errors but with the same size detector are shown in Figures 6.11 and 6.12 and second, detection systems designed for the same pointing error but utilizing different size detectors are shown in Figures 6.12 and 6.13.

The curves shown in Figures 6.14 through 6.16 show the matched filter to a particular point target located within the scan. Notice each of the filters exhibits a band pass characteristic. This is because of the additional noise component (background). The oscillations observed in the point target spectra of Figures 6.6 to 6.8 have been suppressed to provide a look at realizable filters.

The probability of detection for the threshold detector was shown in Part IV to be

$$Q_d = \text{SNR} \sqrt{M} \left[\sum_k^{\infty} |\bar{f}_k|^2 \frac{1}{1 + MQ_k \text{BNR}^2} \right]^{\frac{1}{2}}$$

Figures 6.17 through 6.20 show Q_d as a function of SNR, BNR and M.

The probabilities of detection for point targets located at specific points in the scan have also been plotted. The probability of detection for a specific point target is shown as the

width of the detector is varied. As width is increased, so is the area scanned by the detector. Figure 6.5 shows the difference in spectra between a rectangular detector and a square detector which have approximately the same surface area. It should be obvious however that the rectangular detector scans much more area per nutation than a square detector of identical surface area.

The envelopes of signal coefficients (magnitude only) for a point target are plotted in Figures 6.6 through 6.8. Phase information depends only on the location of the target relative to the initial point for the nutation cycle which is along the x axis. This has not been plotted. Changes in the magnitude due to changes in detector size are shown.

Figures 6.9 and 6.10 show the envelopes of coefficients for the signal that is averaged with respect to a Gaussian pointing error. The bandwidth of the averaged signal is much less than a point target as expected. The figures show the spectra for two different standard deviations of pointing error.

Matched filters (magnitude only) for the threshold

$$Q'_d = \text{SNR}' \sqrt{M} \frac{\sum_k f_k(\vec{r}_0) \bar{f}_k^* \frac{1}{1+MQ_k \text{BNR}^2}}{\left[\sum_k |\bar{f}_k|^2 \frac{1}{1+MQ_k \text{BNR}^2} \right]^{1/2}}$$

where

$$\text{SNR}' = \frac{1}{M} \sum_{n=1}^M a_n \sqrt{T} / \sqrt{\frac{N}{2}}$$

Figures 6/21 through 6/24 show Q'_d as a function of SNR', BNR and M.

The parameters of the nutating optical system have been varied to show their effect on Q_d and Q'_d .

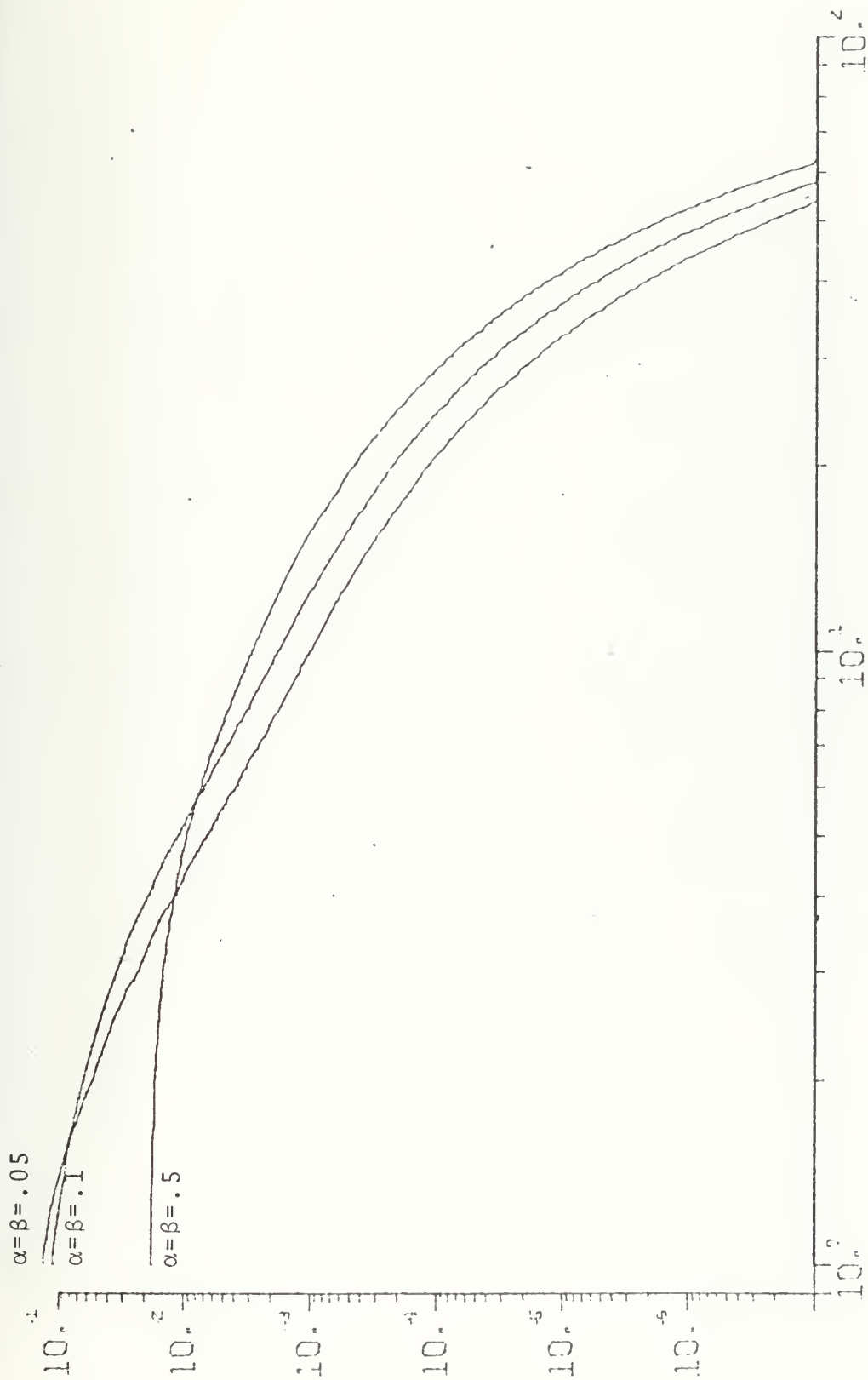


Figure 6.2. Background Power Spectral Density vs. Frequency (Hz).
 Detector parameters: $\text{RHO}=10$, $\text{SIG}=.5$, $w=10$, $h=1$

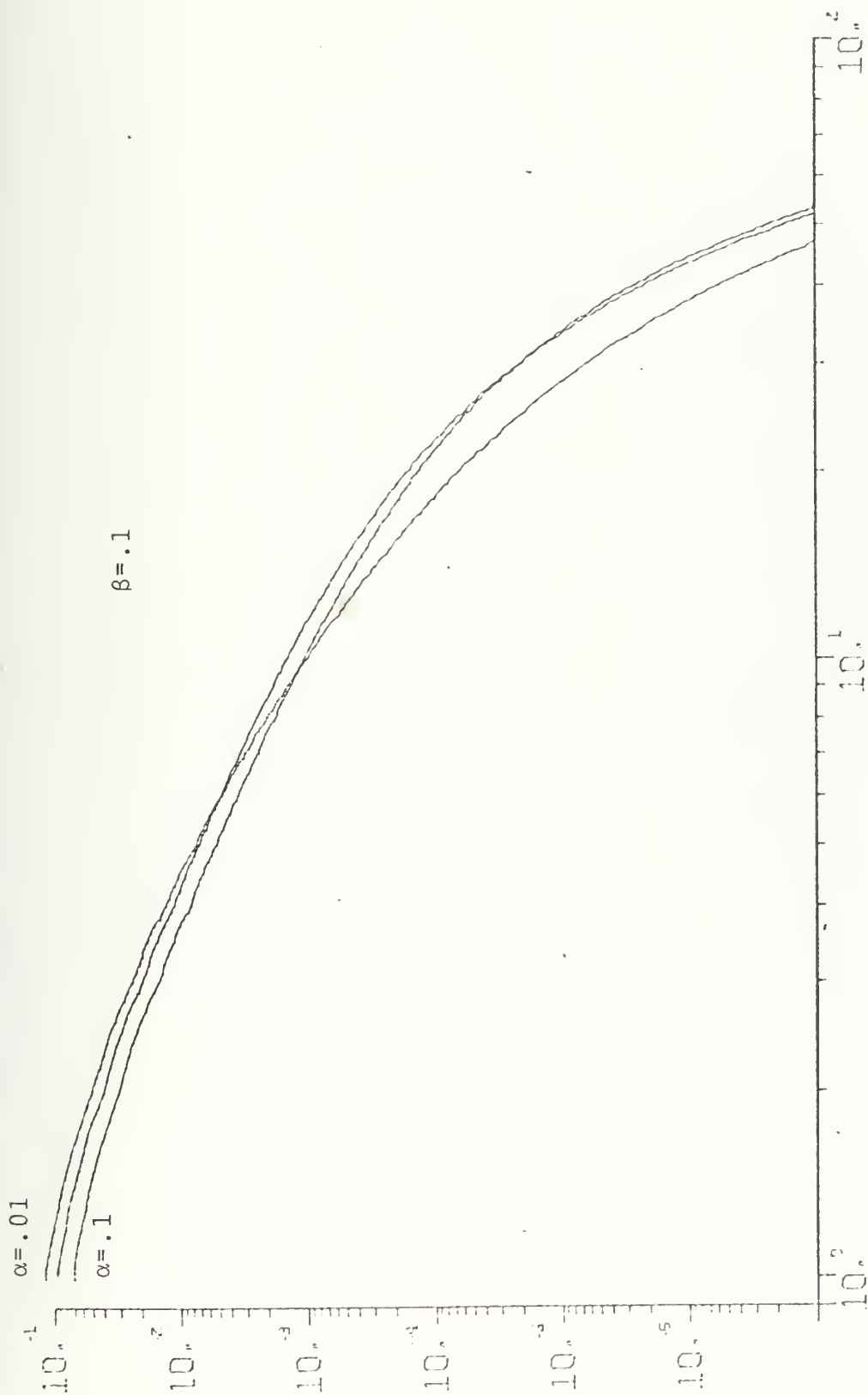


Figure 6.3. Background Power Spectral Density vs. Frequency (Hz).
Detector parameters: $\text{RHO}=15$, $\text{SIG}=.5$, $w=30$, $h=1$

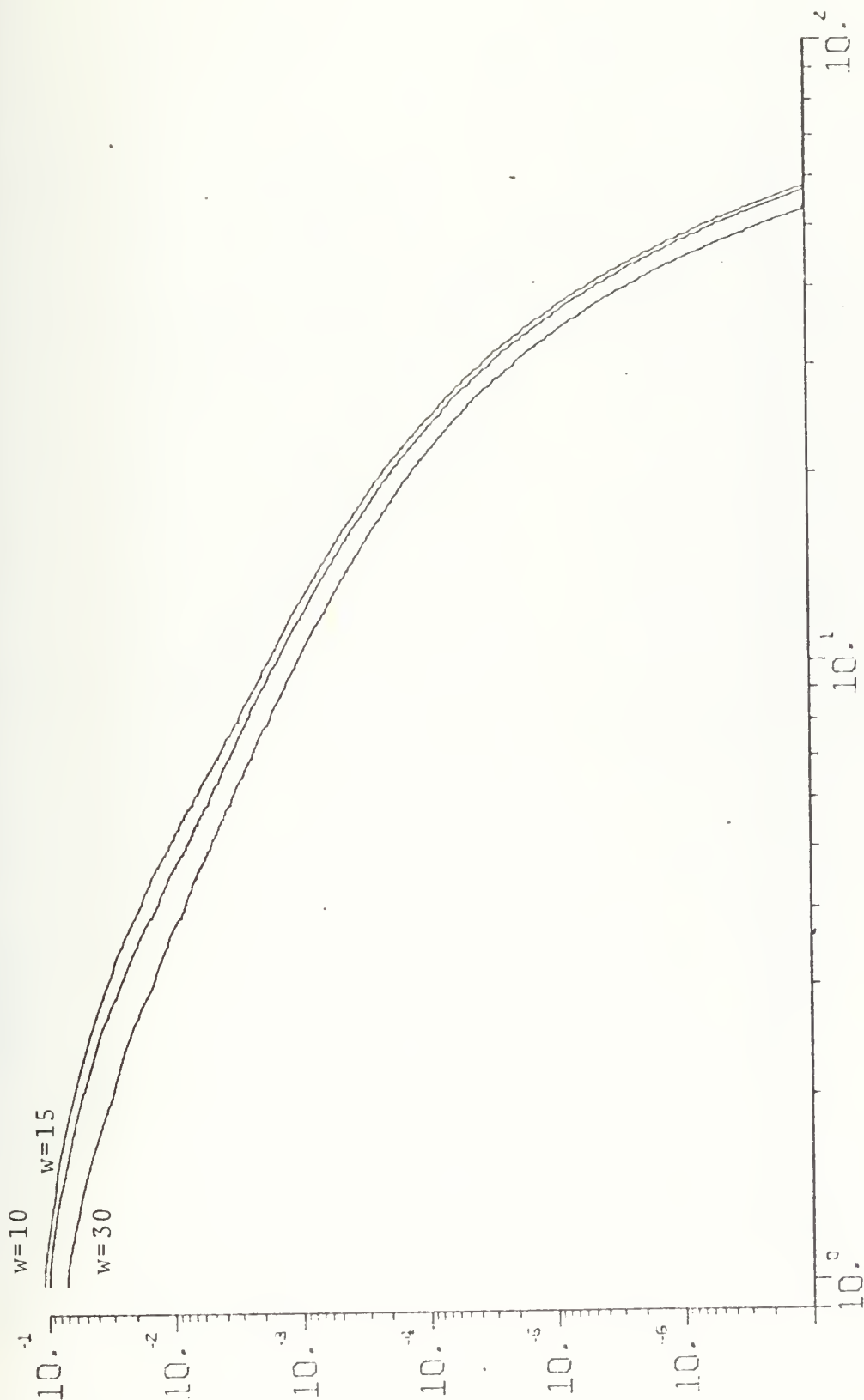


Figure 6.4. Background Power Spectral Density vs. Frequency (Hz).

Common detector parameters: $\text{RHO}=15$, $\text{SIG}=.5$, $h=1$

Background parameters: $\alpha=\beta=.1$

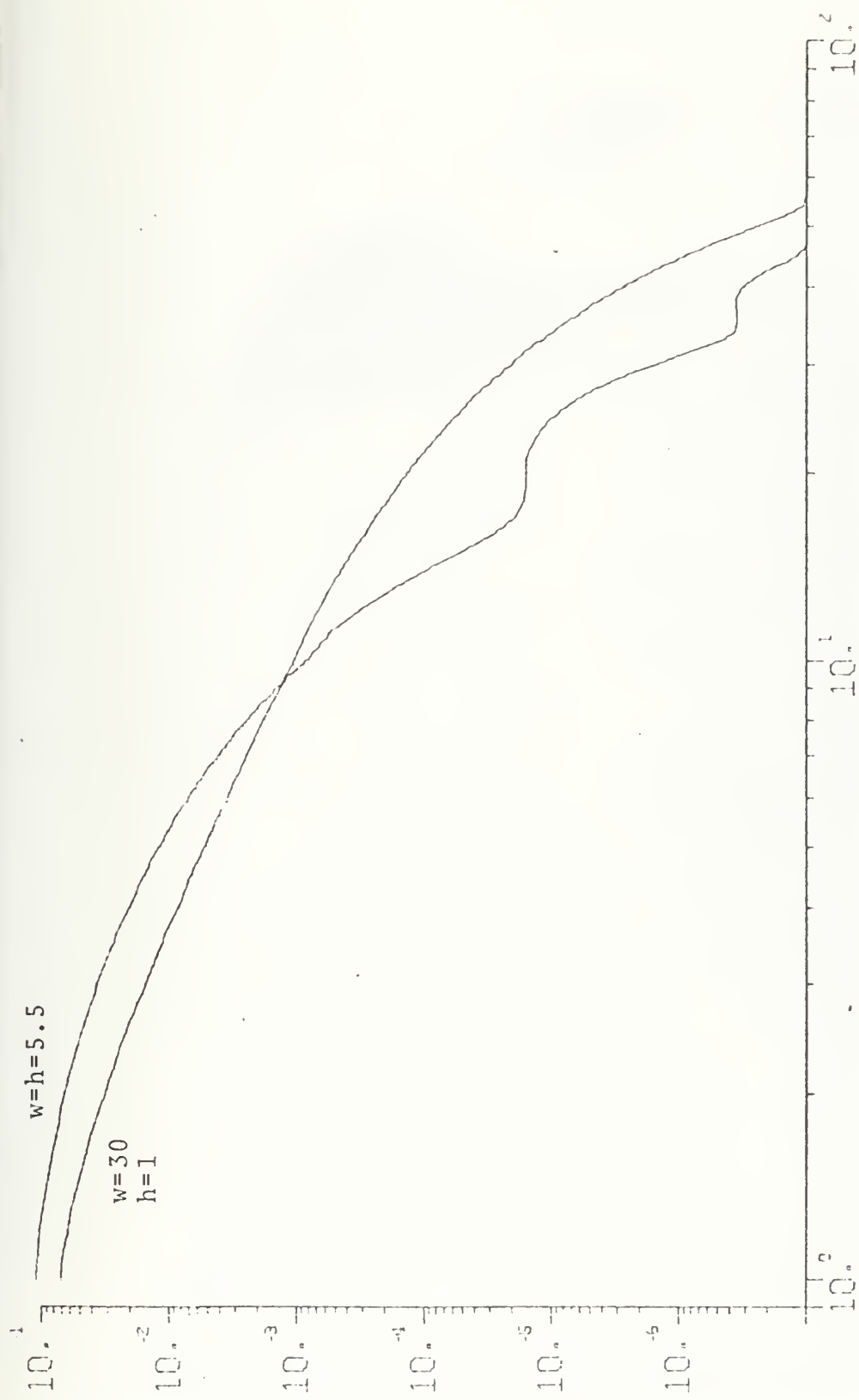


Figure 6.5. Background Power Spectral Density vs. Frequency (Hz)
 Common detector parameters: $\text{RHO}=15$, $\text{SIG}=.5$
 Background parameters: $\alpha=\beta=.1$

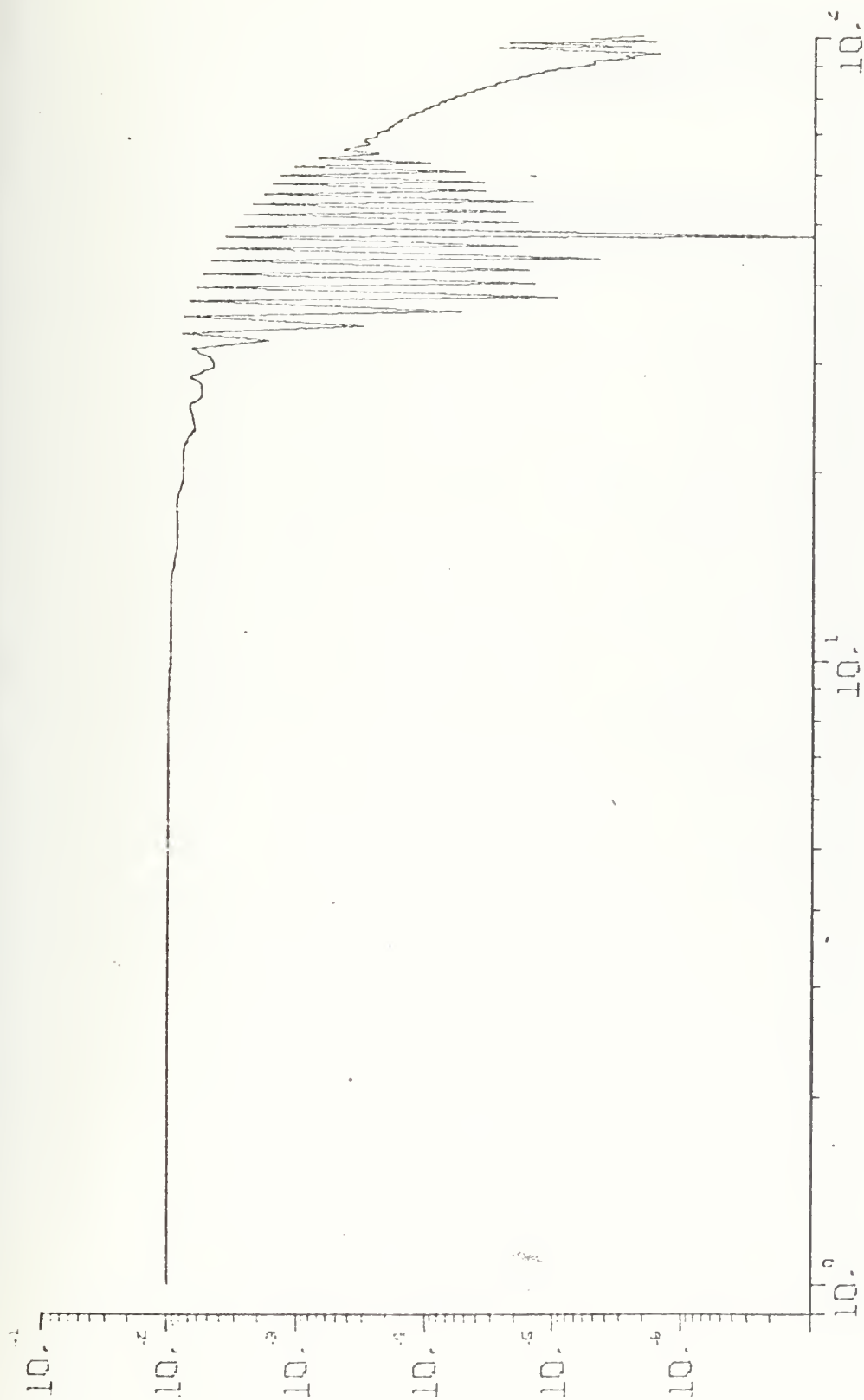


Figure 6.6. Point Target Spectrum Envelope vs. Frequency (Hz)

Detector parameters: $RHO=15$, $SIG=.5$, $w=30$,
 $h=1$, $x_0=15$, $y_0=0$

Target location: $R_x=0$, $R_y=0$

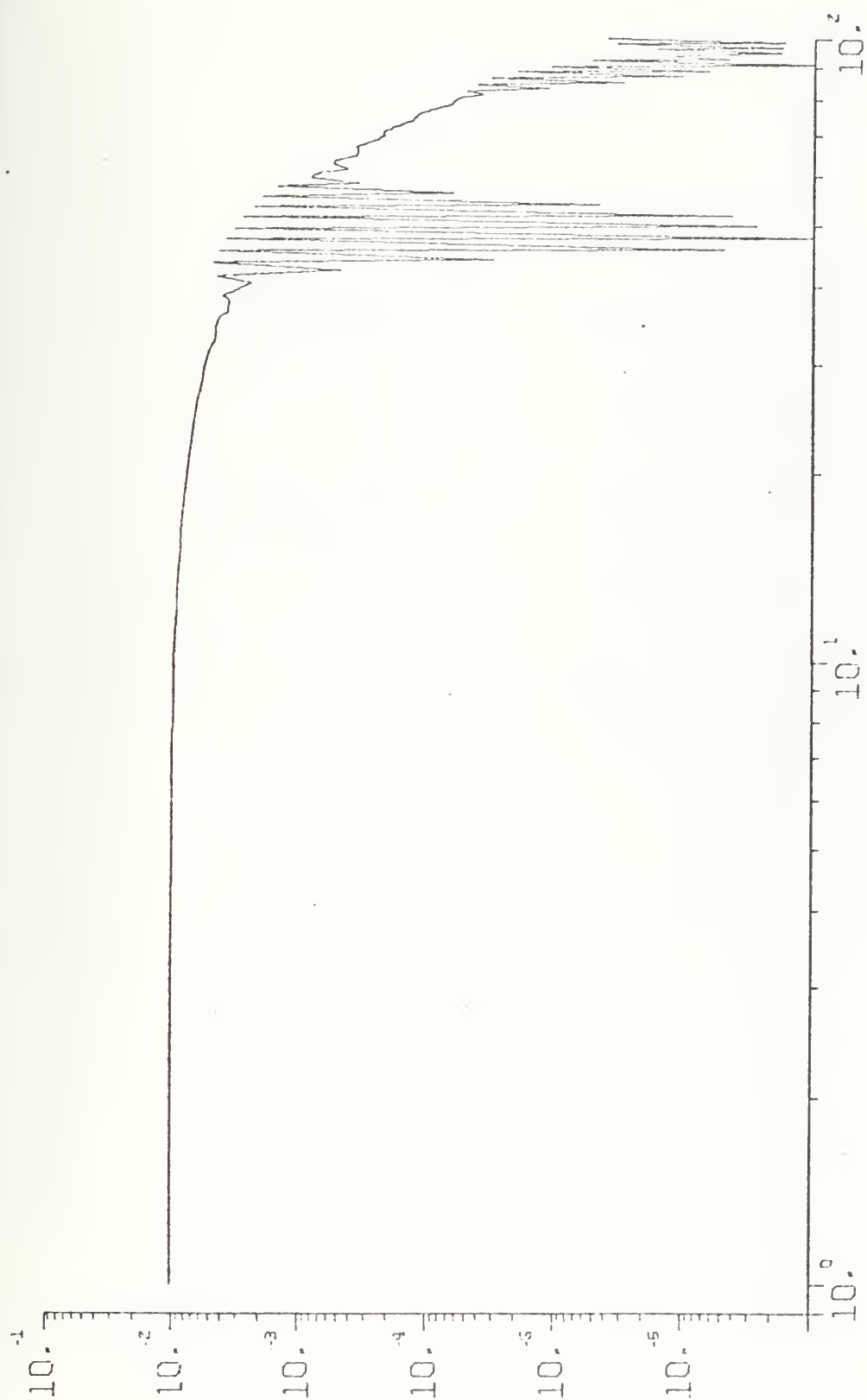


Figure 6.7. Point Target Spectrum Envelope vs. Frequency (Hz).

Detector parameters: $\text{RHO}=15$, $\text{SIG}=.5$, $w=10$, $h=1$,
 $x_0=15$, $y_0=0$

Target location: $R_x=0$, $R_y=0$

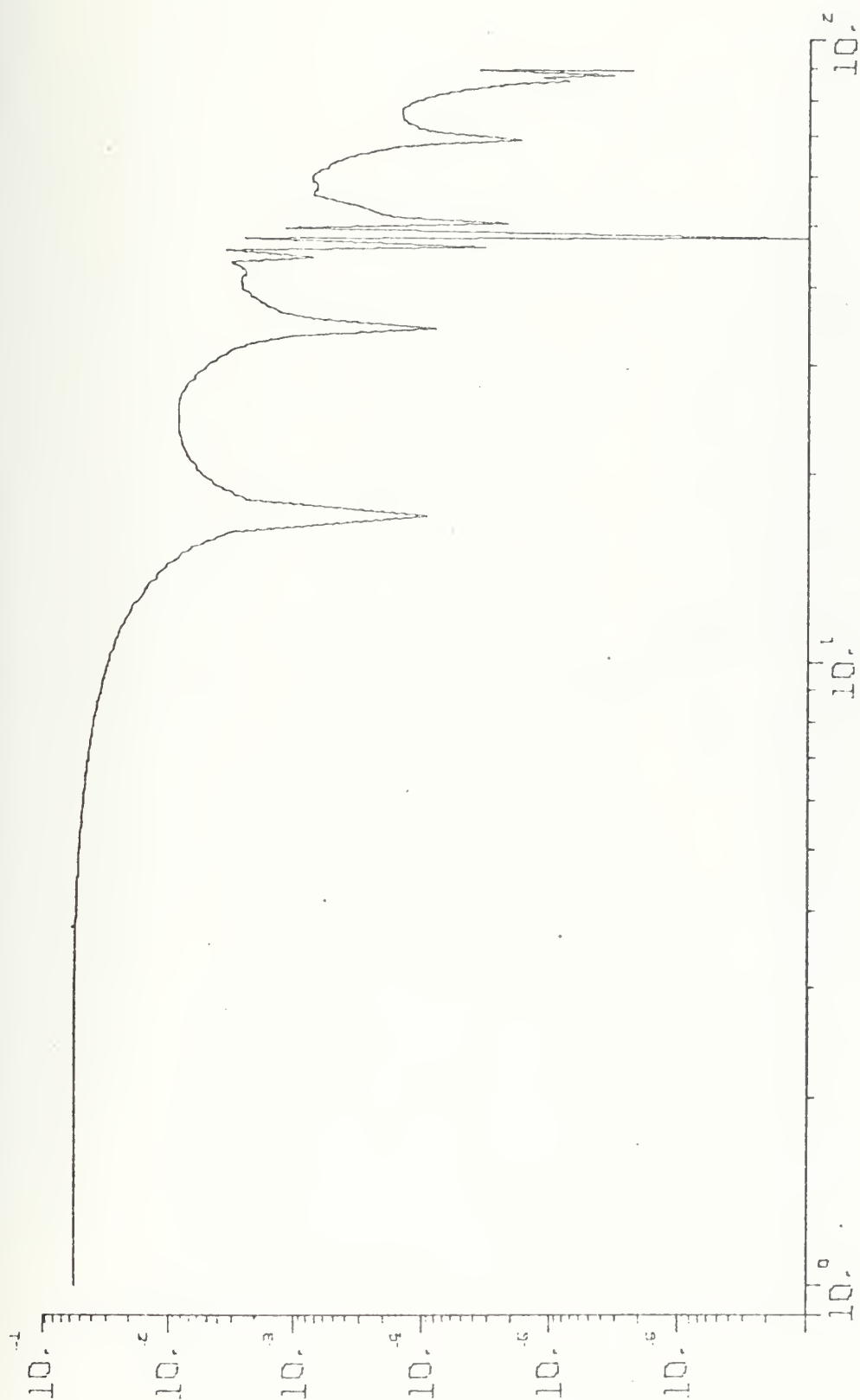


Figure 6.8. Point Target Spectrum Envelope vs. Frequency (Hz)

Detector parameters: $RHO=15$, $SIG=.5$, $w=5.5$,
 $h=5.5$, $x_o=15$, $y_o=0$

Target parameters: $R_x=0.0$, $R_y=0.0$

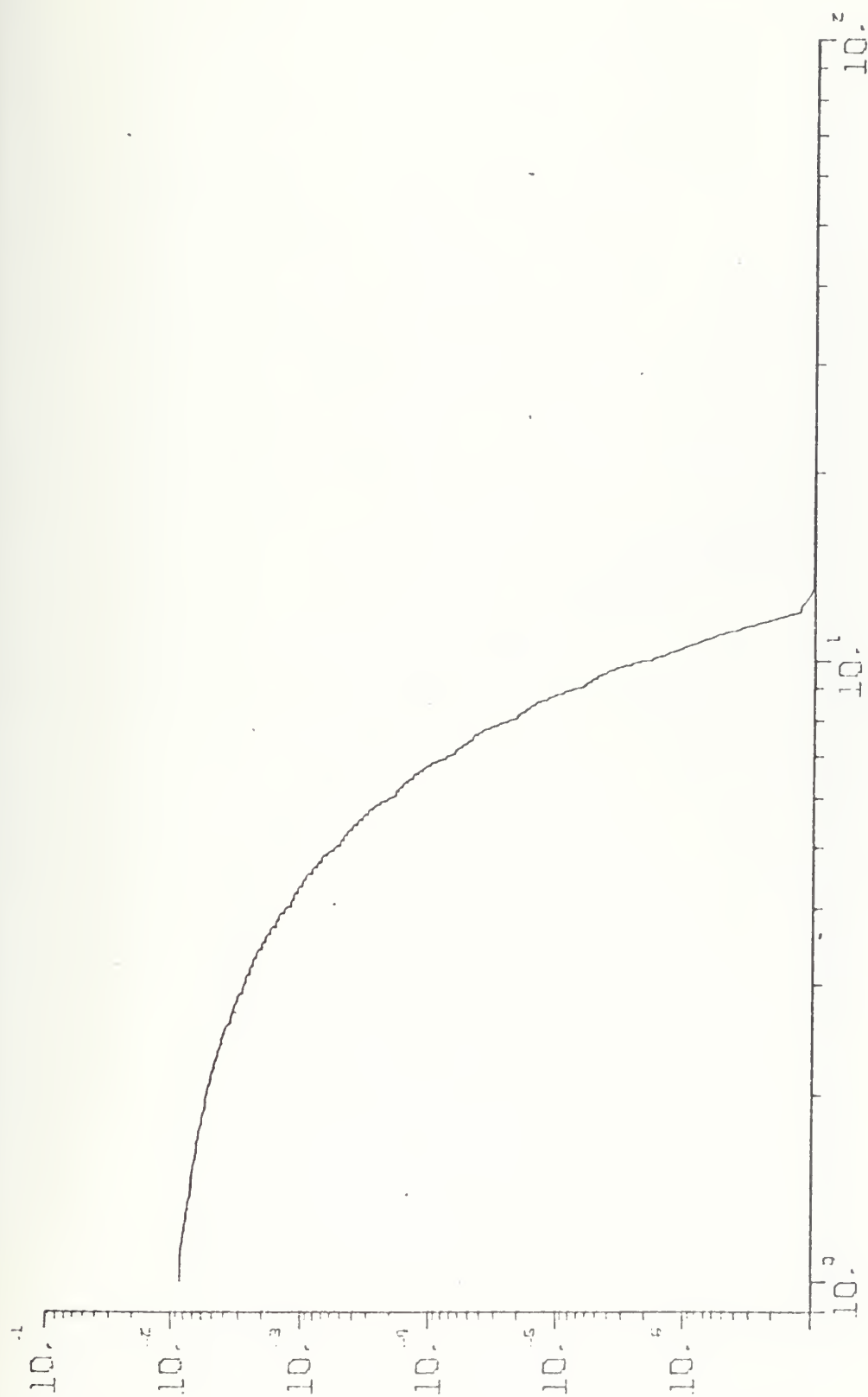


Figure 6.9. Averaged Signal Spectrum vs. Frequency (Hz).
 Detector parameters: $\text{RHO}=15$, $\text{SIG}=5$, $w=30$, $h=1$,
 $x_0=15$, $y_0=0$
 Std. Dev. of Gaussian Pointing error = 7.5

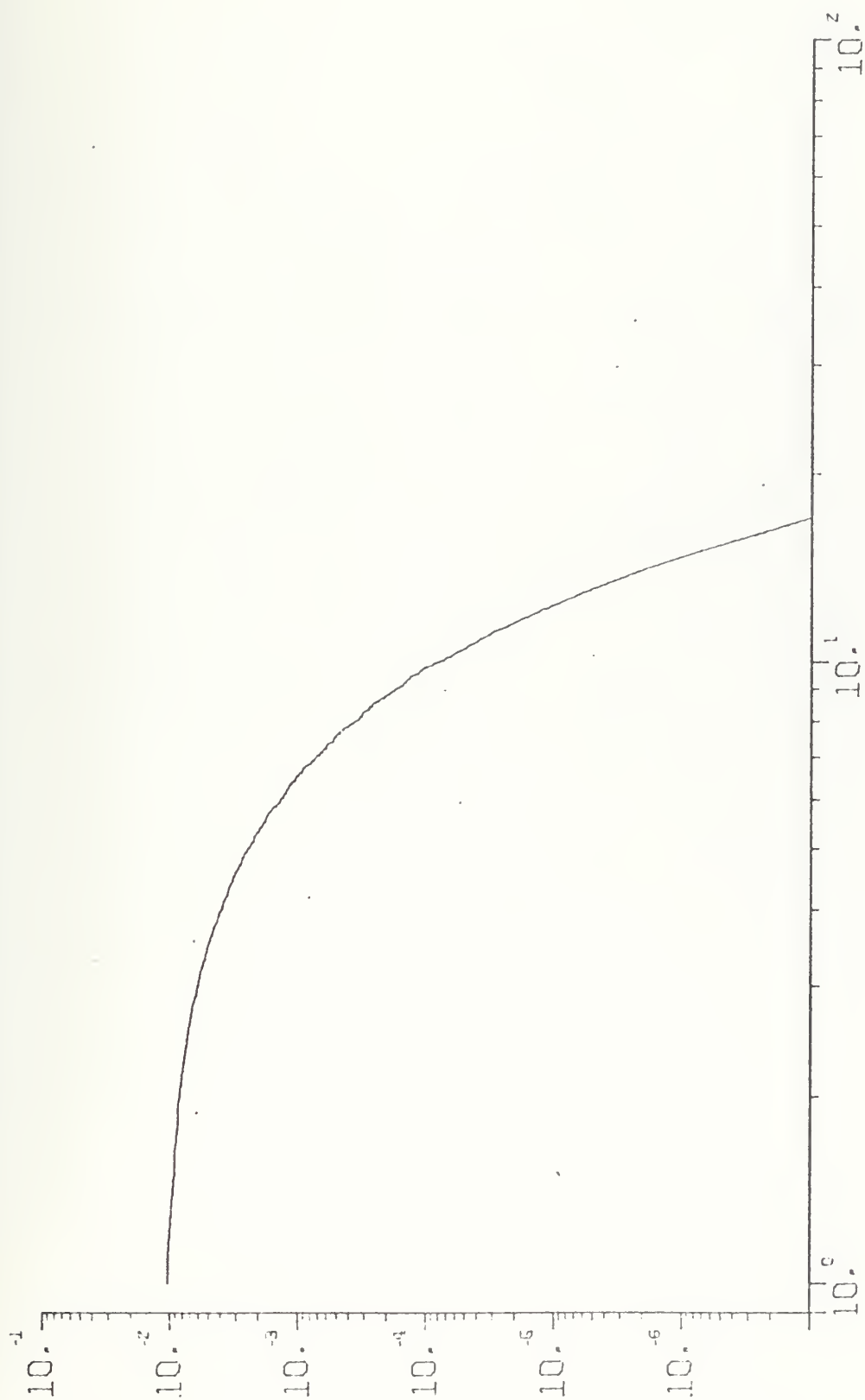


Figure 6.10. Averaged Signal Spectrum Envelope vs. Frequency.

Detector parameters: $\text{RHO}=15$, $\text{SIG}=.5$, $w=30$, $h=1$,
 $x_0=15$, $y_0=1$

Std. Dev. of Gaussian Pointing error = .5

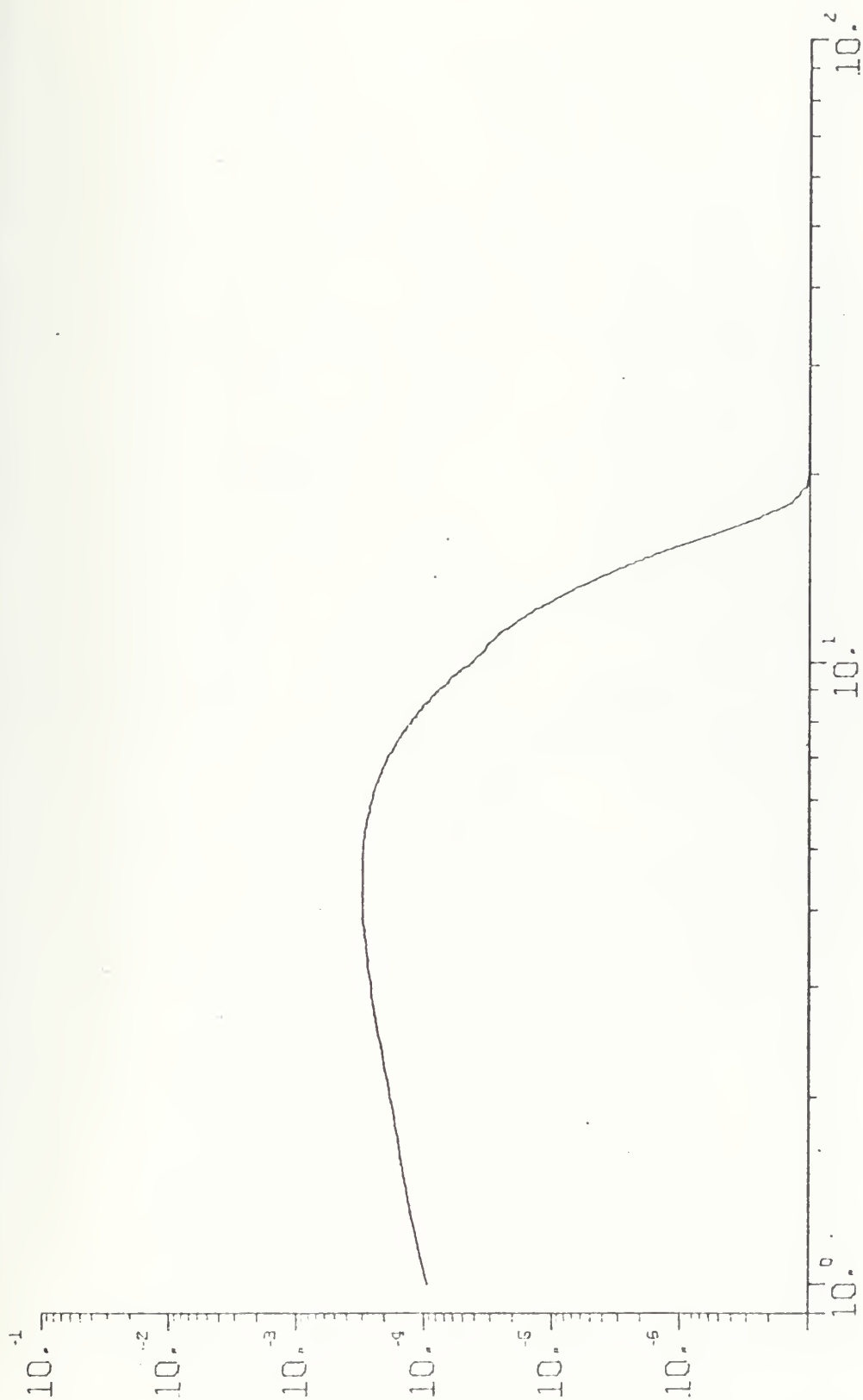


Figure 6.11. Filter Spectrum for Threshold Detector vs. Frequency (Hz)
 Detector parameters: $\text{RHO}=15$, $\text{SIG}=.5$, $w=30$, $h=1$,
 $x_0=15$, $y_0=0$
 Std. Dev. of Gaussian Pointing error = 5.0



Figure 6.12. Filter Spectrum of Threshold Detector vs. Frequency (Hz)

Detector parameters: $\text{RHO}=15$, $\text{SIG}=.5$, $w=30$, $h=1$,

$x_0=15$, $y_0=0$

Std. Dev. of Gaussian pointing error = 7.5

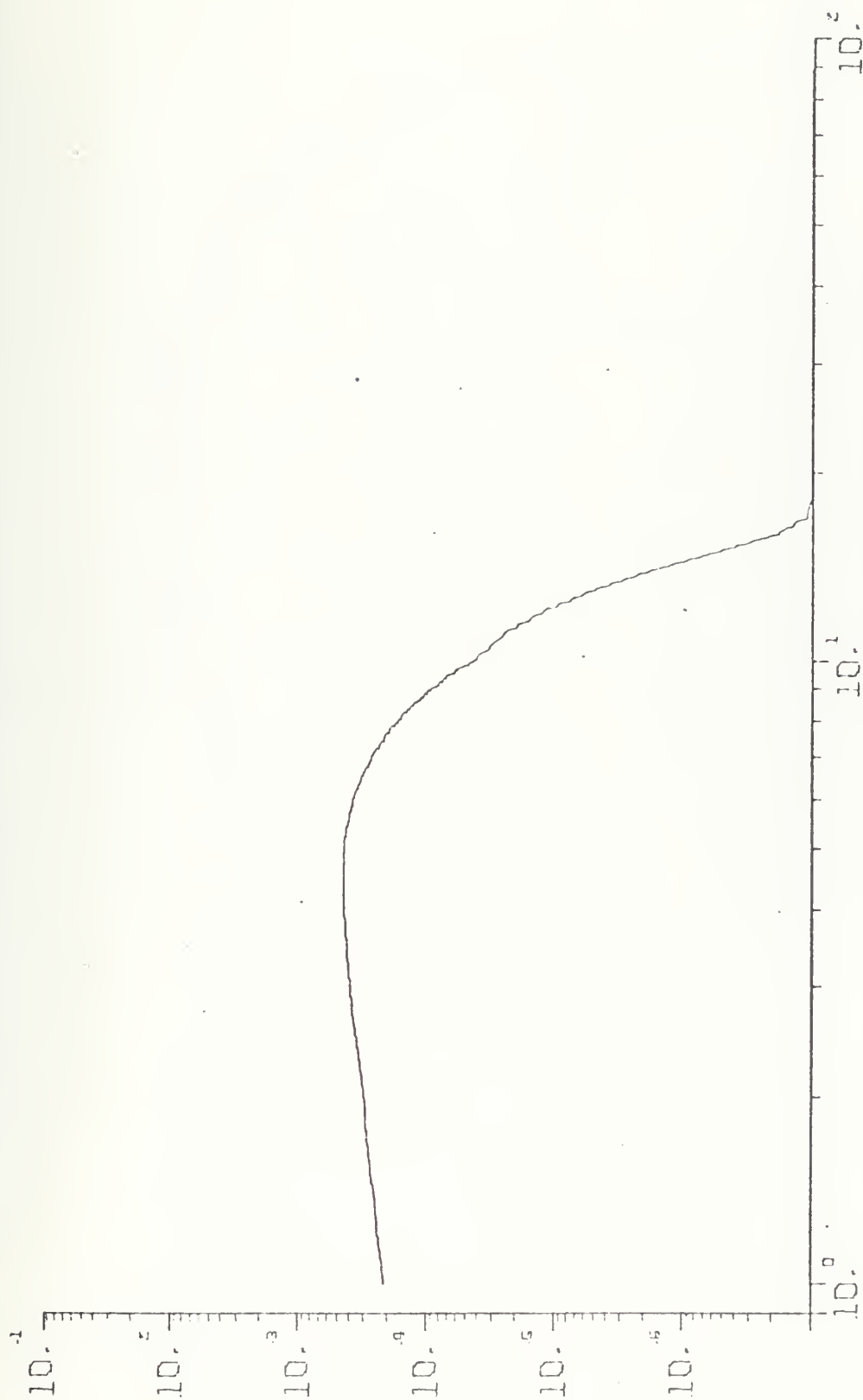


Figure 6.13. Filter Spectrum for Threshold Detector vs. Frequency (Hz)
 Detector parameters: $RHO=15$, $SIG=.5$, $w=5.5$, $h=5.5$,
 $x_0=15$, $y_0=0$
 Std. Dev. of Gaussian pointing error = 5.0

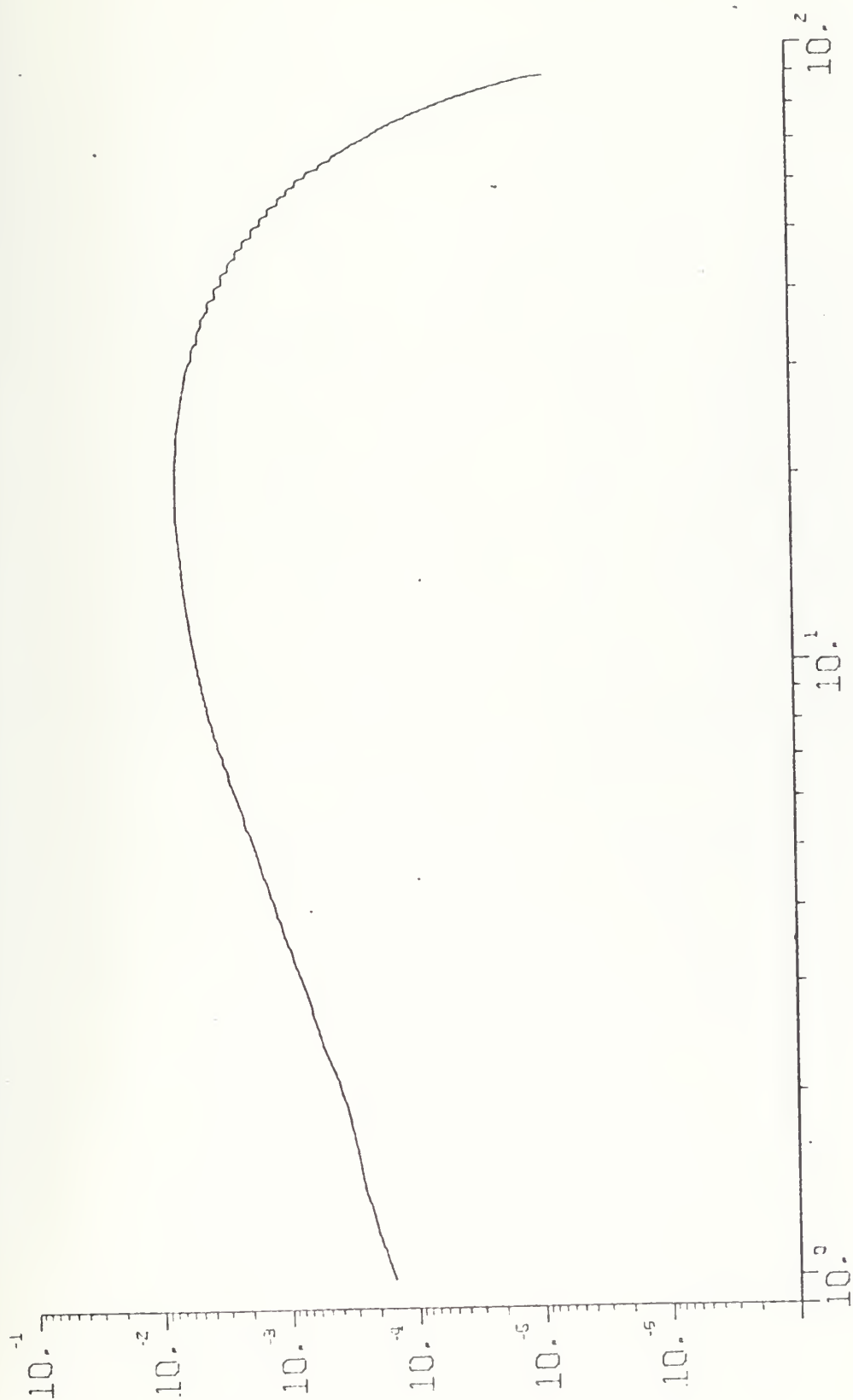


Figure 6.14. Filter Envelope (Matched to Point Target) vs. Frequency (Hz).

Detection Parameters: $RHO=15$, $SIG=.5$, $w=30$, $h=1$,
 $x_0=15$, $y_0=0$

Target location: $R_x=0$, $R_y=0$

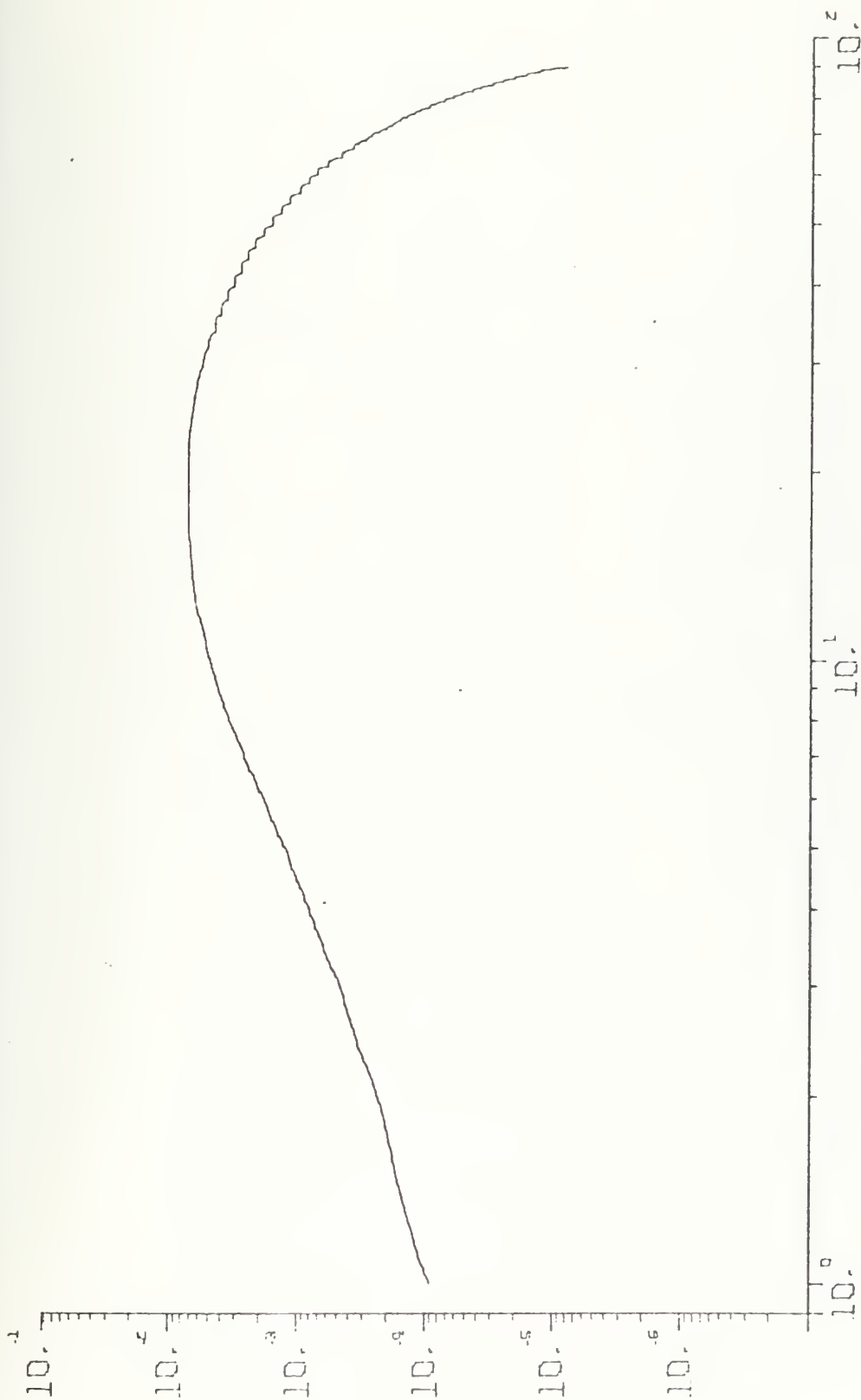


Figure 6.15. Filter Envelope (Matched to Point Target) vs. Frequency (Hz)

Detector parameters: $RHO=15$, $SIG=.5$, $w=10$, $h=1$,
 $x_0=15$, $y_0=0$

Target location: $R_x=0$, $R_y=0$

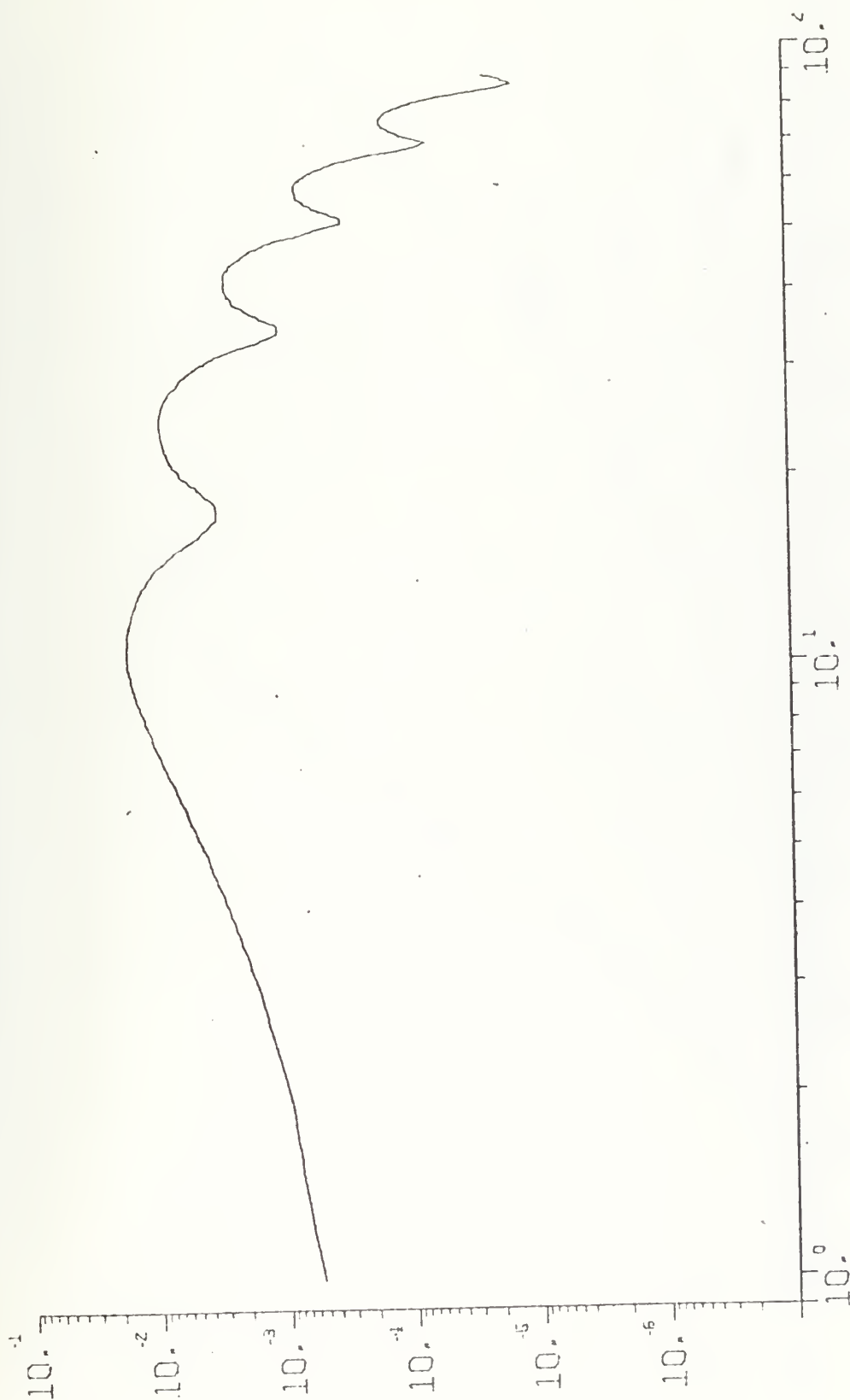


Figure 6.16. Filter Envelope (Matched to Point Target) vs. Frequency (Hz)

Detection Parameters: $RHO=15$, $SIG=.5$, $w=5.5$, $h=5.5$,
 $x_0=15$, $y_0=0$

Target location: $R_x=0$, $R_y=0$

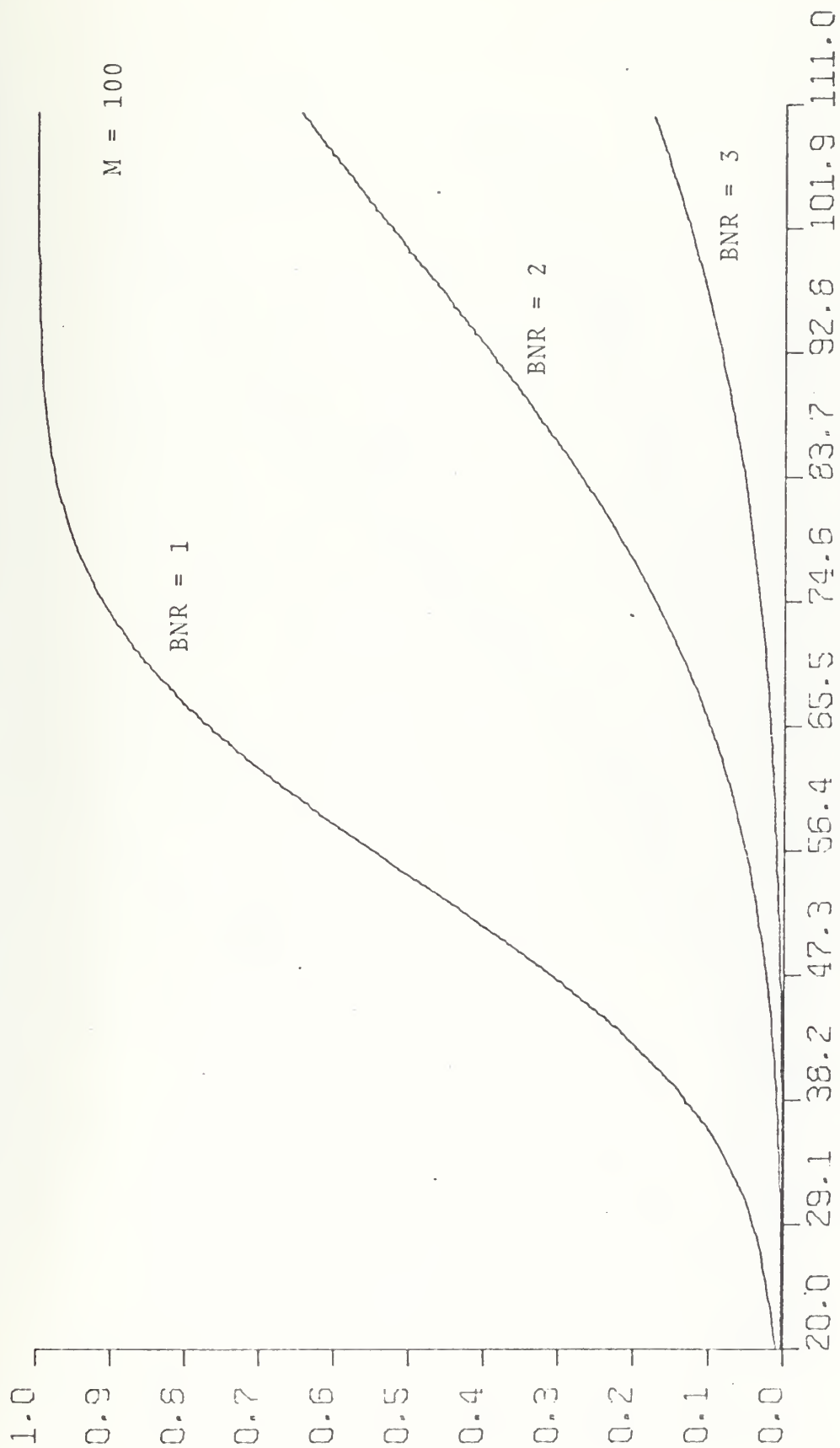


Figure 6.17. Probability of Detection vs. Signal-to-Noise Ratio.

Detector parameters: $RHO=15$, $SIG=.5$, $w=10$, $h=1$,
 $x_0=15$, $y_0=0$

Std. Dev. of Gaussian pointing error = 5.0

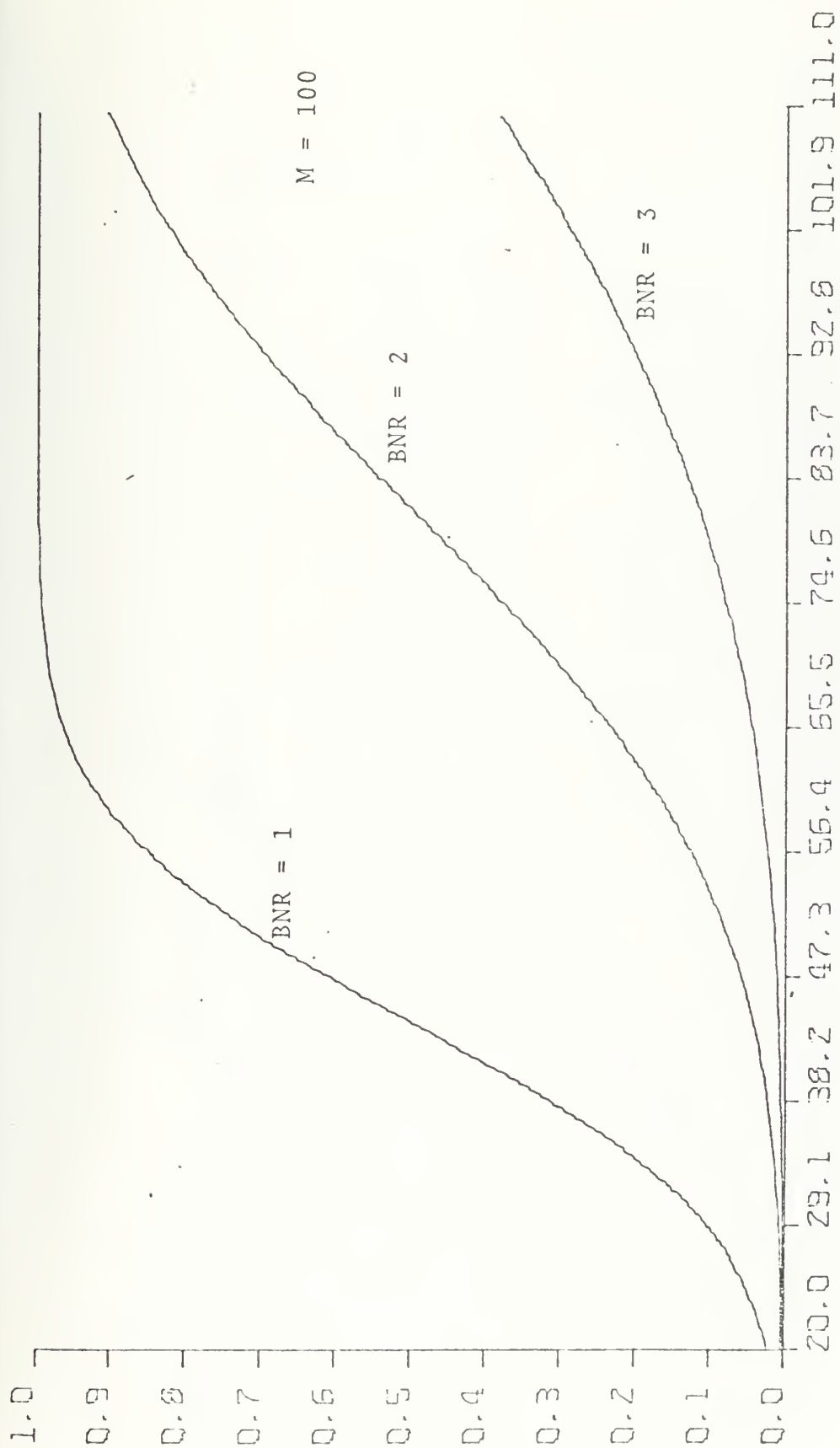


Figure 6.18. Probability of Detection vs. Signal-to-Noise Ratio.

Detector parameters: $\text{RHO}=15$, $\text{SIG}=.5$, $w=30$, $h=1$,
 $x_0=15$, $y_0=0$

Std. Dev. of Gaussian pointing error = 7.5

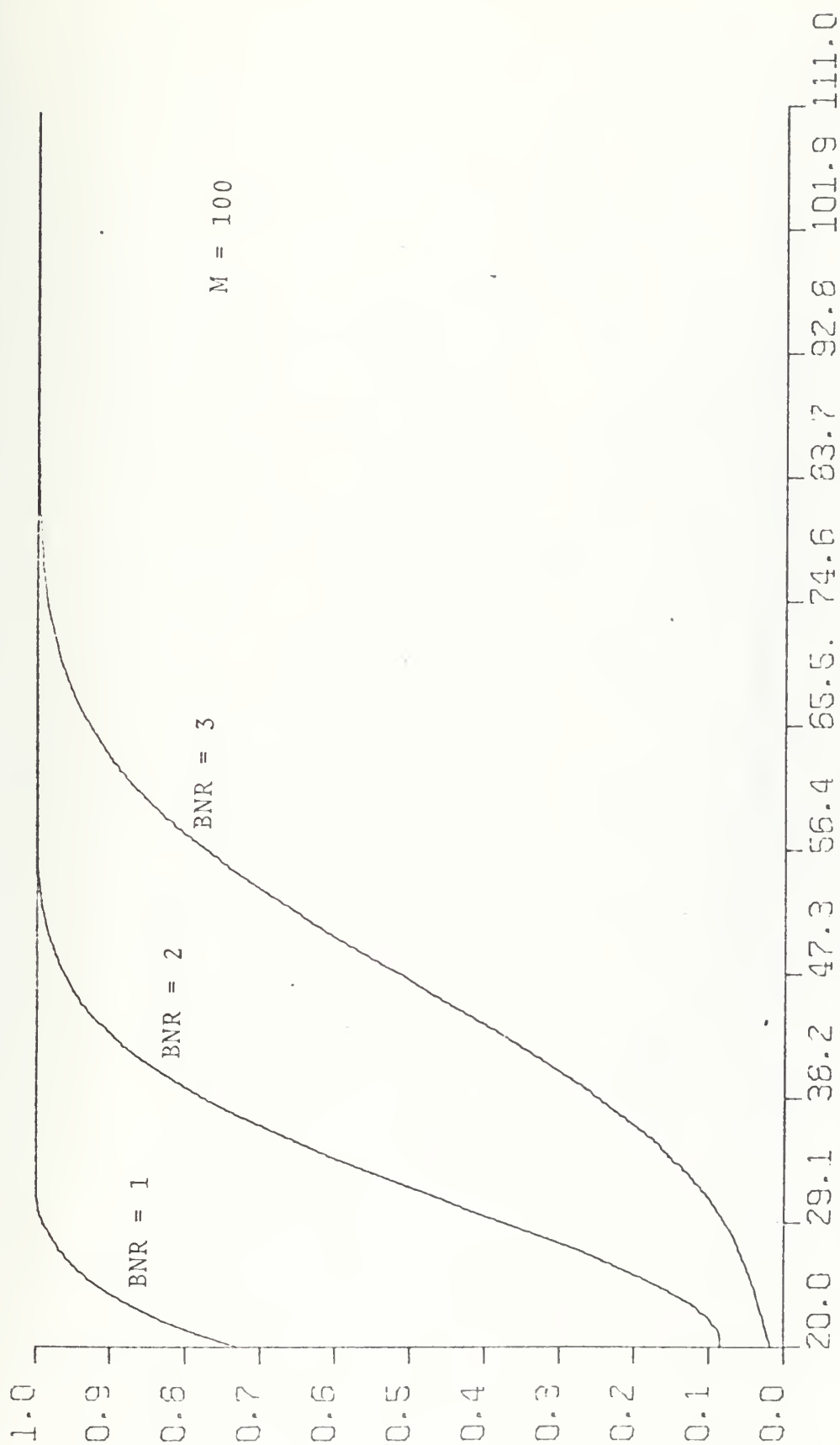


Figure 6.19. Probability of Detection vs. Signal-to-Noise Ratio.

Detector Parameters: $\text{RHO}=15$, $\text{SIG}=.5$, $w=5.5$, $h=5.5$,
 $x_0=15$, $y_0=0$

Std. Dev. of Gaussian pointing error = 5.0

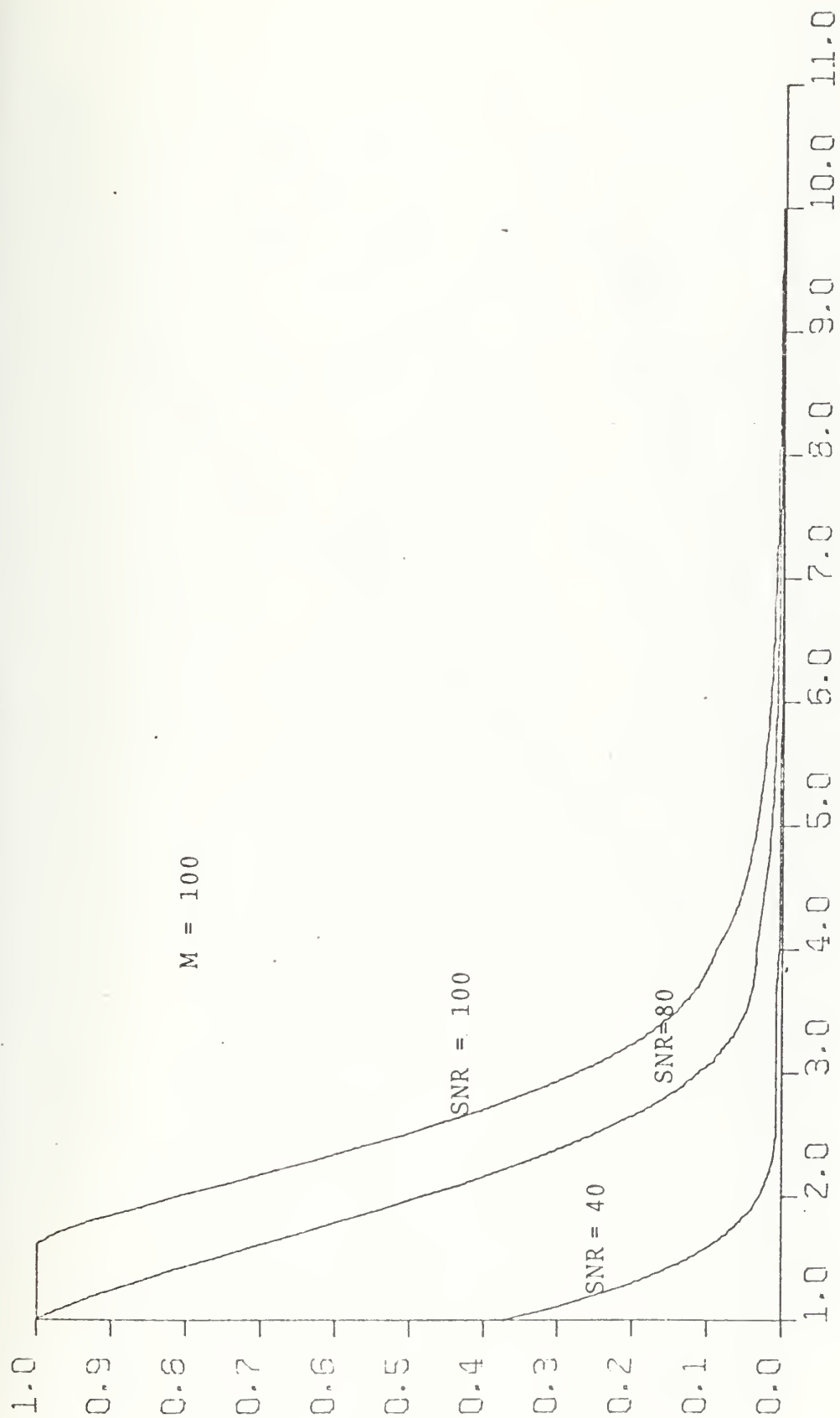


Figure 6.20. Probability of Detection vs. Background-to-Noise Ratio.

Detector parameters: $RHO=15$, $SIG=.5$, $w=30$, $h=1$,
 $x_o=15$, $y_o=0$

Std. Dev. of Gaussian pointing error = 7.5

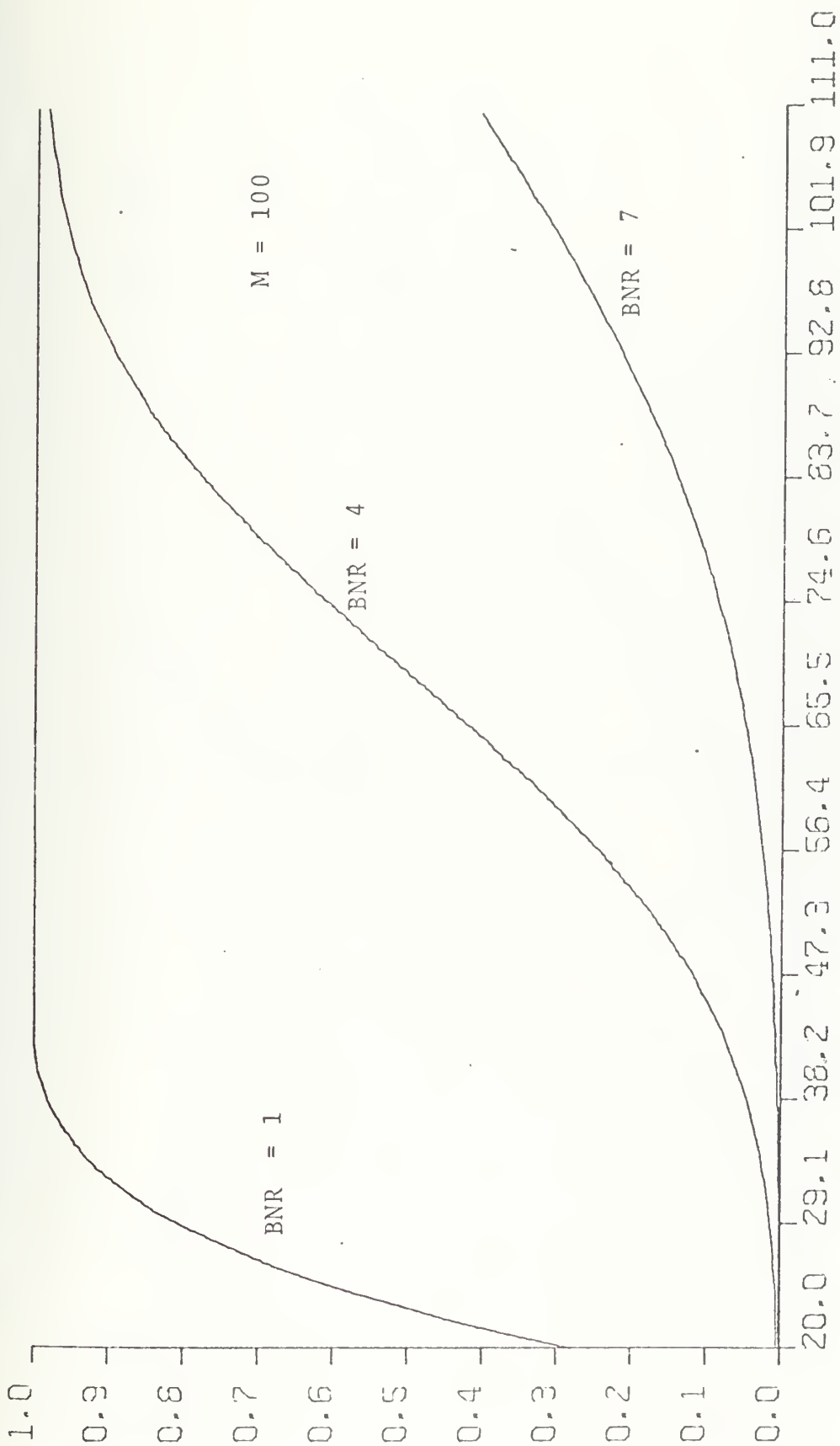


Figure 6.21. Probability of Detection vs. Signal-to-Noise Ratio.

Detector Parameters: $\text{RHO}=15$, $\text{SIG}=.5$, $w=30$, $h=1$,
 $x_0=15$, $y_0=0$

Std. Dev. of Gaussian pointing error = 7.5

Target location: $R_x=0$, $R_y=0$

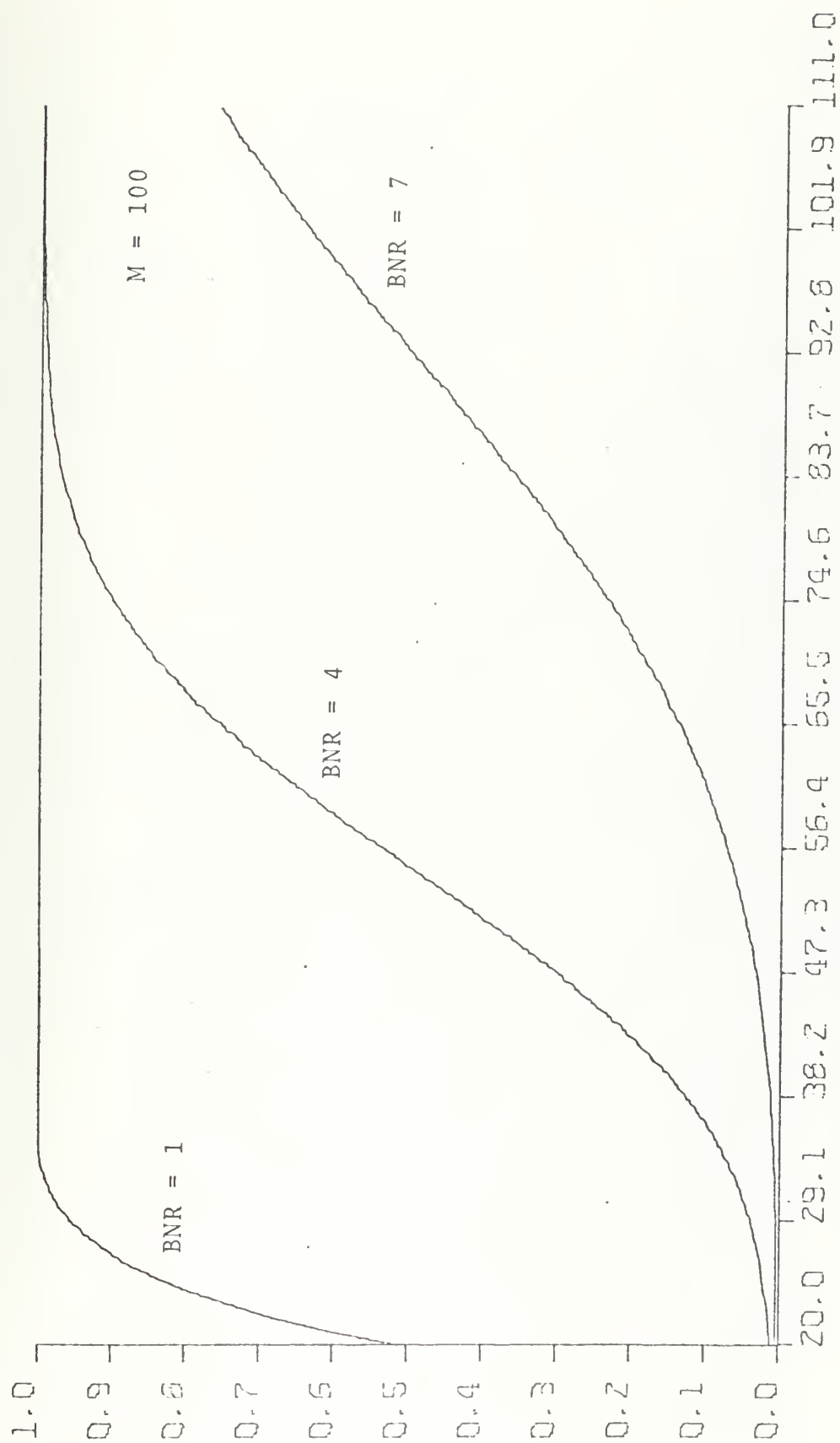


Figure 6.22. Probability of Detection vs. Signal-to-Noise Ratio.

Detector parameters: $\text{RHO}=15$, $\text{SIG}=.5$, $w=10$, $h=1$,
 $x_0=15$, $y_0=0$

Std. Dev. of Gaussian pointing error = 5
 Target location: $R_x=0$, $R_y=0$

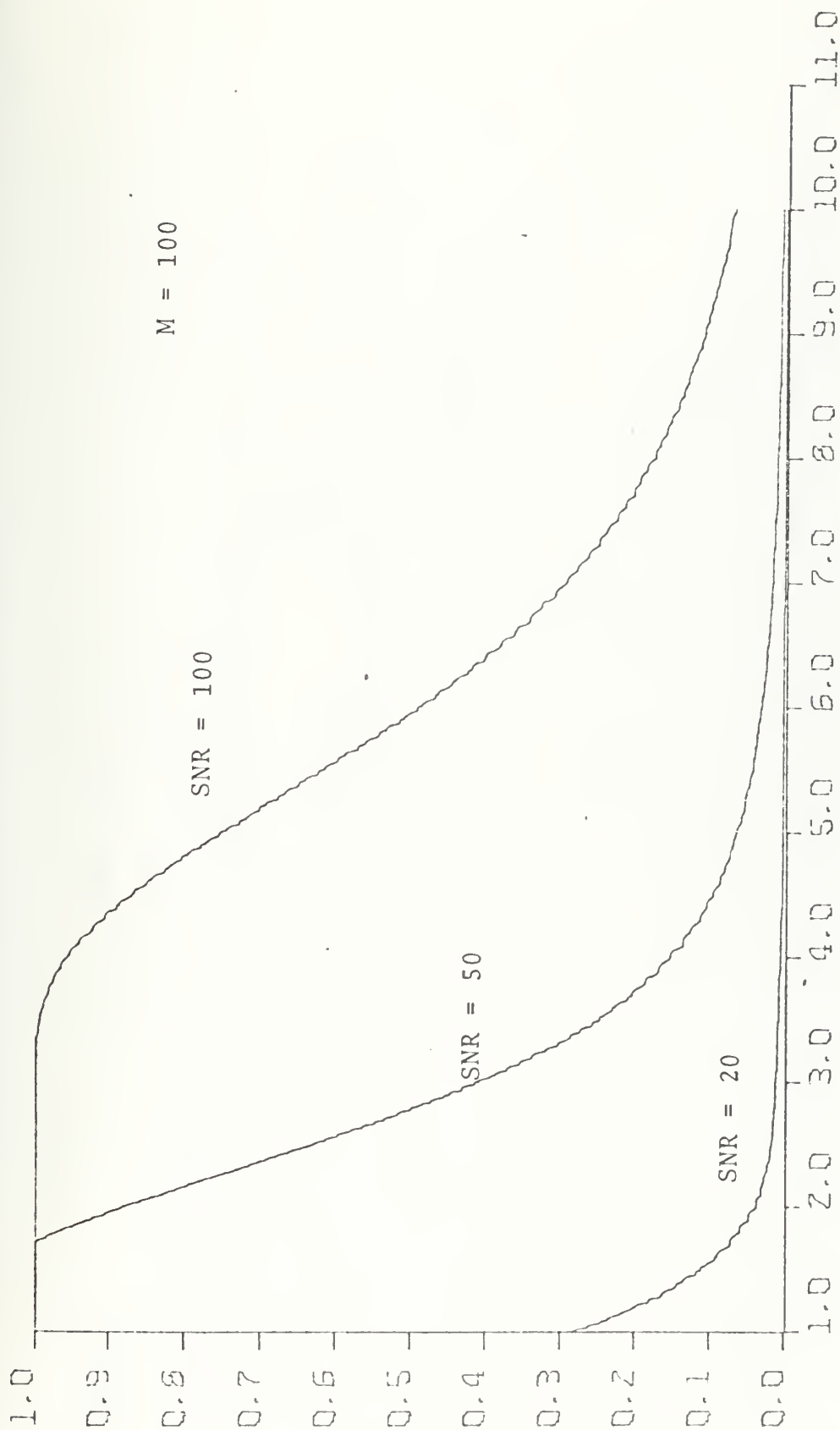


Figure 6/23. Probability of detection vs. Background-to-Noise Ratio.
 Detector parameters: $RHO=15$, $SIG=.5$, $w=30$,
 $h=1$, $x_0=15$, $y_0=0$
 Std. Dev. of Gaussian pointing error = 7.5
 Target location = $R_x=0$, $R_y=0$

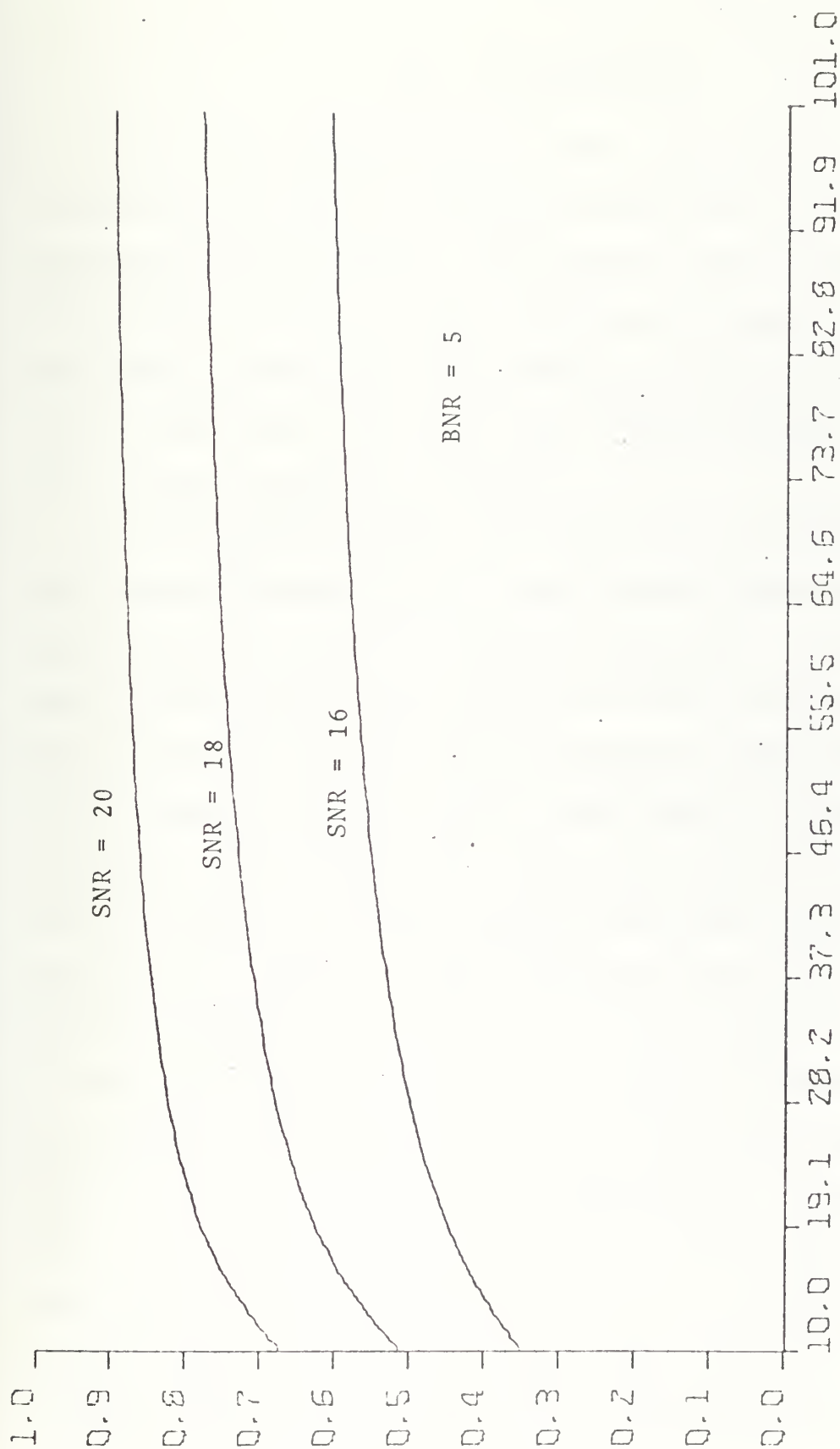


Figure 6.24. Probability of Detection vs. Number of Nutations.
 Detector parameters: $\text{RHO}=15$, $\text{SIG}=5$, $w=5.5$, $h=5.5$,
 $x_0=15$, $y_0=0$
 Std. Dev. of Gaussian pointing error = 5
 Target location = $R_x=0$, $R_y=0$

VII. CONCLUSIONS

The problem investigated in this thesis was to determine an optimum processor to be used in detecting targets with an infrared nutating system. The nature of the system divided the problem into two areas: optimizing a spatial processor according to size and shape and optimizing a temporal processor that takes the output time varying voltage and decides if a target is actually present.

General equations for the output from a nutating detector were known from Samuelsson's work, however these equations had not been solved for a specific detector. At the same time it was observed that the form of the covariance function for the noise offered an easy solution to integral equation of the Karhunen-Loeve expansion which made statistical detection theory appealing. Some work had been done on the form of temporal processor using statistical detection theory but this was limited to only one nutation because of the common background noise component between nutations.

Harger's derivations provided a means for describing a temporal processor using statistical detection theory that based its decisions on multiple observations and included the background noise. His work was extended here to include unknown parameters, amplitude and position, which more closely characterized the system. This extension, called a threshold detector, was shown to be optimum in the case of

small signal-to-noise ratios where detection is most difficult. The derivation also used the Gaussian assumption to describe the background. This may or may not be correct. But in practice, the detector's performance may not suffer greatly if this assumption is wrong.

To implement the threshold detector, the integrals describing the detector output were solved using the Gaussian quadrature method of numerical integration. Checking the computed coefficients by a summation provided a means of accepting the validity of the integrations. The form of the threshold detection system using a rectangular detector was determined and the frequency spectrum of the optimum filter was shown. To specify performance, the probability of detection is plotted against signal-to-noise and background-to-noise ratios and the number of nutations on which the decision was based. The signal spectrum for a point target and background power spectral density is also plotted.

A designer may find these results useful in developing a system or investigating the performance of an actual system as compared to the optimum. He may also use these results to determine the size of a rectangular spatial filter to be used.

Future work should include extending these results to spatial filters that are circular or elliptic. The same numerical integration algorithm could probably be used. The threshold detector was found to be highly sensitive to background correlation lengths. Thus, some form of adaptive processor should be included to minimize the effect of

background. At the present time, a measurement program is underway at Naval Weapons Center, China Lake, California to determine average background correlation lengths but for different environments, these correlation lengths could be expected to vary considerably.

APPENDIX A

DERIVATION OF SIGNAL SPECTRAL COEFFICIENTS

The radiance on the detector is periodic because of the nutation therefore it can be expressed in a Fourier series,

$$H(t) = \sum_n^{\infty} H_n e^{jn\omega_0 t} \quad (1A)$$

where

$$H_n = \frac{1}{T} \int_0^T H(t) e^{-jn\omega_0 t} dt \quad (2A)$$

But,

$$H(t) = \int N'(\underline{r}) \tau(\underline{r} - \underline{\rho}(t)) d^2 \underline{r} . \quad (3A)$$

Substituting (3A) in (2A)

$$H_n = \int d^2 \underline{r} N'(\underline{r}) \frac{1}{T} \int_0^T dt \tau(\underline{r} - \underline{\rho}(t)) e^{-jn\omega_0 t} \quad (4A)$$

The transmittance, τ , may be expressed in terms of the inverse Fourier transform, assuming an infinite image plane,

$$\tau(\underline{r} - \underline{\rho}(t)) = \int d^2 \underline{k} \tau^*(\underline{k}) e^{-j2\pi \underline{k} \cdot (\underline{r} - \underline{\rho}(t))} . \quad (5A)$$

Rewriting the exponent,

$$\underline{k} \cdot (\underline{r} - \underline{\rho}(t)) = \underline{k} \cdot \underline{r} - \rho k_x \cos \omega_0 t - \rho k_y \sin \omega_0 t \quad (6A)$$

Equation (4A) can be rewritten,

$$H_n = \int d^2 \tilde{r} N'(\tilde{r}) \frac{1}{T} \int_0^T dt \int d^2 \tilde{k} \tau^*(\tilde{k}) e^{-j2\pi \tilde{k} \cdot \tilde{r}} \\ \cdot e^{jnA \sin(\omega_0 t + \theta)} e^{-jn\omega_0 t}$$

where

$$A = \sqrt{k_x^2 + k_y^2} \\ \theta = \tan^{-1} k_x/k_y. \quad (7A)$$

Observe that

$$N'(\tilde{k}) = \int d^2 \tilde{r} N'(\tilde{r}) e^{-j2\pi \tilde{k} \cdot \tilde{r}} \quad (8A)$$

thus

$$H_n = \int d^2 \tilde{k} N'(\tilde{k}) \tau^*(\tilde{k}) e^{jn\theta} \frac{1}{T} \int_0^T dt e^{-jn(\omega_0 t + \theta)} \\ \cdot e^{jnA \sin(\omega_0 t + \theta)} \quad (9A)$$

Using the relation

$$J_n(z) = \frac{1}{T} \int_0^T e^{-jn\phi} e^{jz \sin \phi} d\phi, \quad (10A)$$

the expression for the coefficients becomes

$$H_n = \int d^2 \tilde{k} N'(\tilde{k}) \tau^*(\tilde{k}) e^{jn\theta} J_n \left(2\pi \rho \sqrt{k_x^2 + k_y^2} \right). \quad (11A)$$

Let

$$\phi = \tan^{-1} k_y/k_x$$

then

$$j^n e^{-jn\phi} = e^{jn\theta}$$

Rewriting (11A)

$$H_n = j^n \int d^2 \tilde{k} N'(\tilde{k}) \tau^*(\tilde{k}) e^{-jn\phi} J_n \left(2\pi\rho \sqrt{k_x^2 + k_y^2} \right). \quad (12A)$$

APPENDIX B

DERIVATION OF BACKGROUND CORRELATION COEFFICIENTS

The n^{th} power spectrum component of the background at frequency $n\omega_0$ is given by

$$\beta_n = \frac{1}{T} \int_0^T R_B(\tau) e^{-jn\omega_0 \tau} d\tau \quad (1B)$$

But $R_B(\tau)$ is the correlation function of detector output averaged with respect to the starting time.

$$R_B(\tau) = \frac{1}{T} \int_0^T E[B(t+\tau)B(t)] dt \quad (2B)$$

Using the expression for $B(t)$ from Part II,

$$R_B(\tau) = \frac{1}{T} \int_0^T dt E \left[\int N'(\underline{r}) \tau(\underline{r}_1 - \underline{\rho}(t+\tau)) d^2 \underline{r}_1 \right. \\ \left. \cdot \int N'(\underline{r}_2) \tau(\underline{r}_2 - \underline{\rho}(t)) d^2 \underline{r}_2 \right] \quad (3B)$$

Interchanging the order of expectation and integration,

$$R_B(\tau) = \frac{1}{T} \int_0^T dt \int d^2 \underline{r}_1 \int d^2 \underline{r}_2 \tau[\underline{r}_1 - \underline{\rho}(t+\tau)] \\ \cdot \tau[\underline{r}_2 - \underline{\rho}(t)] E[N'(\underline{r}_1)N'(\underline{r}_2)] \quad (4B)$$

Assuming stationary background,

$$E[N'(\underline{r}_1)N'(\underline{r}_2)] = \phi_B'(\underline{r}_1 - \underline{r}_2) \quad (5B)$$

where $\phi'_B(\underline{r}_1 - \underline{r}_2)$ is the background covariance function on the image plane.

It is now convenient to express the integrand in terms of two-dimensional spatial Fourier transform. To begin with

$$\tau(\underline{r}) = \int \tau(\underline{k}) e^{j2\pi \underline{k} \cdot \underline{r}} d^2 \underline{k} \quad (6B)$$

where $\tau(\underline{k})$ is the Fourier transform of the aperture function $\tau(\underline{r})$ and $\underline{k} = (k_x, k_y)$. Then

$$\begin{aligned} & \tau[\underline{r}_1 - \underline{\rho}(t+\tau)] \tau[\underline{r}_2 - \underline{\rho}(t)] \\ &= \int d^2 \underline{k}_1 \tau(\underline{k}_1) \int d^2 \underline{k}_2 \tau^*(\underline{k}_2) e^{j2\pi (\underline{k}_1 \cdot \underline{r}_1 - \underline{k}_2 \cdot \underline{r}_2)} \\ & \quad \cdot e^{-j2\pi [\underline{k}_1 \cdot \underline{\rho}(t+\tau) - \underline{k}_2 \cdot \underline{\rho}(t)]} \end{aligned} \quad (7B)$$

Substituting (5B) and (7B) in (4B) and interchanging the order of integration,

$$\begin{aligned} R_B(\tau) &= \int d^2 \underline{k}_1 \tau(\underline{k}_1) \int d^2 \underline{k}_2 \tau^*(\underline{k}_2) \\ & \quad \cdot \frac{1}{T} \int_0^T dt e^{-j2\pi [\underline{k}_1 \cdot \underline{\rho}(t+\tau) - \underline{k}_2 \cdot \underline{\rho}(t)]} \\ & \quad \cdot \int d^2 \underline{r}_1 e^{j2\pi \underline{k}_1 \cdot \underline{r}_1} \int d^2 \underline{r}_2 \phi'_B(\underline{r}_1 - \underline{r}_2) e^{-j2\pi \underline{k}_2 \cdot \underline{r}_2} \end{aligned} \quad (8B)$$

The last integral becomes, with $\underline{R} = \underline{r}_1 - \underline{r}_2$,

$$\left[\int d^2 \underline{R} \phi'_B(\underline{R}) e^{-j2\pi \underline{k}_2 \cdot \underline{R}} \right] e^{-j2\pi \underline{k}_2 \cdot \underline{r}_1} \quad (9B)$$

But the bracket above is the Fourier transform of $\phi'_B(\underline{r})$, or the Wiener spectrum of background on the image plane. Let

$$W'_B(\underline{k}_2) = \int \phi'_B(\underline{R}) e^{-j2\pi \underline{k}_2 \cdot \underline{R}} d^2 \underline{R} \quad (10B)$$

If $F_o(\underline{k})$ is the Fourier transform of the point spread function and $W_B(\underline{k})$ is the Wiener spectrum of background on the object plane, then

$$W'_B(\underline{k}) = |F_o(\underline{k})|^2 W_B(\underline{k}) \quad (11B)$$

This relation is analogous to the output noise spectrum expression due to a noise input to a linear system. In terms of $W'_B(\underline{k})$ the last line of (8B) is

$$W'_B(\underline{k}) \int e^{j2\pi(\underline{k}_1 - \underline{k}_2) \cdot \underline{r}_1} d^2 \underline{r}_1 = W'_B(\underline{k}) \delta(\underline{k}_1 - \underline{k}_2) \quad (12B)$$

Substituting this into (8B) and performing the integration with respect to \underline{k}_2 ,

$$R_B(\tau) = \int d^2 \underline{k} |\tau(\underline{k})|^2 W'_B(\underline{k}) \cdot \frac{1}{T} \int_0^T e^{j2\pi \underline{k} \cdot [\underline{\rho}(t+\tau) - \underline{\rho}(t)]} dt \quad (13B)$$

Since $\underline{\rho}(t) = (\rho \cos \omega_o t, \rho \sin \omega_o t)$,

$$\begin{aligned} \underline{k} \cdot [\underline{\rho}(t+\tau) - \underline{\rho}(t)] &= k_x \rho \cos \omega_o (t+\tau) + k_y \rho \sin \omega_o (t+\tau) \\ &\quad - k_x \rho \cos \omega_o t - k_y \rho \sin \omega_o t \\ &= A(\tau) \cos \omega_o t + B(\tau) \sin \omega_o t = c(\tau) \cos(\omega_o t - \psi(t)) \end{aligned}$$

where

$$A(\tau) = \rho [k_x \cos \omega_o \tau + k_y \sin \omega_o \tau - k_x]$$

$$B(\tau) = \rho [-k_x \sin \omega_o \tau + k_y \cos \omega_o \tau - k_y]$$

$$C(\tau) = \sqrt{A^2(\tau) + B^2(\tau)} = \rho \sqrt{2(1 - \cos \omega_o \tau) (k_x^2 + k_y^2)}$$

and

$$\psi(\tau) = \tan^{-1} \frac{B(\tau)}{A(\tau)} \quad (14B)$$

Therefore the last integral of (13B) is

$$\frac{1}{T} \int_0^T e^{j2\pi c \cos(\omega_o \tau + \psi)} dt = J_o(2\pi c) \quad (15B)$$

where $J_o(\cdot)$ is the zeroth order Bessel function. Therefore, the correlation function $R_B(\tau)$ is given by

$$R_B(\tau) = \int |\tau(\underline{k})|^2 W'_B(\underline{k}) J_o\left(4\pi \rho \underline{k} \sin \frac{\omega_o \tau}{z}\right) d^2 \underline{k} \quad (16B)$$

where

$$\underline{k} = \sqrt{k_x^2 + k_y^2} \quad \text{and} \quad d^2 \underline{k} = dk_x dk_y.$$

Finally, the power spectrum coefficient β_n is, from (1B)

$$\begin{aligned} \beta_n &= \int |\tau(\underline{k})|^2 W'_B(\underline{k}) d^2 \underline{k} \\ &\cdot \frac{1}{T} \int_0^T J_o\left(2a \sin \frac{\omega_o \tau}{z}\right) e^{-jn\omega_o \tau} d\tau \end{aligned} \quad (17B)$$

where $a = 2\pi k\rho$. The last integral becomes with $x = \omega_o \tau/2$,

$$\begin{aligned} &\frac{1}{T} \int_0^\pi J_o(2a \sin x) \cos 2nx \, dx \\ &- j \frac{1}{\pi} \int_0^\pi J_o(2a \sin x) \sin 2n\pi \, dx \end{aligned} \quad (18B)$$

The cosine integral equals $J_n^2(a)$ and the sine integral vanishes [2]. Therefore on using (18B)

$$\beta_n = \int |\tau(\underline{k})|^2 |F_o(\underline{k})|^2 W_B(\underline{k}) J_n^2(2\pi\rho\underline{k}) d^2\underline{k} . \quad (19B)$$

This is the general power spectrum expression for a nutating detector output. The power at frequency $n\omega_o$ is expressed in terms of aperture transform $\tau(\underline{k})$, optical transfer function $F_o(\underline{k})$, Wiener spectrum of background $W_B(\underline{k})$ and nutation radius through $J_n^2(2\pi\rho\underline{k})$. The integration is over the entire \underline{k} -plane.

APPENDIX C

EXPECTATION OF Λ_{12}

The essential calculation required to find

$$\Lambda_{12}(\{Z_n\}) = E_B[\Lambda_{12}(\{Z_n\}|B)] \quad (1C)$$

for Gaussian background B is the expectation

$$I = E_B \left[\exp \left\{ \int_0^T A(t)B(t)dt - c \int_0^T B^2(t)dt \right\} \right]$$

where

$$c = M/N$$

and

$$A(t) = \frac{2}{N} \sum_{n=1}^M (Z_n(t) - S_n(t)) \quad (2C)$$

B(t) may be expanded in its Karhunen-Loeve (K-L) representation provided the mean square value

$$E(B^2(t)) < \infty \quad (3C)$$

and thus the integral equation

$$\lambda_i \phi_i(t) = \int_0^T R_B(t,u) \phi_i(u)du \quad 0 \leq t \leq T \quad (4C)$$

can be solved. λ_i are called the eigenvalues of the equation and $\phi_i(t)$ are called the eigenfunctions.

Using Mercer's theorem, the correlation function of the background may be expressed as

$$R_B(t, u) = \sum_k^{\infty} \lambda_k \phi_k(t) \phi_k^*(u) \quad (5C)$$

The K-L expansion of $B(t)$ is

$$B(t) = \sum_k^{\infty} b_k \phi_k(t)$$

with

$$b_k = \int_0^T B(t) \phi_k^*(t) dt \quad 0 \leq t \leq T \quad (6C)$$

where the coefficients, b_k , are uncorrelated and because $B(t)$ is Gaussian the coefficients are statistically independent with means μ_k and variances λ_k .

Also expanding $A(t)$,

$$A(t) = \sum_k^{\infty} a_k \phi_k(t)$$

with

$$a_k = \int_0^T A(t) \phi_k^*(t) dt, \quad 0 \leq t \leq T. \quad (7C)$$

Rewriting in terms of the expansions

$$I = E_B \left[\exp \left\{ \int_0^T \left(\frac{1}{2} \sum_n^{\infty} \sum_k^{\infty} a_n b_k^* + \frac{1}{2} \sum_n^{\infty} \sum_k^{\infty} a_n^* b_k \right) \phi_k(t) \phi_n^*(t) dt - c \int_0^T \sum_n^{\infty} \sum_k^{\infty} b_n b_k^* \phi_k(t) \phi_n^*(t) dt \right\} \right]. \quad (8C)$$

Using

$$\delta_{xy} = \int_0^T \phi_x(t) \phi_y^*(t) dt$$

$$I = E_{bn} \left[\exp \left\{ \sum_n^{\infty} \left(\frac{1}{2} a_n b_n^* + \frac{1}{2} a_n^* b_n \right) - c \sum_n^{\infty} b_n b_n^* \right\} \right] \quad (9C)$$

Using the independence of the coefficients

$$\begin{aligned} I &= \prod_n^{\infty} E_{bn} \exp \left\{ \frac{1}{2} a_n b_n^* + \frac{1}{2} a_n^* b_n - c |b_n|^2 \right\} \\ &= \prod_n^{\infty} \exp \left\{ \frac{|a_n|^2}{4c} \right\} E_{bn} \exp \left\{ -c \left| b_n - \frac{a_n}{2c} \right|^2 \right\} \end{aligned} \quad (10C)$$

For Gaussian random variables

$$E(w_{xx}^*) = \frac{\exp[w m_x m_x^* / (1 - 2w\lambda)]}{1 - 2w\lambda}$$

where

$$m_x = E(x)$$

$$\lambda = E[(x - m_x)(x^* - m_x^*)] \quad (11C)$$

and w is a constant.

$$\text{Let } x = b_n - a_n/2c$$

$$\text{and } m_x = \mu_n - a_n/2c$$

then

$$E_{bn} \exp \left\{ -c \left| b_n - \frac{a_n}{2c} \right|^2 \right\} = \frac{\exp \left\{ -c \left| \mu_n - a_n/2c \right|^2 (1 + 2c\lambda_n) \right\}}{(1 + 2c\lambda_n)} \quad (12c)$$

Substituting (12C) into (10C), and separating terms

$$\begin{aligned}
I = & \prod_n^B (1 + 2c\lambda_n)^{-1} \exp \left\{ \frac{1}{2} \sum_n^\infty \frac{|a_n|^2 \lambda_n}{1 + 2c\lambda_n} \right\} \\
& \cdot \exp \left\{ - \frac{c}{2} \sum_n^\infty \frac{\mu_n^* (\mu_n - a_n/c)}{1 + 2c\lambda_n} \right\} \\
& \cdot \exp \left\{ - \frac{c}{2} \sum_n^\infty \frac{\mu_n (\mu_n^* - a_n^*/c)}{1 + 2c\lambda_n} \right\} \quad (13C)
\end{aligned}$$

This result can be written in closed form by using the definition $A_n = (a, \phi_n)$

$$\frac{1}{2} \sum_n^\infty \frac{|a_n|^2 \lambda_n}{1 + 2c\lambda_n} = \frac{N}{4M} \int_0^T dt_1 A(t_1) \int_0^T dt_2 A(t_2) q(t_1, t_2) \quad (14C)$$

where

$$q(t_1, t_2) = \frac{2M}{N} \sum_n^\infty \frac{\lambda_n}{1 + 2c\lambda_n} \phi_n(t_1) \phi_n^*(t_2) \quad (15C)$$

is such that operating on $q(t_1, t_2)$ with

$$\int_0^T \int_0^T \left[R_B(t_1, t_2) + \frac{1}{\sqrt{M}} R_N(T_1, t_2) \right] (\cdot) dt_1 dt_2 \quad (16C)$$

and using Mercer's theorem yields

$$\frac{N}{2M} q(t_1, t_2) + \int_0^T R_B(T_2, t_3) q(t_3, t_1) dt_3 = R_B(T_1, t_2) \quad (17C)$$

Likewise,

$$\begin{aligned}
& - \frac{c}{2} \sum_n^\infty \frac{\mu_n^* (\mu_n - a_n/c) + \mu_n (\mu_n^* - a_n^*/c)}{1 + 2c\lambda_n} \\
& = \frac{1}{2} \int_0^T \left(m_b(t) - \frac{A(t)}{c} \right) h(t) dt \quad (18C)
\end{aligned}$$

where

$$h(t) = \sum_n^{\infty} \frac{2\mu_n}{1 + 2c\lambda_n} \phi_n(t) \quad (19C)$$

such that

$$Nh(t) + 2M \int_0^T R_B(t_3, t) h(t_3) dt_3 = Mm_b(t) \quad (20C)$$

Taking the logarithm of both sides of equation (13C) and using the equations above

$$\begin{aligned} \ln I &= \sum_n^{\infty} (1 + 2c\lambda_n)^{-1} \\ &+ \frac{N}{4M} \int_0^T dt_1 \left\{ \frac{2}{N} \sum_{\ell=1}^M (Z_{\ell}(t_1) - S_{\ell}(t_1)) \right\} \\ &\cdot \int_0^T dt_2 \left\{ \frac{2}{N} \sum_{m=1}^M (Z_m(t_2) - S_m(t_2)) \right\} q(t_1, t_2) \\ &- \int_0^T \left[m_b(t) - \frac{N}{M} \left\{ \frac{2}{N} \sum_{\ell=1}^M (Z_{\ell}(t) - S_{\ell}(t)) \right\} \right] h(t) dt \\ \ln I &= \sum_n^{\infty} (1 + 2b\lambda_n)^{-1} \\ &+ \frac{1}{NM} \int_0^T \int_0^T \left[\sum_{\ell=1}^M Z_{\ell}(t_1) \sum_{m=1}^M Z_m(t_2) - \sum_{\ell=1}^M S_{\ell}(t_1) \sum_{m=1}^M Z_m(t_2) \right. \\ &- \sum_{m=1}^M S_m(t_2) \sum_{\ell=1}^M Z_{\ell}(t_1) + \sum_{\ell=1}^M S_{\ell}(t_1) \sum_{m=1}^M S_m(t_2) \left. \right] q(t_1, t_2) dt_1 dt_2 \\ &- \int_0^T m_b(t) h(t) dt \\ &+ \frac{2}{M} \int_0^T \sum_{\ell=1}^M (Z_{\ell}(t) - S_{\ell}(t)) h(t) dt. \end{aligned} \quad (21C)$$

The likelihood ratio desired is

$$\Lambda_{12}(\{Z_n\}) = \exp \left\{ \frac{2}{N} \sum_{n=1}^M \int_0^T Z_n(t) S_n(t) dt - \frac{1}{N} \sum_{n=1}^M \int_0^T S_n^2(t) dt \right\} \cdot I. \quad (22C)$$

Taking the logarithm of both sides and substituting the expression for $\ell_n(I)$,

$$\begin{aligned} \ln \Lambda_{12}(\{Z_n\}) &= \frac{2}{N} \sum_{n=1}^M \int_0^T Z_n(t) S_n(t) dt \\ &- \frac{1}{N} \sum_{n=1}^M \int_0^T S_n^2(t) dt \\ &+ \sum_k^{\infty} \ell_n \left(1 + \frac{2M}{N} \lambda_k \right)^{-1} \\ &+ \frac{1}{NM} \int_0^T \int_0^T \left\{ \sum_{\ell=1}^M Z_{\ell}(t_1) \sum_{m=1}^M Z_m(t_2) \right. \\ &- \sum_{\ell=1}^M S_{\ell}(t_1) \sum_{m=1}^M Z_m(t_2) - \sum_{m=1}^M S_m(t_2) \sum_{\ell=1}^M Z_{\ell}(t_1) \\ &+ \left. \sum_{\ell=1}^M S_{\ell}(t_1) \sum_{m=1}^M S_m(t_2) \right\} q(t_1, t_2) dt_1 dt_2 \\ &- \int_0^T m_b(t) h(t) dt + \frac{2}{M} \int_0^T \sum_{\ell=1}^M (Z_{\ell}(t) - S_{\ell}(t)) h(t) dt \end{aligned} \quad (23C)$$

APPENDIX D

KARHUNEN-LOEVE REPRESENTATION OF EQUIVALENT SIGNAL-TO-NOISE RATIO

The variance of the threshold statistic

$$W = \sum_{n=1}^M \int_0^T z_n(t) \bar{q}(t) dt$$

where

$$\bar{q}(t) = \frac{2}{N} \left[\bar{f}(t) - \int_0^T \bar{f}(u) q(u, t) du \right] \quad (1D)$$

under hypotheses H_0 and H_1 is

$$\text{VAR} = \frac{NM}{z} \int_0^T \bar{q}^2(t) dt + M^2 \int dt \cdot \bar{q}(t) \int du \bar{q}(u) R_y(t, u) \quad (2D)$$

Substituting (1D) into the first term of the variance expression

$$\begin{aligned} \frac{NM}{z} \int_0^T \bar{q}^2(t) dt = \frac{2M}{N} \int_0^T dt \left[\bar{f}^2(t) - 2\bar{f}(t) \int_0^T \bar{f}(u) q(t, u) du \right. \\ \left. + \int_0^T \int_0^T \bar{f}(u) \bar{f}(v) q(t, u) q(t, v) dudv \right] \quad (3D) \end{aligned}$$

Using the Karhunen-Loeve representation

$$\begin{aligned} \frac{NM}{z} \int_0^T \bar{q}^2(t) dt = \frac{2M}{N} \left[\sum_k^\infty \sum_\ell^\infty \bar{f}_k \bar{f}_\ell^* \int_0^T \phi_k(t) \phi_\ell^*(t) dt \right. \\ \left. - 2 \sum_k^\infty \sum_\ell^\infty \bar{f}_k \bar{f}_\ell^* \frac{\frac{2M}{N} \lambda_n}{1 + \frac{2M}{N} \lambda_n} \int_0^T \phi_k(t) \phi_m^*(t) dt \int_0^T \phi_m(u) \phi_\ell^*(u) du \right] \end{aligned}$$

$$+ \sum_k^{\infty} \sum_{\ell}^{\infty} \sum_m^{\infty} \sum_n^{\infty} \bar{f}_k \bar{f}_{\ell}^* \frac{\frac{2m}{N} \lambda_m}{1 + \frac{2m}{N} \lambda_m} \frac{\frac{2m}{N} \lambda_n}{1 + \frac{2m}{N} \lambda_n} \int_0^T \phi_m(t) \phi_n^*(t) dt$$

$$\left[\int_0^T \phi_k(u) \phi_m^*(u) dt \int_0^T \phi_n(v) \phi_{\ell}^*(v) dt \right] \quad (4D)$$

Using

$$\delta_{nk} = \int_0^T \phi_n(t) \phi_k^*(t) dt,$$

then

$$\frac{NM}{z} \int_0^T \bar{q}^2(t) dt = \frac{2M}{N} \sum_k^{\infty} \bar{f}_k \bar{f}_k^* \left(1 - 2 \frac{\frac{2M}{N} \lambda_k}{1 + \frac{2M}{N} \lambda_k} + \left(\frac{\frac{2M}{N} \lambda_k}{1 + \frac{2M}{N} \lambda_k} \right)^2 \right)$$

$$= \frac{2M}{N} \sum_k^{\infty} \bar{f}_k \bar{f}_k^* \left(\frac{1}{1 + \frac{2M}{N} \lambda_k} \right)^2. \quad (5D)$$

The second term may be expressed in a similar manner to give

$$\text{VAR} = \frac{2M}{N} \sum_k^{\infty} \bar{f}_k \bar{f}_k^* \left(\frac{1}{1 + \frac{2M}{N} \lambda_k} \right)^2 + \left(\frac{2M}{N} \right)^2 \sum_k^{\infty} \bar{f}_k \bar{f}_k^* \left(\frac{1}{1 + \frac{2M}{N} \lambda_k} \right)^2 \lambda_k$$

$$\text{VAR} = \frac{2M}{N} \sum_k^{\infty} \bar{f}_k \bar{f}_k^* \frac{1}{1 + \frac{2M}{N} \lambda_k}. \quad (6D)$$

The equivalent signal to noise ratio in Part II is

$$d = \frac{\sum_{n=1}^M \bar{a}_n \int_0^T \bar{f}(t) \bar{q}(t) dt}{\sqrt{\text{VAR}}}. \quad (7D)$$

The K-L representation of the numerator is

$$\sum_{n=1}^M \bar{a}_n \int_0^T \bar{f}(t) \bar{q}(t) dt = \sum_{n=1}^M \bar{a}_n \left[\frac{2}{N} \sum_k^{\infty} |\bar{f}_k|^2 / \left(1 + \frac{2M}{N} \lambda_k \right) \right]. \quad (8D)$$

d may now be represented by dividing (8D) by the square root of (6D)

$$d = \frac{\frac{2}{N} \sum_{n=1}^M a_n \sum_k |\bar{f}_k|^2 / (1 + \frac{2M}{N} \lambda_k)}{\left[\frac{2M}{N} \sum_k |\bar{f}_k|^2 / 1 + \frac{2M}{N} \lambda_k \right]^{\frac{1}{2}}}$$

$$d = \frac{\frac{1}{M} \sum_{n=1}^M a_n \sqrt{M} \left[\sum_k |\bar{f}_k|^2 / (1 + \frac{2M}{N} \lambda_k) \right]^{\frac{1}{2}}}{\sqrt{N/2}} . \quad (9D)$$

APPENDIX E

NON-ZERO TERMS FOR NUMERICAL INTEGRATION

Equation (5.5) for the radiance function for a point target may be written as

$$I = \frac{j^2}{\pi} \int e^{-x^2-y^2} e^{-j(P_x+Q_y)} \frac{\sin \alpha x}{x} \frac{\sin \beta y}{y} \cdot e^{-jn\phi} J_n \left(c \sqrt{x^2+y^2} \right) dx dy$$

where

$$\alpha = w/\sqrt{2}\sigma$$

$$\beta = h/\sqrt{2}\sigma$$

$$c = \sqrt{2}\rho/\sigma$$

$$P = \frac{\sqrt{2}}{\sigma} (r_x - x_0)$$

$$Q = \frac{\sqrt{2}}{\sigma} (r_y - y_0)$$

and

$$\phi = \tan^{-1} y/x \quad (1E)$$

Let $E(x,y)$ be that part of the integral that is even about both planar axis which is

$$E(x,y) = \frac{j^n}{\pi} e^{-x^2-y^2} \frac{\sin \alpha x}{x} \frac{\sin \beta y}{y} J_n \left(c \sqrt{x^2+y^2} \right). \quad (2E)$$

Using Euler's relation the integral becomes

$$I = \int E(x,y) [\cos(Px+Qy) + j\sin(Px+Qy)] [\cos n\phi - j\sin n\phi] dx dy \quad (3E)$$

Using trigonometric identities

$$I = \int E(x,y) \sum_{i=1}^{\infty} T_i dx dy$$

where

$$T_1 = \cos Px \cos Qy \cos n\phi$$

$$T_2 = -\sin Px \sin Qy \cos n\phi$$

$$T_3 = -\sin Px \cos Qy \sin n\phi$$

$$T_4 = -\cos Px \sin Qy \sin n\phi$$

$$T_5 = -j \sin Px \cos Qy \cos n\phi$$

$$T_6 = -j \cos Px \sin Qy \cos n\phi$$

$$T_7 = -j \cos Px \cos Qy \sin n\phi$$

$$T_8 = +j \sin Px \sin Qy \sin n\phi \quad (4E)$$

To save computation time it is necessary to determine which of the eight integrals are always zero and for which n they are zero.

Observe that

$$\begin{aligned} \cos n\phi &= R_e e^{jn\phi} = R_e (e^{j\phi})^n \\ &= R_e (\cos\phi + j \sin\phi)^n \\ &= R_e \left(\frac{x}{\sqrt{x^2+y^2}} + j \frac{y}{\sqrt{x^2+y^2}} \right)^n \\ &= \left(\frac{1}{x^2+y^2} \right)^{n/2} R_e (x + jy)^n. \end{aligned} \quad (5E)$$

Likewise

$$\sin n\phi = \left(\frac{1}{x^2+y^2} \right)^{n/2} I_m(x+jy)^n . \quad (6E)$$

The first term in brackets is always even and may be made part of $E(x,y)$. The second term in brackets may be expanded by the binomial expansion with the general term

$$(x)^{n-k} (jy)^k . \quad (7E)$$

The first integral of (4E) becomes

$$I_1 = \int E(x,y) \cos Px \cos Qy R_e(x+jy)^n dx dy \quad (8E)$$

For I_1 to be non-zero, $Re(x+jy)^n$ must be even in x and even in y . From (7E) this is true only of even n ; for odd n , I_1 will always be zero.

Examining the other seven integrals yields

$$I = \begin{cases} \int E(x,y) [\cos Px \cos Qy \cos n\phi \\ \quad + j \sin Px \sin Qy \sin n\phi] dx dy & n \text{ even} \\ \int E(x,y) [\cos Px \sin Qy \sin n\phi \\ \quad + j \sin Px \cos Qy \cos n\phi] dx dy & n \text{ odd} \end{cases} \quad (9E)$$

Observing that symmetry about the x - and y -axis is necessary for this integral to be non-zero and integrating only when the integral is non-zero permits one to integrate only over the first quadrant.

APPENDIX F
SUMMATION CHECK

The signal for a point target was shown in Part II to be

$$H(\omega_0 t) = \int N'(\underline{r}) \tau(\underline{r} - \underline{\rho}(t)) d^2 \underline{r} . \quad (1F)$$

Assuming an infinite image plane, $H(\omega_0 t)$ may be written in terms of the Fourier transform as

$$H(\omega_0 t) = \int N'(\underline{k}) \tau^*(\underline{k}) e^{-j2\pi \underline{k} \cdot \underline{\rho}(t)} d^2 \underline{k} \quad (2F)$$

For a rectangular detector (2F) may be written as

$$H(\omega_0 t) = \int e^{-2\pi^2 \sigma^2 (k_x^2 + k_y^2)} \frac{\sin \pi w k_x}{\pi k_x} \frac{\sin \pi h k_y}{\pi k_y} \\ \cdot \int e^{j2\pi \underline{k} \cdot (\underline{\rho}(t) - \underline{r}_0)} \cdot e^{-j2\pi (k_x x_0 + k_y y_0)} d^2 \underline{k} \quad (3F)$$

Let

$$x = \sqrt{2} \sigma \pi k_x$$

$$y = \sqrt{2} \sigma \pi k_y$$

and noting the integral may be separated into twoparts

$$H(\omega_0 t) = \frac{1}{\pi} \int e^{-x^2} \sin \frac{wx}{\sqrt{2}\sigma} e^{j\frac{\sqrt{2}}{\sigma} x(\rho \cos \omega_0 t - (r_x - x_0))} dx \\ \cdot \frac{1}{\pi} \int e^{-y^2} \frac{\sin \frac{hy}{\sqrt{2}\sigma}}{y} e^{j\frac{\sqrt{2}}{\sigma} y(\rho \sin \omega_0 t - (r_y - y_0))} dy . \quad (4F)$$

Since the integration is $-\infty$ to $+\infty$ only even integrands will be non-zero. Rewriting (4F)

$$H(\omega_0 t) = \frac{2}{T} \int_0^\infty e^{-x^2} \frac{\sin \frac{wx}{\sqrt{2}\sigma}}{x} \cos\left(\frac{\sqrt{2}}{\sigma} x[\rho \cos \omega_0 t - (r_x - x_0)]\right) dx$$

$$\cdot \frac{2}{\pi} \int_0^\infty e^{-y^2} \frac{\sin \frac{hy}{\sqrt{2}\sigma}}{y} \cos\left(\frac{\sqrt{2}}{\sigma} y[\rho \sin \omega_0 t - (r_y - y_0)]\right) dy. \quad (5F)$$

The general form of the integral is

$$R = R(B) = \frac{2}{\pi} \int_0^\infty e^{-u^2} \frac{\sin Bu}{u} \cos(Cu) du. \quad (6F)$$

Differentiating with respect to B

$$\frac{dR(B)}{dB} = \frac{2}{\pi} \int_0^\infty e^{-u^2} \cos Bu \cos Cu du. \quad (7F)$$

But the solution to (7F) is known [2]:

$$\frac{dR(B)}{dB} = \frac{1}{2\sqrt{\pi}} \left\{ e^{-\frac{(B-C)^2}{4}} + e^{-\frac{(B+C)^2}{4}} \right\}. \quad (8F)$$

Since the constant of integration $R(0) = 0$,

$$R(B) = \frac{1}{2\sqrt{\pi}} \left[\int_0^\infty e^{-\frac{(v-c)^2}{4}} dv + \int_0^\infty e^{-\frac{(w+c)^2}{4}} dw \right] \quad (9F)$$

Let

$$P = \frac{v-c}{2}$$

and

$$Q = \frac{w+c}{2}$$

then

$$\begin{aligned}
 R(B) &= \frac{1}{2} \left\{ \frac{2}{\sqrt{\pi}} \int_{-C/2}^{\frac{B-C}{2}} e^{-P^2} dP + \frac{2}{\sqrt{\pi}} \int_{-C/2}^{\frac{B+C}{2}} e^{-Q^2} dQ \right\} \\
 &= \frac{1}{2} \left\{ \text{Erf} \left(\frac{B-C}{2} \right) + \text{Erf} \left(\frac{B+C}{2} \right) \right\} \quad (10F)
 \end{aligned}$$

where

$$\text{Erf}(z) = \frac{2}{\sqrt{\pi}} \int_0^z e^{-y^2} dy . \quad (11F)$$

Substituting the result (10F) into (5F)

$$\begin{aligned}
 H(\omega_0 t) &= \frac{1}{4} \left\{ \text{Erf} \left(\frac{\sqrt{2}}{T} [\rho \cos \omega_0 t - r_x + x_0] + \frac{1}{\sqrt{2}\sigma} w \right) \right. \\
 &\quad - \text{Erf} \left(\frac{\sqrt{2}}{\sigma} [\rho \cos \omega_0 t - r_x + x_0] - \frac{1}{\sqrt{2}\sigma} w \right) \\
 &\quad + \text{Erf} \left(\frac{\sqrt{2}}{\sigma} [\rho \sin \omega_0 t - r_y + y_0] + \frac{1}{\sqrt{2}\sigma} h \right) \\
 &\quad \left. - \text{Erf} \left(\frac{\sqrt{2}}{\sigma} [\rho \sin \omega_0 t - r_y + y_0] - \frac{1}{\sqrt{2}\sigma} h \right) \right\}. \quad (12F)
 \end{aligned}$$

The mean square voltage of the background may also be solved in a like manner.

From Part V, the mean square voltage was shown to be

$$\bar{e}_B^2 = \int |\tau(\tilde{k})|^2 |F_0(\tilde{k})|^2 W_B(\tilde{k}) d^2 \tilde{k} \quad (13F)$$

which for a rectangular detector becomes

$$\bar{e}_B^2 = \sigma_\beta^2 \cdot 2\alpha \int \frac{\sin^2(\pi k_x W)}{\pi^2 k_x^2} \frac{e^{-4\pi^2 \sigma^2 k_x^2}}{\alpha^2 + (2\pi k_x)^2} dk_x$$

$$\sigma_B \cdot 2\beta \int \frac{\sin^2(\pi k_y h)}{\pi^2 k_y^2} \frac{e^{-4\pi^2 \sigma^2 k_y^2}}{\beta^2 + (2\pi k_y)^2} dk_y \quad (14F)$$

Letting

$$t = 2\pi k$$

the general form of the integral to be solved is

$$R(\mu) = \frac{1}{\pi} \int_0^\infty \frac{\sin^2(\mu t/2)}{t^2/4} \frac{e^{-\sigma^2 t^2}}{\alpha^2 + t^2} dt \quad (15F)$$

Taking the first and second derivatives one has

$$\frac{dR(\mu)}{d\mu} = \frac{1}{\pi} \int_0^\infty \frac{\sin(2\mu t)}{t} \frac{e^{-\sigma^2 t^2}}{\alpha^2 + t^2} dt \quad (16F)$$

and

$$\frac{d^2 R(\mu)}{d\mu^2} = \frac{2}{\pi} \int_0^\infty \frac{\cos(2\mu t)}{\alpha^2 + t^2} e^{-\sigma^2 t^2} dt \quad (17F)$$

The solution to the second derivative is known [2]:

$$\begin{aligned} \frac{d^2 R(\mu)}{d\mu^2} = \frac{e^{\sigma^2 \alpha^2}}{2\alpha} \left[e^{-\alpha\mu} \operatorname{Erfc} \left(\alpha\sigma - \frac{\mu}{2\sigma} \right) \right. \\ \left. + e^{\alpha\mu} \operatorname{Erfc} \left(\alpha\sigma + \frac{\mu}{2\sigma} \right) \right] \end{aligned} \quad (18F)$$

where

$$\operatorname{Erfc}(z) = \frac{2}{\sqrt{\pi}} \int_z^\infty e^{-y^2} dy \quad (19F)$$

is the complimentary error function.

With lengthy and tedious calculations it can be shown by using the relation

$$R(\mu) = \int_0^\mu dv \left[\int_0^v F(w) dw \right] \quad (20F)$$

with initial conditions equal to zero and

$$F(w) = \frac{d^2 R(\mu)}{d\mu^2} \quad (21F)$$

that

$$\begin{aligned} R(\mu) = & \frac{\mu}{\alpha^2} \left[1 - \operatorname{Erfc} \left(\frac{\mu}{2\sigma} \right) - \frac{2\sigma}{\sqrt{\pi}u} \left(1 - e^{-(\mu/2\sigma)^2} \right) \right] \\ & + \frac{e^{\sigma^2 \alpha^2}}{2\alpha^3} \left[e^{\alpha\mu} \operatorname{Erfc} \left(\alpha\sigma + \frac{\mu}{2\sigma} \right) \right. \\ & + e^{-\alpha\mu} \operatorname{Erfc} \left(\alpha\sigma - \frac{\mu}{2\sigma} \right) \\ & \left. - 2 \operatorname{Erfc} (\alpha\sigma) \right] \end{aligned} \quad (22F)$$

The mean square voltage thus becomes

$$\bar{e}_B^2 = 4\alpha\beta\sigma_B^2 R(w;\alpha)R(h;\beta) \quad (23F)$$

APPENDIX G - CALCULATED COEFFICIENTS

k	β_k	$\text{Re} [H_k(\vec{r}_0)]$	$I_m[H_k(\vec{r}_0)]$	$\text{Re} [H_k]$	$I_m [H_k]$
0	1.595402650-01	1.061436980-02	0.0	9.567495280-03	0.0
1	1.013595010-01	-1.060998540-02	0.0	-8.943580190-03	0.0
2	1.565698180-02	1.059048110-02	0.0	-7.339049060-03	0.0
3	2.565698180-02	-1.055309480-02	0.0	-5.345911170-03	0.0
4	1.345674690-02	1.049249150-02	0.0	-3.503965200-03	0.0
5	7.811798200-03	-1.041447230-02	0.0	-2.093884650-03	0.0
6	5.056152240-03	1.032658290-02	0.0	-1.153693110-03	0.0
7	3.548767670-03	-1.023710170-02	0.0	-5.914255920-04	0.0
8	2.603966130-03	1.0013710170-02	0.0	-2.840736630-04	0.0
9	1.952342900-03	-1.001806960-02	0.0	-1.285358490-04	0.0
10	1.486512530-03	9.8664556920-03	0.0	-5.501636690-05	0.0
11	1.152092890-03	-9.689057150-03	0.0	-2.234935440-05	0.0
12	9.102821760-04	9.507762740-03	0.0	-8.339829000-06	0.0
13	7.306937930-04	-9.345730870-03	0.0	-3.185540300-06	0.0
14	5.9221218820-04	9.1973224900-03	0.0	-1.122360500-06	0.0
15	4.820620460-04	-9.027501930-03	0.0	-3.725174180-07	0.0
16	3.9383391550-04	8.800019980-03	0.0	-1.223773100-07	0.0
17	3.233341580-04	-8.528254070-03	0.0	-3.7798188670-08	0.0
18	2.670342850-04	8.276802050-03	0.0	-1.1330933520-08	0.0
19	2.216413290-04	-8.095520360-03	0.0	-3.2537333590-09	0.0
20	1.844381670-04	7.9468559010-03	0.0	-8.9977383590-10	0.0
21	1.535616710-04	-7.718267950-03	0.0	-2.400047440-10	0.0
22	1.278681530-04	7.3736642140-03	0.0	-6.180585160-11	0.0
23	1.065734000-04	-7.037064830-03	0.0	-1.538011190-11	0.0
24	8.972745590-05	6.787143380-03	0.0	-3.701729760-12	0.0
25	6.217242790-05	-6.6787143380-03	0.0	-8.524683440-13	0.0
26	5.1913333850-05	6.521018750-03	0.0	-1.946869020-13	0.0
27	4.326807300-05	-6.029920580-03	0.0	-4.261203350-14	0.0
28	3.606692340-05	5.716740220-03	0.0	-9.050288080-15	0.0
29	3.004243950-05	-5.788110610-03	0.0	-1.866579100-15	0.0
30	2.501366890-05	5.673940540-03	0.0	-3.741026050-16	0.0
31	2.080139220-05	-4.975521320-03	0.0	-7.291044630-17	0.0
32	1.7226430060-05	4.603569170-03	0.0	-1.382694600-17	0.0
33	1.429805020-05	-4.705050700-03	0.0	-2.35592914030-18	0.0
34	1.182094870-05	4.472553870-03	0.0	-4.59291473080-19	0.0
35	9.760252520-06	-4.408003460-03	0.0	-8.054273080-20	0.0
36	8.0477791020-06	4.467845180-03	0.0	-1.377614770-20	0.0
37	6.54370995540-06	-1.746571140-03	0.0	-2.2994456340-21	0.0
38	5.437089300-06	1.963190140-03	0.0	-3.747505420-22	0.0
39		-5.963190140-03	0.0	-5.966157790-23	0.0

4	4	5	1	7	3	9	7	0	-	6
3	6	3	6	4	9	6	9	7	-	6
2	9	6	4	7	0	2	5	-	6	
2	4	1	2	2	7	2	5	-	6	
1	9	5	8	0	1	2	1	-	6	
1	5	8	4	7	7	1	0	-	6	
1	2	7	8	0	1	0	3	-	6	
1	0	2	9	8	4	2	2	-	6	
1	8	2	5	9	8	6	4	-	6	
6	1	3	8	2	2	8	4	-	6	
5	2	8	0	6	6	7	6	-	6	
4	2	0	2	9	1	8	1	-	6	
3	3	3	5	9	5	3	8	-	6	
2	6	3	5	4	9	3	5	-	6	
2	0	7	7	3	6	4	6	-	6	
1	6	3	2	6	0	0	6	-	6	
1	2	7	8	8	5	8	7	-	6	
9	1	2	8	1	2	3	2	-	6	
7	7	5	9	5	9	8	4	-	6	
6	0	9	5	1	0	1	8	-	6	
4	6	3	7	4	8	6	0	-	6	
3	5	6	6	0	4	1	3	-	6	
2	7	3	1	6	2	6	5	-	6	
2	0	8	3	4	6	4	3	-	6	
1	5	8	1	7	7	9	2	-	6	
1	1	9	5	3	7	7	5	-	6	
8	9	3	7	9	3	8	3	-	6	
6	7	3	7	0	5	1	5	-	6	
5	0	2	2	7	7	0	0	-	6	
3	7	2	4	8	9	2	7	-	6	
2	7	4	6	4	8	6	4	-	6	
2	0	1	3	1	4	2	8	-	6	
1	4	6	7	0	5	8	2	-	6	
7	6	5	2	3	4	2	2	-	6	
5	4	7	0	4	4	2	2	-	6	
3	7	5	8	7	2	7	4	-	6	
2	7	2	8	7	3	9	9	-	6	
1	9	0	3	1	6	4	9	-	6	
1	3	1	5	9	0	2	0	-	6	
9	0	1	3	9	4	0	2	-	6	
6	1	0	8	9	0	3	4	-	6	
2	7	0	1	6	2	5	8	-	6	
1	7	6	0	2	1	0	1	-	6	
1	1	3	1	0	5	2	1	-	6	
7	1	6	4	8	9	0	3	-	6	
4	7	0	3	1	7	7	7	-	6	

APPENDIX H

COMPUTER PROGRAM TO CALCULATE THE FOURIER COEFFICIENTS OF THE BACKGROUND CORRELATION FUNCTION, A POINT TARGET AND AN AVERAGED TARGET OVER A GAUSSIAN POINTING ERROR FOR A ROTATING OPTICAL SYSTEM WITH A RECTANGULAR DETECTOR.

AA = BACKGROUND CORRELATION FUNCTION COEFF(ZERO ORDER)
 ALFA = BACKGROUND CORRELATION COEFFICIENTS (VECTOR)
 FNO = SIGNAL FOURIER COEFFICIENT (ZERO ORDER)
 FN = SIGNAL FOURIER COEFFICIENTS (VECTOR)
 FAVGO = AVERAGED SIGNAL COEFF (ZERO ORDER)
 FAVG = AVERAGED SIGNAL FOURIER COEFF (VECTOR)
 RHO = ROTATION RADIUS
 SIG = STANDARD DEVIATION OF BLUR CIRCLE
 WI = WIDTH OF DETECTOR (X-DIRECTION)
 H = HEIGHT OF DETECTOR (Y-DIRECTION)
 AL = INVERSE CORR LENGTH OF BACKGROUND (X-DIRECTION)
 BE = INVERSE CORR LENGTH OF BACKGROUND (Y-DIRECTION)
 PO = STANDARD DEVIATION OF POINTING ERROR
 XO = DETECTOR COORDINATE X-DIRECTION
 YO = DETECTOR COORDINATE Y-DIRECTION
 RX = POINT TARGET COORDINATE X-DIRECTION
 RY = POINT TARGET COORDINATE Y-DIRECTION
 R, RANGLE = POLAR COORDINATES OF POINT TARGET
 NS = NUMBER OF FIRST COEFFICIENT DESIRED
 NUM = NUMBER OF LAST COEFFICIENT DESIRED
 IAVE=1 "SIGNAL" WILL CALCULATE AVERAGE SIGNAL COEFF
 IAVE=0 "SIGNAL" WILL CALCULATE POINT TARGET COEFF

IMPLICIT REAL*8 (A-H,O-Z)
 DIMENSION ALFA(120)
 COMPLEX*16 FN(120), FNO, FAVG(120), FAVGO
 COMMON /DTPRM/ RHO, SIG, WI, H, AL, BE, RX, RY, XO, YO
 COMMON /AVPRM/ NUM, IAVE, PO
 COMMON /START/ NS
 COMMON /ANGL/ RANGL
 READ 2, RHO, SIG, WI, H, AL, BE
 READ 2, XO, YO, R, ANGL
 READ 3, NS, NUM, IAVE, PO
 RANGL=0.0174500*ANGL
 RX=R*DCOS(RANGL)
 RY=R*DSIN(RANGL)
 RANGL=DATAN2(RY-YO, RX-XO)
 CALL SUMCK
 CALL BKGRN(ALFA, AA)
 CALL SIGNAL(FN, FNO)
 WRITE (9) RHO, SIG, WI, H, AL, BE, RX, RY, XO, YO, PO
 IAVE=1
 IF(IAVE.EQ.1) RX=0.000
 IF(IAVE.EQ.1) RY=0.000
 CALL SUMCK
 CALL SIGNAL(FAVG, FAVGO)
 WRITE (9) FNO, FN, AA, ALFA
 WRITE (9) FAVGO, FAVG
 FORMAT(10I5)
 FORMAT(8D10.0)
 FORMAT(3I5, 1D10.0)
 FORMAT(8E10.4)
 STOP
 END

SUBROUTINE BKGRN(VP,V)

SUBROUTINE BKGRN COMPUTES THE COEFFICIENTS OF THE
BACKGROUND CORRELATION FUNCTION UP TO 120 ORDERS.
HIGHER ORDERS MAY EASILY BE COMPUTED BY ONLY CHANGING
THE DIMENSION STATEMENTS.

ZP = VALUES OF RADII FOR DIFFERENT ANNULI
Z = WORKING VECTOR FOR RADII
MAXR = MAXIMUM RADIUS OF OUTER ANNULUS
NIZ1 = DIMENSION OF ZP
VP = WORKING VECTOR IN FIRST PART AND RETURN VECTOR
IN THE SECOND PART
V = ZERO ORDER COEFFICIENT

IMPLICIT REAL*8 (A-H,O-Z)
DIMENSION VP(1),DN(50,120)
DIMENSION DI(50),ZP(20),Z(50)
DIMENSION R(24),W(24),TH(25)
COMMON /AVPRM/ NUM,IAVE,PO
COMMON /DTPRM/ RHO,SIG,WI,H,AL,BE,RX,RY,XO,YO
COMMON /BKPRM/ A,B,C,D
COMMON /NFIRST/ NFIRST
DATA MAXR/4/,NR/1/,NIZ1/20/
DATA ZP/0.0D0,1.2D0,2.4D0,5.5D0,8.6D0,11.8D0,15.0D0,20.
1D0,25.0D0,30.0D0,40.0D0,50.0D0,60.0D0,70.0D0,80.0D0,
290.0D0,100.0D0,150.0D0,200.0D0,400.0D0/
NFIRST=0
PI = DARCOS(-1.0D0)

CALCULATE CONSTANTS FOR INTEGRAL

CONST = AL*BE*SIG**2/PI/PI
A=WI/2.0D0/SIG
B=H/2.0D0/SIG
C = (AL*SIG)**2
D = (BE*SIG)**2
E = RHO/SIG

SET ANNULI FOR SPECIFIC PARAMETERS

150 DO 150 I=1,NIZ1
Z(I)=ZP(I)/E
I = 0
IF(Z(NIZ1).GT.MAXR)GO TO 210
DZ = PI/NR/E
MMM=50-NIZ1
DO 200 I=1,MMM
Z(I+NIZ1) = Z(NIZ1) + I*DZ
IF(Z(I+NIZ1).GT.MAXR)GO TO 210
200 CONTINUE

MAX = NUMBER OF ANNULI

210 MAX=1+NIZ1-1

PRINT 4,RHO,SIG,H,WI,AL,BE,A,B,C,D,E,DZ
PRINT 4,(Z(I),I=1,MAX)
DO 300 I=1,MAX

COMPUTE RADII,WEIGHTS AND ANGLES FOR EACH ANNULUS


```

C      CALL WAA(Z(I),Z(I+1),R,TH,W,NPQ)
C
C      NFIRST=1
C      DI(I) = 0.DO
C      DO 115 NN=1,NUM
115    DN(I,NN) = 0.DO
C
C      COMPUTE FUNCTION FOR EACH RADIUS
C
C      DO 280 K=1,NPQ
C      CALL BESSL (R(K)*E,VP,VJN,NUM)
C      RV=VJN**2/DEXP(R(K)**2)
C      EP=DEXP(R(K)**2)
C      DO 120 NN=1,NUM
120    VP(NN)=VP(NN)**2/EP
C      REC=0.DO
C
C      COMPUTE FUNCTION FOR EACH ANGLE
C
C      DO 270 J=1,NPQ
270    REC=REC+FU(R(K)*DCOS(TH(J)),R(K)*DSIN(TH(J)))
C      V=0.DO
C      DO 130 NN=1,NUM
130    DN(I,NN)=DN(I,NN)+REC*VP(NN)*W(K)
280    DI(I) = DI(I) + REC*RV*W(K)
300    CONTINUE
C
C      SUM VALUE FROM EACH ANNULUS
C
C      DO 400 I=1,MAX
400    J = MAX + 1 - I
C      V = V + DI(J)
C      V=V*CONST
C      PRINT 3,N,V,DI(MAX)
C      NBQ=0
C      PRINT 13,NBQ,V
C      PRINT 4,(DI(I),I=1,MAX)
C      DO 500 NP=1,NUM
C      VQM=0.DO
C      VP(NP)=0.DO
C      DO 600 I=1,MAX
C      J=MAX+1-I
C      VP(NP)=VP(NP)+DN(J,NP)
C      IF(DN(J,NP).GT.VQM) VQM=DN(J,NP)
600    CONTINUE
C      VP(NP)=VP(NP)*CONST
C      PRINT 13,NP,VP(NP)
C      PRINT 14,NP,VQM,DN(MAX,NP)
500    CONTINUE
C
C      CALCULATE SUM FOR INTEGRATION CHECK
C
C      SUM=V
C      DO 700 J=1,NUM
C      I=NUM+1-J
C      SUM=SUM+2.DO*VP(I)
700    CONTINUE
C      PRINT 12,SUM
C      RETURN
1    FORMAT(10I5)
2    FORMAT(8E10.0)
3    FORMAT(2I10,1P2E15.6)
4    FORMAT(1P8E15.6)
12   FORMAT(5X,G20.13)
13   FORMAT(5X,I4,6X,G20.13)
14   FORMAT(5X,I4,6X,G20.13,6X,G20.13)
16   FORMAT(3(1PD20.12))
C      END

```


FUNCTION FU(X,Y)

FUNCTION FU IS AN AUXILIARY ROUTINE FOR BKGRN THAT
COMPUTES THAT PART OF THE INTEGRAND NOT RADIALY
SYMMETRIC.

IMPLICIT REAL*8 (A-H,O-Z)
COMMON /BKPRM/ A,B,C,D
P1=1.D0
IF(X.NE.0.D0) P1=DSIN(A*X)/(A*X)
IF(Y.NE.0.D0) P1=P1*DSIN(B*Y)/(B*Y)
FU=P1**2/(C+X**2)/(D+Y**2)
RETURN
END

SUBROUTINE SIGNAL(REC,RECO)

SUBROUTINE SIGNAL COMPUTES THE FOURIER COEFFICIENTS OF
A POINT TARGET OR AVERAGED COEFFICIENTS OVER A
GAUSSIAN POINTING ERROR

ZP = VALUES OF RADII FOR DIFFERENT ANNULI
Z = WORKING VECTOR FOR RADII
MAXR = MAXIMUM RADIUS OF OUTER ANNULUS
NIZ1 = DIMENSION OF ZP
REC = RETURN VECTOR OF COEFFICIENTS
RECO = ZERO ORDER COEFFICIENT

IMPLICIT REAL*8 (A-H,O-Z)
DIMENSION BN(120)
DIMENSION DI(50),DNJ(50,120),DN(50,120),Z(50),ZP(20)
DIMENSION R(24),W(24),TH(24)
COMPLEX*16 REC(1),VEC(120),RECO,VS,F,WP
COMMON /AVPRM/ NUM,IAVE,PO
COMMON /DTPRM/ RHO,SIG,WI,H,AL,BE,RX,RY,XO,YO
COMMON /SIPRM/ A,B,C,PX,QX
COMMON /NFIRST/ NFIRST
COMMON /START/ NS
COMMON /ANGL/ RANGL
DATA ZP/0.0D0,1.2D0,2.4D0,5.5D0,8.6D0,11.8D0,15.0D0,20.
1D0,25.0D0,30.0D0,40.0D0,50.0D0,60.0D0,70.0D0,80.0D0,
290.0D0,100.0D0,150.0D0,200.0D0,400.0D0/
DATA MAXR/77,NR/17,NIZ1/20/
NFIRST=0
VS=DCMPLX(0.0D0,-1.0D0)
PI = DAPCOS(-1.0D0)
PI2 = PI/2.0D0
KKK=0

CALCULATE CONSTANTS FOR INTEGRAL

GAMA=SIG
IF(IAVE.EQ.1) GAMA=DSQRT(SIG**2+PO**2)
SG = DSQRT(2.0D0)*GAMA
A=WI/SG
B=H/SG
CONST=A*B/PI/PI
C = 1.0D0
PX=-XO
QX=-YO
IF(IAVE.EQ.0) PX=PX+RX
IF(IAVE.EQ.0) QX=QX+RY
PX=PX*DSQRT(2.0D0)/GAMA
QX=QX*DSQRT(2.0D0)/GAMA
E = 2.0D0*RHO/SG

SET ANNULI FOR SPECIFIC PARAMETERS

DZ = 0.0D0
DO 150 I=1,NIZ1
150 Z(I)=ZP(I)/(2.0D0*E)
I = 0
IF(Z(NIZ1).GT.MAXR)GO TO 210
DZ=15.0D0*PI/E
MMM=50-NIZ1
DO 200 I=1,MMM
200 Z(I+NIZ1) = Z(NIZ1) + I*DZ
IF(Z(I+NIZ1).GT.MAXR)GO TO 210
CONTINUE
PRINT 17,Z(I+NIZ1)


```

C
C
C      MAX = NUMBER OF ANNULI

210  MAX=I+NI Z1-1
      GO TO 212
211  MAX=I
212  PRINT 4,RHD,SIG,WI,H,AL,BE,RX,RY,XO,YO,PX,QX
215  PRINT 4,(Z(I),I=1,MAX)
220  DO 300 I=1,MAX

C
C
C      COMPUTE RADII,WEIGHTS AND ANGLES FOR EACH ANNULUS

      CALL WAA(Z(I),Z(I+1),R,TH,W,NPQ)
      NFIRST=1
      NPR=NPQ
      DI(I) = 0.DO
      DO 115 NN=NS,NUM
115  DNJ(I,NN)=0.DO
      DN(I,NN) = 0.DO
      IF(KKK.EQ.1) GO TO 300
      DO 280 K=1,NPQ
      RK2=R(K)**2
      IF(RK2.GT.174) GO TO 285
      EP=DEXP(RK2)
      IF(EP.GT.1.D 50) GO TO 285
      CALL BESSL (R(K)*E,BN,VJN,NUM)
      RV=VJN/EP
      RECO=F(R(K),TH,0)

C
C
C      COMPUTE FUNCTION FOR EACH RADIUS

      RECO=RECO*RV*W(K)
      PP=RECO
      DI(I)=DI(I)+PP
      DO 130 NN=NS,NUM
      BN(NN)=BN(NN)/EP
      REC(NN)=F(R(K),TH,NN)
      REC(NN)=REC(NN)*BN(NN)*W(K)
      PP=REC(NN)
      DN(I,NN)=DN(I,NN)+PP
      PP=REC(NN)*VS
      DNJ(I,NN)=DNJ(I,NN)+PP
130  CONTINUE
280  CONTINUE
300  CONTINUE

C
C
C      SUM VALUE FROM EACH ANNULUS

      VZ = 0.DO
      V1 = 0.DO
      V2 = 0.DO
      DO 400 I=1,MAX
      J = MAX + 1 - I
      IF(DABS(DI(J)).GT.DABS(VZ)) VZ=DI(J)
400  IF(DI(J).LE.0.DO) V1 = V1+DI(J)
      IF(DI(J).GT.0.DO) V2 = V2+DI(J)
      RECO=DCMPLX(V1+V2,0.DO)
      RECO=RECO*CONST
      NBQ=0
      PRINT 4,(DI(I),I=1,MAX)
      PRINT 19,NBQ,RECO
      PRINT 14,NBQ,VZ,DI(MAX)
      DO 500 NP=NS,NUM
      VQM = 0.DO
      V1 = 0.DO
      V1J=0.DO
      V2 = 0.DO
      V2J=0.DO

```



```

DO 600 I=1,MAX
J=MAX+1-I
IF(DN(J,NP).LT.0.DO) V1=V1+DN(J,NP)
IF(DNJ(J,NP).LT.0.DO) V1J=V1J+DNJ(J,NP)
IF(DN(J,NP).GE.0.DO) V2=V2+DN(J,NP)
IF(DNJ(J,NP).GE.0.DO) V2J=V2J+DNJ(J,NP)
IF(DABS(DN(J,NP)).GT.DABS(VQM)) VQM=DN(J,NP)
600 CONTINUE
REC(NP)=DCMPLX(V1+V2,V1J+V2J)
REC(NP)=REC(NP)*CONST
PRINT 19,NP,REC(NP)
PRINT 14,NP,VQM,DN(MAX,NP)
500 CONTINUE
725 CONTINUE
VS=DCMPLX(0.DO,1.DO)
DO 800 NP=NS,NUM
800 REC(NP)=REC(NP)*VS**NP
IF(IAVE.EQ.0) GO TO 960
SUM=RECO
IF(NS.NE.1) SUM=0.0DO
PRINT 19,NBQ,RECO

C
C
C CALCULATE SUM FOR INTEGRATION CHECK
DO 900 I=NS,NUM
PQ=REC(I)
PRINT 19,I,REC(I)
900 SUM=SUM+2.DO*PQ
PRINT 18,SUM,SUMJ
RETURN
960 CONTINUE
VS=DCMPLX(0.DO,-1.DO)
PRINT 19,NPQ,RECO
SUM=RECO
IF(NS.NE.1) SUM=0.DO
SUMJ=0.DO
DO 950 NP=NS,NUM
VEC(NP)=REC(NP)*DCMPLX(DCOS(NP*RANGL),DSIN(NP*RANGL))
PRINT 19,NP,VEC(NP)
PP=VEC(NP)
SUM=SUM+2.DO*PP
PP=VEC(NP)*VS
SUMJ=SUMJ+PP
950 CONTINUE
PRINT 18,SUM,SUMJ
RETURN
285 KKK=1
GO TO 300
1 FORMAT(10I5)
2 FORMAT(8E10.0)
3 FORMAT(2I10,1P2E15.6)
4 FORMAT(1P8E15.6)
5 FORMAT(2I5)
6 FORMAT(1P2E15.6)
12 FORMAT(5X,G20.13)
13 FORMAT(5X,I4,6X,G20.13)
14 FORMAT(5X,I4,6X,G20.13,6X,G20.13)
15 FORMAT(2X,I3,2X,1PE15.6,2X,1PE15.6,2X,I3,2X,1PE15.6,2X
1,1PE15.6)
16 FORMAT(3(1PD20.12))
17 FORMAT(5X,'MAX NOT LARGE ENOUGH ZMAX=',F15.8)
18 FORMAT(2X,'SUM=',G20.13,'SUMJ=',G20.13)
19 FORMAT(5X,I4,6X,G25.13,G20.13)
END

```


FUNCTION F (R,TH,NN)

FUNCTION F IS AN AUXILIARY ROUTINE FOR SIGNAL THAT
COMPUTES THAT PART OF THE INTEGRAND NOT RADially
SYMMETRIC

```

IMPLICIT REAL*8 (A-H,O-Z)
COMPLEX*16 F
DIMENSION TH(1)
DIMENSION AAE(24),BBE(24),AAO(24),BBO(24)
COMMON /SIPRM/ A,B,C,PX,QX
DATA NPR/24/
JJ=(-1)**NN
AA=0.0D0
BB=0.0D0
IF(NN.GT.0) GO TO 5
DO 1 J=1,NPR
X=R*DCOS(TH(J))
Y=R*DSIN(TH(J))
DSX=DSIN(PX*X)
DSY=DSIN(QX*Y)
DCX=DCOS(PX*X)
DCY=DCOS(QX*Y)
P1=1.D0
IF(X.NE.0.D0) P1=DSIN(A*X)/(A*X)
IF(Y.NE.0.D0) P1=P1*DSIN(B*Y)/(B*Y)
AAE(J)=DCX*DCY*P1
BBE(J)=DSX*DSY*P1
AAO(J)=-DCX*DSY*P1
BBO(J)=-DSX*DCY*P1
1 CONTINUE
5 IF(JJ.LT.0) GO TO 10
DO 20 J=1,NPR
AA=AA+AAE(J)*DCOS(NN*TH(J))
BB=BB+BBE(J)*DSIN(NN*TH(J))
20 CONTINUE
F=DCMPLX(AA,BB)
IF(NN.EQ.0) F=DCMPLX(AA,0.D0)
RETURN
10 DO 40 J=1,NPR
AA=AA+AAO(J)*DSIN(NN*TH(J))
BB=BB+BBO(J)*DCOS(NN*TH(J))
40 CONTINUE
F=DCMPLX(AA,BB)
RETURN
END

```


C
C
C
C
C
C
C
C
C
SUBROUTINE WAA(R1,R2,R,TH,W,N)

SUBROUTINE WAA COMPUTES THE RADIAL POINTS,WEIGHTS AND
ANGLES AT WHICH THE INTEGRAND MUST BE EVALUATED.

NP = DEGREE OF GAUSSIAN LA
R = RADIAL POINTS TO BE USED
TH = ANGLES TO BE USED
W = WEIGHTS TO BE USED
NFIRST PREVENTS COMPUTING G-L POINTS MORE THAN ONCE

IMPLICIT REAL*8(A-H,O-Z)
DIMENSION R(1),W(1),TH(1)
REAL*8 RC(24),WC(24)
COMMON /NFIRST/ NFIRST
DATA NP/24/
PI=DARCCS(-1.00)
PIN=PI/2.00/NP
IF(NFIRST.NE.0)GO TO 99
CALL GLO24(RC,WC,0.00,1.00)
DO 10 I=1,NP
TH(I)=(I-.500)*PIN
NFIRST = 1
99 CONTINUE
N = NP
T = R2 - R1
TW = T*(R2 + R1)
F = TW*PI/NP
DO 100 I=1,NP
RX = R1
RX = RX*R1
RY = R2
RY = RY*R2
R(I) = DSQRT(RX + RC(I)*(RY - RX))
W(I) = WC(I)*F
100 CONTINUE
RETURN
END

C
C
C
C

SUBROUTINE GL024(X,A,C,D)

GAUSSIAN-LEGENDER INTEGRATION ROUTINE (24 POINTS)

DOUBLE PRECISION DMC,DPC

DOUBLE PRECISION C,D,X(24),A(24),XX(12), AA(12)

DATA XX(1),AA(1),XX(2),AA(2),XX(3),AA(3),XX(4),AA(4),X

1 XX(6),AA(6),XX(7),AA(7),XX(8),AA(8),XX(9),AA(9),XX(10

2 XX(11),AA(11),XX(12),AA(12)/

*.9951872199970213601799974097D-0,.12341229799987199546

*.9747265559713094981983919930D-0,.28531388628933663181

*.9382745520027327585236490017D-0,.44277438817419806163

*.8864155270044010342131543419D-0,.59298584915436780746

*.8200019859739029219539498726D-0,.73346481411080305734

*.7401241915785543642438281031D-0,.86190161531953275917

*.6480936519369755692524957869D-0,.97613652104113888269

*.5454214713888395356583756172D-0,.10744427011596563478

*.4337935076260451384870842319D-0,.11550566805372560135

*.3150426796961633743867932913D-0,.12167047292780339120

*.1911188674736163091586398207D-0,.12583745634682829612

*.6405689286260562608504308262D-1,.12793819534675215697

DMC = .5D0*(D-C)

DPC = .5D0*(D+C)

DO 2 I=1,12

NI = 25 - I

X(I) = -DMC*XX(I) + DPC

X(NI) = DMC*XX(I) + DPC

A(I) = DMC*AA(I)

2 A(NI) = DMC*AA(I)

RETURN

END

SUBROUTINE BESSL (AG,BF,BZ,NUM)

SUBROUTINE BESSL COMPUTES BESSEL FUNCTIONS OF THE
RECEIVED ARGUMENT

AG = ARGUMENT OF BESSEL FUNCTION
BF = RETURN VECTOR OF BESSEL FUNCTIONS
BZ = ZERO ORDER BESSEL FUNCTION
NUM = HIGHEST ORDER OF BESSEL FUNCTION TO BE RETURNED
NY,NX = ORDERS CALCULATED BY ASYMPTOTIC EXPANSION

IMPLICIT REAL*8 (A-H,O-Z)
DIMENSION BF3(1000),BF(1)
NZ=1000
KT=0
IF(AG.LT.0) KT=1
IF(AG.LT.0.DO) AG=DABS(AG)
X=AG
NY=IFIX(SNGL(AG))
IF(NY.LE.1) NF=16
IF(NY.EQ.2) NF=20
IF(NY.EQ.3) NF=24
IF(NY.GE.4.AND.NY.LT.6) NF=6*NY
IF(NY.GE.6.AND.NY.LT.10) NF=5*NY
IF(NY.GE.10.AND.NY.LT.15) NF=4*NY
IF(NY.GE.15.AND.NY.LT.29) NF=3*NY
IF(NY.GE.29.AND.NY.LT.80) NF=2*NY
IF(NY.GE.80.AND.NY.LT.150) NF=IFIX(1.5*FLOAT(NY))
IF(NY.GE.150.AND.NY.LT.330) NF=IFIX(1.4*FLOAT(NY))
IF(NY.GE.330) NF=IFIX(1.25*FLOAT(NY))
IF(IFIX(FLOAT(NF)/2.).LT.IFIX(FLOAT(NF+1)/2.)) NF=NF+1
IF(NY.LT.1) NF=8
NY=NF
NX=NY-1

SET ORDERS > NY TO ZERO

DO 1 I=NY,NZ
BF3(I)=0.DO
CONTINUE

COMPUTE ASYMPTOTIC EXPANSION

DO 2 MU=NX,NY
Z=X/DFLOAT(MU)
AMU=DFLOAT(MU)
A = DSQRT(1.DO-Z**2)
A1=1.5DO*(DLOG((1.DO+A)/Z)-A)
DEL = DEXP(2.DO/3.DO*DLOG(A1))
X1 = DEXP(2.DO/3.DO*DLOG(AMU)+DLOG(DEL))
CALL TABLE (X1,AIV,AIPV)
D1 = DEXP(1.DO/3.DO*DLOG(AMU))
D2 = DEXP(5.DO/3.DO*DLOG(AMU))
BO = -5.DO/(48.DO*DEL**2)+(1.DO/DSQRT(DEL))*(5.DO/(24.
DO*A**3)-1.DO/(8.DO*A))
F1 = DEXP(0.25DO*DLOG(4.DO*DEL)-0.5DO*DLOG(A))
BF3(MU)=F1*(AIV/D1+AIPV*BO/D2)
CONTINUE
NY2=NY-2

USE RECURSIVE EQUATION TO GENERATE ORDERS < NX

DO 4 I=1,NY2
N=NY2-I+1
BF3(N) = (2.DO*DFLOAT(N+1)/X)*BF3(N+1)-BF3(N+2)


```

4      CONTINUE
      SUM = 2.D0*BF3(1)/X-BF3(2)
      DO 76 I=2,NY2,2
      SUM = SUM+2.D0*BF3(I)
76     CONTINUE

C
C
C      COMPUTE NORMALIZING CONSTANT

      SNORM = 1.D0/SUM
      DO 77 I=1,NUM
      BF(I)=SNORM*BF3(I)

C
C
C      ODD ORDER BESSEL FUNCTIONS ARE ODD

77     IF(KT.EQ.1) BF(I)=BF(I)*(-1.D0)**I
      CONTINUE
      BZ = (2.D0*BF3(1)/X-BF3(2))*SNORM
      RETURN
      END

```


SUBROUTINE TABLE(X,AIV,AIPV)

SUBROUTINE TABLE IS AN AUXILIARY ROUTINE FOR BESSL
THAT COMPUTES AIRY FUNCTIONS

```

IMPLICIT REAL*8 (A-H,O-Z)
DIMENSION AI(50),AIP(50),ABI(15),ABIP(15)
DATA AI/4*0.0D0,.562280D0,4*0.0D0,.560462D0,4*0.0D0,
1.558724D0,4*0.0D0,.557058D0,4*0.0D0,.555456D0,4*0.0D0,
2.553912D0,4*0.0D0,.552421D0,4*0.0D0,.550980D0,4*0.0D0,
3.549584D0,4*0.0D0,.548230D0/
DATA AIP/4*0.0D0,.566873D0,4*0.0D0,.569448D0,4*0.0D0,
1.571927D0,4*0.0D0,.574320D0,4*0.0D0,.576635D0,4*0.0D0,
2.578878D0,4*0.0D0,.581056D0,4*0.0D0,.583174D0,4*0.0D0,
3.585235D0,4*0.0D0,.587245D0/
DATA ABI/4*0.0D0,.548230D0,.545636D0,.543180D0,
1.540844D0,.538618D0,.536489D0,.534448D0,.532488D0,
2.530601D0,.528783D0,.527027D0/
DATA ABIP/4*0.0D0,.587245D0,.591120D0,.594823D0,
1.598372D0,.601782D0,.605068D0,.608239D0,.611305D0,
2.614275D0,.617156D0,.619954D0/
L=0
Y = DEXP(DLOG(1.5D0)-1.5D0*DLOG(X))
W = DEXP(DLOG(2.D0/3.D0)+1.5D0*DLOG(X))
L=1
IF(Y.GT.1.5D0) GO TO 14
IF(Y.GT.0.499999D0) GO TO 1
L=2
W1 = 10.D0 * Y
IW1=IFIX(SNGL(W1))
W2=W1+1.
IW2=IFIX(SNGL(W2))
IZ=IW1*10
IF(IW1.LT.IW2) IZ=IZ+5
IY=IZ-5
IF(IY.EQ.0) GO TO 13
GO TO 8
1 Y = 10.D0 * Y
IY=IFIX(SNGL(Y))
IF(IY-Y) 2,4,6
2 IZ=IY+1
GO TO 8
4 AIV=AI(IY)
AIPV=AIP(IY)
GO TO 19
6 IZ=IY
IY=IY-1
DP=Y-FLOAT(IY)
IF(L.EQ.2) DP=DP/5.D0
IF(L.EQ.1) GO TO 12
AIV = (1.D0-DP)*AI(IY)+DP*AI(IZ)
AIPV = (1.D0-DP)*AIP(IY)+DP*AIP(IZ)
GO TO 19
12 AIV = (1.D0-DP)*ABI(IY)+DP*ABI(IZ)
AIPV = (1.D0-DP)*ABIP(IY)+DP*ABIP(IZ)
GO TO 19
13 DP = Y/5.D0
AIV = (1.D0-DP)*0.564190D0+DP*AI(IZ)
AIPV = (1.D0-DP)*0.564190D0+DP*AIP(IZ)
19 AIV = DEXP(-DLOG(2.D0)-0.25D0*DLOG(X)-W+DLOG(AIV))
AIPV = DEXP(0.25D0*DLOG(X)-W+DLOG(AIPV))
AIPV = AIPV * (-.5D0)
RETURN
14 PRINT 30
30 FORMAT(5X,'HAVE EXCEEDED TABLE VALUES')
RETURN
END

```


SUBROUTINE SUMCK

SUBROUTINE SUMCK COMPUTES THE ANALYTICAL EXPRESSION
FOR THE INFINITE SUM OF COEFFICIENTS

SISUM = INFINITE SUM OF POINT TARGET (IAVE=1) OR
AVERAGED TARGET (IAVE=0) COEFFICIENTS
BKSUM = INFINITE SUM OF BACKGROUND COEFFICIENTS

IMPLICIT REAL*8 (A-H,O-Z)
COMMON /DTPRM/ RHO,SIG,WI,H,AL,BE,RX,RY,XO,YO
COMMON /AVPRM/ NUM,IAVE,PO
COMMON /ANGL/ RANGL
W=WI
CONST=0.2500D0
GAMA=DSQRT(SIG**2+PO**2)
IF(IAVE.EQ.0) GAMA=SIG
DIV=2.0D0*DSQRT(2.0D0)*GAMA
IF(IAVE.EQ.0) GO TO 10

COMPUTE SUM OF AVERAGED COEFFICIENTS

A=DERF((2.0D0*(XO+RHO)+W)/DIV)
B=DERF((2.0D0*(XO+RHO)-W)/DIV)
C=DERF((2.0D0*(YO+H)/DIV)
D=DERF((2.0D0*(YO)-H)/DIV)
SISUM=CONST*(A-B)*(C-D)
R1=R(W,AL,SIG)
R2=R(H,BE,SIG)

COMPUTE SUM OF BACKGROUND COEFFICIENTS

BKSUM=4.0D0*AL*BE*R1+R2/(W*H)**2
PRINT 5,BKSUM,SISUM
RETURN
CONTINUE

COMPUTE SUM OF POINT TARGET COEFFICIENTS

A=DERF((2.0D0*(XO+RHO*DCOS(RANGL)-RX)+W)/DIV)
B=DERF((2.0D0*(XO+RHO*DCOS(RANGL)-RX)-W)/DIV)
C=DERF((2.0D0*(YO+RHO*DSIN(RANGL)-RY)+H)/DIV)
D=DERF((2.0D0*(YO+RHO*DSIN(RANGL)-RY)-H)/DIV)
GO TO 4
FORMAT(2X,'BKSUM=',D15.8,10X,'SISUM=',D15.8)
END

C
C
C
C
C

FUNCTION R(U,Z,SIG)

FUNCTION R IS AN AUXILIARY ROUTINE FOR BKSUM

```

IMPLICIT REAL*8 (A-H,O-Z)
PI=DARCOS(-1.00)
R=0.00
F1=-((U/(2.00*SIG))**2)
E1=DEXP(F1)
E2=(Z*SIG)**2
E2=DEXP(E2)
F31=7*U
E3=DEXP(E31)
E4=DEXP(-E31)
X1=U/(2.00*SIG)
Y1=1.00-DERF(X1)
X2=Z*SIG+U/(2.00*SIG)
Y2=1.00-DERF(X2)
X3=Z*SIG-U/(2.00*SIG)
Y3=1.00-DERF(X3)
X4=Z*SIG
Y4=1.00-DERF(X4)
R=(U/(Z**2))*(1.00-Y1-(SIG*2.00/(DSQRT(PI)*U))*(1.00-E
R=R+(E2/(2.00*Z**3))*(E3*Y2+E4*Y3-2.00*Y4)
RETURN
END

```


BIBLIOGRAPHY

1. Abramowitz, M. and Stegun, I., Handbook of Mathematical Functions, U.S. Gov. Printing Office, 1964.
2. Gradsheyn, I.S. and Ryzhik, I. W., Table of Integrals Series and Products, Academic Press, 1965.
3. Harger, R. O., "Signal Sequence Detection Given Noisy, Common Background Image Sets," IEEE Trans. Aerosp. Electron. Sys., Vol. AES-8, pp. 174-185, March 1972.
4. Helstrom, C. W., Statistical Theory of Signal Detection, 2d ed., Pergamon Press, 1968.
5. Hudson, R. D., Jr., Infrared Systems Engineering, pp. 27, Wiley, 1969.
6. Hughes Aircraft Company Report 2341.4/18, Application of Detection Theory to IR Scanning Systems, by R. Yoshitani, October 1970.
7. Papoulis, A., Probability, Random Variables and Stochastic Processes, pp. , McGraw-Hill, 1965.
8. Papoulis, A., Systems and Transforms with Applications in Optics, McGraw-Hill, 1968.
9. Peirce, W. H., "Numerical Integration Over the Planar Annulus," J. Soc. Indust. Appl. Math. Vol. 5, No. 2, pp. 66-73, June 1957.
10. Saab Report RAD-0-70:33, Description of Signal and Background Noise in IR Systems with Transform Methods (in Swedish), by H. Samuelsson, 1970.
11. Samuelsson, H., "Infrared Systems: I. Expressions for Signal and Background Induced Noise with Space Filters," IEEE Trans. Aerosp. Electron. Sys., Vol. AES-7, pp. 27-33, January 1971.
12. Stroud, A. H., Approximate Calculation of Multiple Integrals, Prentice-Hall, Inc., 1971.
13. Stroud, A. and Secrest, D., Gaussian Quadrature Formulas, Prentice-Hall, Inc., 1966.
14. University of Michigan, Willow Run Labs., Rept. 2389-87-T, ASTIA Doc. 480352, "Spacial Frequency Filtering," by J. L. Alward, Dec. 1965.

15. Van Trees, H. L., Detection, Estimation and Modulation Theory, Part 1, Wiley, 1968.

INITIAL DISTRIBUTION LIST

	No. Copies
1. Defense Documentation Center Cameron Station Alexandria, Virginia 22314	2
2. Library, Code 0212 Naval Postgraduate School Monterey, California 93940	2
3. Prof. Harold A. Titus, Code 52Ts Department of Electrical Engineering Naval Postgraduate School Monterey, California 93940	3
4. Dr. Fletcher Phillips Code 3025 Naval Weapons Center China Lake, California 93555	1
5. Dr. Reo Yoshitani Hughes Aircraft Company 8433 Fallbrook Ave. Canoga Park, California 91304	1
6. Prof. Allen E. Fuhs, Code 57Fu Department of Aeronautics Naval Postgraduate School Monterey, California 93940	1
7. Prof. Richard Franke, Code 53Fe Department of Mathematics Naval Postgraduate School Monterey, California 93940	1
8. LT William E. Major, USN U.S. Naval Destroyer School Newport, Rhode Island 02840	1
9. Prof. John P. Powers, Code 52Pw Department of Electrical Engineering Naval Postgraduate School Monterey, California 93940	1
10. CDR Lindsey Smith, USN Code Air 533C Naval Air Systems Command Washington, D.C. 20360	1

UNCLASSIFIED

Security Classification

DOCUMENT CONTROL DATA - R & D

(Security classification of title, body of abstract and indexing annotation must be entered when the overall report is classified)

ORIGINATING ACTIVITY (Corporate author)

Naval Postgraduate School
Monterey, California 93940

2a. REPORT SECURITY CLASSIFICATION

Unclassified

2b. GROUP

REPORT TITLE

OPTIMUM THRESHOLD DETECTION FOR AN
INFRARED ROTATING DETECTION SYSTEM

DESCRIPTIVE NOTES (Type of report and, inclusive dates)

Electrical Engineer's Thesis; March 1973

AUTHOR(S) (First name, middle initial, last name)

William E. Major, II; Lieutenant, United States Navy

REPORT DATE

March 1973

7a. TOTAL NO. OF PAGES

135

7b. NO. OF REFS

15

CONTRACT OR GRANT NO.

9a. ORIGINATOR'S REPORT NUMBER(S)

PROJECT NO.

9b. OTHER REPORT NO(S) (Any other numbers that may be assigned
this report)

DISTRIBUTION STATEMENT

Approved for public release; distribution unlimited.

SUPPLEMENTARY NOTES

12. SPONSORING MILITARY ACTIVITY

Naval Postgraduate School
Monterey, California 93940

ABSTRACT

A threshold detection system based on the Neyman-Pearson criterion is derived for an infrared rotating optical system. Detection is optimum for small signal-to-noise ratios and a Gaussian uncertainty in the pointing error of the optical system. The signal spectrum and background power spectral density for a rectangular space filter are computed numerically and used to specify the matched filter for the threshold detection system and evaluate its performance.

UNCLASSIFIED

Security Classification

KEY WORDS

LINK A

LINK B

LINK C

ROLE

WT

ROLE

WT

ROLE

WT

SIGNAL PROCESSING

DETECTION THEORY

INFRARED DETECTION

OPTICAL DETECTION

NUTATING DETECTOR

SPATIAL PROCESSING

SPATIAL FILTERING

5 JUN 74
5 JUN 74

22513
22181

Thesis
M2775 Major
c.1

143338

Optimum threshold de-
tection for an infrared
nutating detection sys-
tem.

5 JUN 74
5 JUN 74

22513
22181

Thesis
M2775 Major
c.1

143338

Optimum threshold de-
tection for an infrared
nutating detection sys-
tem.

thesM2775

Optimum threshold detection for an infra



3 2768 001 01175 2

DUDLEY KNOX LIBRARY